

Syracuse University

## SURFACE

---

Biomedical and Chemical Engineering -  
Dissertations

College of Engineering and Computer Science

---

5-2013

# Improving Bioactivity and the Anti-Bacterial Properties of Two-Solution Bone Cement Containing Cross-Linked Polymethylmethacrylate (PMMA) Nanospheres ( $\eta$ -TSBC)

Shailly Jariwala  
*Syracuse University*

Follow this and additional works at: [https://surface.syr.edu/bce\\_etd](https://surface.syr.edu/bce_etd)



Part of the [Biomedical Engineering and Bioengineering Commons](#)

---

### Recommended Citation

Jariwala, Shailly, "Improving Bioactivity and the Anti-Bacterial Properties of Two-Solution Bone Cement Containing Cross-Linked Polymethylmethacrylate (PMMA) Nanospheres ( $\eta$ -TSBC)" (2013). *Biomedical and Chemical Engineering - Dissertations*. 67.

[https://surface.syr.edu/bce\\_etd/67](https://surface.syr.edu/bce_etd/67)

This Dissertation is brought to you for free and open access by the College of Engineering and Computer Science at SURFACE. It has been accepted for inclusion in Biomedical and Chemical Engineering - Dissertations by an authorized administrator of SURFACE. For more information, please contact [surface@syr.edu](mailto:surface@syr.edu).

# **IMPROVING BIOACTIVITY AND THE ANTI-BACTERIAL PROPERTIES OF TWO-SOLUTION BONE CEMENT CONTAINING CROSS-LINKED POLYMETHYLMETHACRYLATE (PMMA) NANOSPHERES ( $\eta$ -TSBC)**

Shailly H. Jariwala

## **ABSTRACT**

The high viscosity standard two-solution bone cements (STSBC) developed in our laboratory exhibits several advantages over other commercial powder-liquid cement formulations. However, the high monomer concentration, viscosity, and exothermal temperature are considered a major limitation to the use of this material. Modified two-solution cements containing cross-linked polymethylmethacrylate (PMMA) nanospheres ( $\eta$ -TSBC), as part of the polymer phase, were fabricated as the first step for optimization of cement viscosity for application of the material in the treatment of vertebral compression fractures using vertebroplasty (VP) and kyphoplasty (KP). The  $\eta$ -TSBC exhibited reduced viscosity, lower polymerization exotherm, and residual monomer in comparison to STSBC. Nevertheless, the  $\eta$ -TSBC lacks bioactivity and has no biologic potential to remodel or integrate into the surrounding bone. Also, addition of radiopacifiers such as barium sulfate and zirconium dioxide is required for fluoroscopy guided procedures and is known to be detrimental to the cement mechanical and bioactive properties. In this sense,  $\eta$ -TSBCs containing strontium-substituted hydroxyapatite (SrHA) microspheres have been developed in this study as a step towards improving bioactivity of these cement formulations. Hydroxyapatite (HA) is a natural bone mineral component and strontium is known to stimulate bone formation and acts as a good contrast agent. In addition to this, recent studies (1-4) have shown that the antibacterial property of hydroxyapatite nanoparticles improved after partial or complete substitution of calcium with strontium ions. The

goal of addition of SrHA microspheres into the  $\eta$ -TSBC formulation is to improve bioactivity by allowing apatite formation on the cement surface that would in turn help making chemical bonds with the HA in the surrounding bone, and also to impart radiopacity and antibacterial properties without the need to incorporate any additional radio contrast or antibiotic filler material. The addition of SrHA microspheres at different concentrations resulted in improving the apatite forming ability of  $\eta$ -TSBCs. The antibacterial properties of  $\eta$ -TSBC containing SrHA microspheres were investigated *in vitro* by culturing *Escherichia coli* (*E.coli*) K12/pRSH103 biofilm which resulted in reduced biofilm growth on the cement surfaces with increasing SrHA concentration, indicating capability of bacterial inhibition. The addition of SrHA microspheres resulted in a reduction of mechanical properties in comparison to  $\eta$ -TSBC, bringing these values closer to the human cancellous bone. However, the mechanical properties were similar to the  $\eta$ -TSBC containing 20% wt/vol  $ZrO_2$  as a radiopacifier, indicating no further detrimental effect of the SrHA addition on the  $\eta$ -TSBC properties while replacing  $ZrO_2$  in order to impart radiopacity and improve bioactivity. These cements were observed to require further optimization to improve interfacial bonding of the SrHA microspheres to the cement matrix for enhancement of mechanical properties of the material. In summary,  $\eta$ -TSBCs containing SrHA microspheres were developed exhibiting a combination of attractive properties and potential for additional modification that will prolong the life and performance of arthroplasties and vertebral augmentation.

IMPROVING BIOACTIVITY AND THE ANTI-BACTERIAL PROPERTIES OF TWO-  
SOLUTION BONE CEMENT CONTAINING CROSS-LINKED  
POLYMETHYLMETHACRYLATE (PMMA) NANOSPHERES ( $\eta$ -TSBC)

By

Shailly H. Jariwala  
B.E, University of Mumbai, Mumbai, India, 2006  
M.S., Syracuse University, Syracuse, New York, 2009

DISSERTATION

Submitted in partial fulfillment of the requirements for the degree of Doctor of Philosophy in  
Bioengineering in the Graduate School of Syracuse University

May 2013

© Copyright 2013 Shailly H. Jariwala

All Rights Reserved

*Dedicated to*

*My grandparents*

*&*

*My parents, Alka and Hemant Jariwala*

## Acknowledgements

The completion of this work is a result of the contribution, support, and efforts of many people involved. Foremost, I would like to express my deepest and sincerest gratitude to my dissertation advisor, Dr. Julie Hasenwinkel, for giving me the opportunity and the resources to gain experience in the field of research and development of Biomaterials. I am thankful to Julie for always supporting me with her patience and knowledge whilst providing an excellent atmosphere to conduct research, think out of the box, and liberty to work in my own way. I would also like to thank her for motivating me to interact with professionals from other sectors that lead to fruitful collaborations. Thank you for your trust, patience, and constant guidance. As a woman about to begin her professional career in the field of Science and Engineering, I admire her ability to successfully balance her professional and personal life along with being an excellent mother/parent and would only hope to one day achieve the same. I will be indebted to her for exceptionally inspiring and enriching my growth as a student and as a researcher.

I would like to thank the members of my committee, Dr. Karin Ruhlandt, Dr. Jeremy Gilbert, Dr. Patrick Mather, Dr. Rebecca Bader, and Dr. Dacheng Ren for their time and effort. In addition, sincere thanks to Dr. Gilbert, with whom I have enjoyed having discussions and suggestions about this project and about science in general, and whose enthusiasm for research has had a lasting effect. I am grateful to Dr. Patrick Mather and the Mather Research Group for all their help in training and usage of laboratory equipment (DSC, Goniometer).

I am grateful to Dr. Dacheng Ren and his Research Group for our collaboration and for all the suggestions, training, and making available resources (*E.coli* bacterial strains) used in this work to test antibiotic properties of the bone cements. I particularly appreciate the helpful training on *E. coli* biofilm culture and agar gel assay experiments from Sarah Smith and

Chanokpon Yongyat. I sincerely acknowledge the help from Sarah Smith on the experiments for 24 hour and long-term antibacterial study performed on SrHA bone cements. Special thanks to Nathaniel Ordway at the Institute of Human Performance (IHP) and State University of New York Upstate Medical University, for helping me capture radiographs of SrHA cements using C-arm fluoroscopy in order to test the optical density of the cements in this work. I am also grateful for the vital help and training from Dr. Danieli Rodrigues and Christopher Ma during the initial phases of this project. I would also like to acknowledge Richard Chave from the Syracuse University machine shop for graciously machining all the Teflon molds used for casting cement samples for various mechanical and bioactivity tests in this work.

I would also like to express my gratitude to the faculty and staff of the Department of Biomedical and Chemical Engineering (BMCE) and Syracuse Biomaterials Institute (SBI), at Syracuse University, particularly Dawn Long, Kristin Lingo, Karen Low, and Michelle Lissner for all their help and support. I thank Syracuse University for the graduate and research assistantships and the Wallace H. Coulter Foundation for the financial support.

I would like to thank Anthony Fernando, Tarun Saxena, Christopher Close, and Shiril Sivan for being phenomenal friends, terrific lab mates, and a fantastic support system throughout my 6 years in Syracuse. A special thanks to Sharvari Waghmare and Rutu Pandya, for being fabulous friends and confidantes. I earnestly thank Orville D'Souza for always believing and having faith in my capabilities and being a tremendous friend even with being miles away. I am grateful to all my friends and colleagues, especially Aditya Pathak, Chintan Doshi, Maitreyee Pandit, Naman Trapasia, Mayank Talati, Vishwanathan Swaminathan, Morteza Haeri, Jua Kim, and Danieli Rodrigues for being such great companies and comfort in Syracuse. I also appreciate

the collaboration, useful insights and friendship from all the people in my lab and the Syracuse Biomaterials Institute and for making the lab a very enjoyable environment to work in.

Most importantly, I wish to thank my entire family for always believing in my dreams, aspirations, and professional goals and for their constant love and support. I cannot thank my family enough for their unconditional love and feel truly blessed to have them as my family. Words are not enough to express gratitude to my parents, and my younger sister Jesal, for understanding my need to go far away from home to achieve better education and for always showing admiration and respect for my choices. Thank you for being so patient, for your constant care, and for being present during the most precious moments of my life. In addition, sincere appreciation for Jesal's ability to tolerate all of my idiosyncrasies and quirks throughout life, and for her and Shalini Burra's support and tolerance, especially during these last few days of working on my dissertation. It would not have been possible to accomplish this goal without you all.

## **Table of Contents**

Abstract.....	i
Acknowledgements.....	vi
List of Figures.....	xiii
List of Tables.....	xix
1 Introduction .....	1
2 Background and significance.....	7
2.1 Two-solution bone cements containing PMMA nanospheres ( $\eta$ -TSBC) .....	8
2.2 Modification of $\eta$ -TSBC to improve bioactivity.....	9
2.3 Applications of bioactive $\eta$ -TSBCs .....	14
3 Goals and hypotheses .....	16
3.1 First goal: Fabricate two-solution bone cements containing strontium-substituted hydroxyapatite (SrHA) microspheres and characterize their bioactive properties .....	16
3.2 Second goal: Evaluate the effect of composition (degree of strontium substitution) and concentration of SrHA microspheres on the flexural, compressive, and fracture toughness properties of $\eta$ -TSBCs.....	17
3.3 Third goal: Investigate the antibiotic properties of the $\eta$ -TSBC containing bioactive strontium-substituted hydroxyapatite microspheres and determine the mechanism behind bacterial inhibition.....	18
4 Injectable, bioactive two-solution bone cements with strontium-substituted hydroxyapatite (SrHA) microspheres .....	20
4.1 Introduction .....	21

4.2	Materials and Methods .....	23
4.2.1	Preparation and characterization of SrHA/SrCaHA microspheres .....	23
4.2.2	Bone cement preparation .....	25
4.2.3	Optical density measurements .....	25
4.2.4	<i>In vitro</i> bioactivity.....	26
4.3	Results .....	28
4.3.1	Characterization of SrHA/SrCaHA microspheres .....	28
4.3.2	Optical Density .....	30
4.3.3	Bioactivity.....	31
4.4	Discussion .....	39
4.5	Conclusions .....	45
5	Biomechanical evaluation of two-solution bone cements with strontium-substituted hydroxyapatite microspheres .....	47
5.1	Introduction .....	48
5.2	Material and Methods.....	52
5.2.1	Preparation of SrHA/SrCaHA cements .....	52
5.2.2	Compression Testing .....	53
5.2.3	Flexural properties .....	54
5.2.4	Fracture toughness .....	55
5.3	Results .....	56

5.3.1	Compressive properties.....	56
5.3.2	Flexural properties .....	58
5.3.3	Fracture toughness .....	62
5.4	Discussion .....	64
5.5	Conclusions .....	69
6	<i>In vitro</i> evaluation of antibacterial properties of two-solution bone cements containing strontium-hydroxyapatite microspheres.....	71
6.1	Introduction .....	72
6.2	Materials and Methods.....	75
6.2.1	Bone cement preparation .....	75
6.2.2	Antibacterial tests: 24 hours and long-term .....	76
6.2.3	Antibacterial inhibition zone test.....	78
6.3	Results .....	79
6.3.1	24 hour antibacterial study.....	79
6.3.2	Long-term antibacterial tests.....	81
6.3.3	Inhibition zone test.....	82
6.4	Discussion .....	83
6.5	Conclusions .....	87
7	Summary.....	88
8	Future Work.....	95

9	Appendices .....	103
9.1	Appendix A: Synthesis of cross-linked PMMA nanospheres .....	103
9.2	Appendix B: Synthesis of SrHA/SrCaHA microspheres .....	106
9.3	Appendix C: Protocol by Kokubo et al. (84) for preparation of Simulated Body Fluid (SBF)	108
10	References .....	112
11	Vita .....	131

**List of Figures**

- Figure 1. SEM micrographs of as prepared, self-assembled (a) SrHA and (b) SrCaHA microspheres (2-5  $\mu\text{m}$  in diameter). (c) FTIR spectra of SrHA and SrCaHA powders indicating the presence of the phosphate ( $\text{PO}_4^{3-}$ ) peaks. Asterisk represents the significant phosphate peaks. (d) EDX spectra of SrHA and SrCaHA powders. The spectrum for SrCaHA powder shows the additional calcium peaks indicating half-substitution of calcium ions with strontium ions..... 29
- Figure 2. Radiographic images of  $\eta$ -TSBC prepared at (a) 0% (controls), (b) 5% SrHA, (c) 10% SrHA, (d) 20% SrHA, (e) 30% SrHA, (f) 20%  $\text{ZrO}_2$ , (g) 5% SrCaHA, (h) 10% SrCaHA, (i) 20% SrCaHA, and (j) 30% SrCaHA. Cements prepared at 0% SrHA/SrCaHA were not completely transparent to X-rays. (k) Comparison of the radiographic contrast values of  $\eta$ -TSBC preparations with increasing concentration of SrHA/SrCaHA microspheres. The data showed a significant linear increase in radiopacity with increasing SrHA/SrCaHA microsphere concentration..... 31
- Figure 3. SEM micrographs and EDX spectra of the SrCaHA cement surfaces before (left panel) and after immersion in SBF at 37°C for 30 days (right panel). From top to bottom: (a) Control (0% wt/vol), (b) 10% wt/vol SrCaHA, (c) 20% wt/vol SrCaHA, and (d) 30% wt/vol SrCaHA. Apatite formation was observed on all the SrCaHA containing cement surfaces after 30 days in SBF along with an increase in the atomic percentage of calcium, phosphorus, and oxygen. (A = apatite layer, C = PMMA cement) ..... 33
- Figure 4. SEM micrographs and EDX spectra of the SrHA cement surfaces before (left panel) and after immersion in SBF at 37°C for 30 days (right panel). From top to bottom: (a) Control (0% wt/vol), (b) 10% wt/vol SrHA, (c) 20% wt/vol SrHA, and (d) 30% wt/vol

SrHA. Apatite formation was observed on all the SrHA containing cement surfaces after 30 days in SBF along with an increase in the atomic percentage of calcium, phosphorus, and oxygen. (A = apatite layer, C = PMMA cement)..... 34

Figure 5. FTIR spectra of apatite layer formed on the surface of 10%, 20%, and 30% wt/vol SrCaHA cements soaked in SBF at 37°C for 30 days. All of the spectra obtained showed the presence of phosphate peaks (Asterisks) confirming the presence of apatite. .... 34

Figure 6. (a) EDX spectra of 0, 10, 20 and 30% SrCaHA samples before and after immersion in SBF for 30 days. (b) EDX spectra of 0, 10, 20 and 30% SrHA samples before and after immersion in SBF for 30 days. Changes in the atomic percentages of C, O, P, Ca, Sr on the 0, 10, 20 and 30% SrCaHA and SrHA sample surfaces (c) before and (d) after immersion in SBF for 30 days. A significant increase in the atomic percentages of O, P, and Ca for all the SrHA and SrCaHA cement compositions was observed after 30 days in SBF. However, no significant changes were observed in the atomic percentages of all the 5 elements for the control samples, before and after immersion in SBF..... 35

Figure 7. (a) SEM micrograph of a 20% SrHA cement surface after being soaked in SBF at 37°C for 30 days, having regions devoid of apatite (C) and regions having apatite (A) formed on its surface. (b) EDX line scan spectra, performed along the line plotted (500 points) on the SEM micrograph region in Figure (a), showing a progressive increase in the intensity of O, P, and Ca levels as one moves from the cement surface onto the apatite layer formed..... 36

Figure 8. SEM micrographs of cross-section of the (a) 10% SrCaHA and (b) 10% SrHA cement samples soaked in SBF for 30 days. (c) EDX spectra across the cross-section of the 10% SrCaHA and 10% SrHA cement surfaces and the (d) Atomic percentage of the elements analyzed by EDX spectra. The EDX spectra of the cross-section surfaces of both the cement compositions clearly showed no presence of any apatite, indicating that apatite was not formed in the bulk of the cement..... 37

Figure 9. SEM micrographs indicating the different thicknesses of the apatite layer formed on surfaces of various cement compositions (a) 20  $\mu\text{m}$  in thickness, (b) 10  $\mu\text{m}$  in thickness, (c) 5  $\mu\text{m}$  in thickness, (d) 3  $\mu\text{m}$  in thickness. (e) Apatite layer thickness measured as a function of the filler concentration. A decrease in apatite thickness was observed for the SrCaHA cements with increasing filler concentration, whereas no particular trend in the apatite thickness was observed for the SrHA cements with increasing filler concentration. .... 38

Figure 10. The changes in the pH of SBF medium containing controls (0% filler), 10% SrHA, 20% SrHA, 10% SrCaHA, and 20% SrCaHA cement samples (n = 3), over a period of 4 weeks. The pH vs. time graph illustrated that pH of the SBF containing control samples remained constant at 7.4, whereas the pH of SBF containing SrHA and SrCaHA cement samples increased significantly over a period of 4 weeks as compared to the control samples, indicating the relative alkaline effect on the pH of the medium due to addition of apatite. .... 39

Figure 11. Compressive properties of two-solution bone cements prepared with increasing concentration of SrHA and SrCaHA microspheres. (a) Compressive strength, (b) Compressive modulus, and (c) Strain to failure. Cements prepared with SrHA and

SrCaHA microspheres have significantly higher compressive strength than  $\eta$ -TSBCs and the compressive strength increased significantly with increasing SrHA/SrCaHA concentration ( $p < 0.05$ ). ..... 58

Figure 12. Flexural properties of  $\eta$ -TSBC, and  $\eta$ -TSBC prepared at 10 and 20% SrHA/SrCaHA and 20% ZrO<sub>2</sub>. (a) Flexural strength, (b) Flexural modulus, and (c) Strain to failure.

The flexural strength reduced significantly with increasing SrHA/SrCaHA concentration ( $p < 0.05$ ). However, no significant differences were observed between strengths of SrHA and SrCaHA cements and between 20% ZrO<sub>2</sub> and SrHA/SrCaHA containing cement compositions. .... 59

Figure 13. SEM micrographs of the fractured surfaces after flexural testing of the following compositions: (a) Controls (b) 20% ZrO<sub>2</sub> (c) 10% SrCaHA (d) 20% SrCaHA (e) 10% SrHA (f) 20% SrHA. .... 60

Figure 14. High magnification SEM micrographs of the fractured surfaces of (a) and (b) 20% SrCaHA cements indicating ductile fracture where regions with higher concentration of nanospheres and depleted matrix was observed. Black arrows indicated the regions having SrHA microspheres embedded in the cement matrix (white region). .... 62

Figure 15. (a) Fracture toughness of  $\eta$ -TSBCs prepared at increasing concentration of SrHA and SrCaHA microspheres. There was no significant effect of addition of SrHA/SrCaHA microspheres on the fracture toughness of  $\eta$ -TSBCs. SEM micrographs of the fractured surfaces depicting the crack propagation in the following cement compositions: (b) Controls (c) 20% ZrO<sub>2</sub> (d) 10% SrCaHA (e) 20% SrCaHA (f) 10% SrHA (g) 20% SrHA. .... 63

- Figure 16. High magnification SEM micrograph of fractured (a) 10% SrCaHA and backscattered SEM micrograph of fractured (b) 20% SrCaHA cement surfaces showing advancement of the main crack via microcracks through the matrix around the SrCaHA beads/agglomerates..... 64
- Figure 18. Long-term antibacterial study. (a) Graph of the *E. coli* biofilm surface coverage (%) as a function of time in culture. The 20% SrHA samples showed continued significant biofilm inhibition up till day 14 as compared to controls. The fluorescence micrographs of *E.coli* biofilm formation on controls, 10% SrHA, and 20% SrHA samples on (b) day 1 (c) day 6 (d) day 10 and (e) day 14 (all at 20X magnification). The least amount of biofilm growth was visible on the 20% SrHA samples on day 14. .... 82
- Figure 19. Antibacterial inhibition zone test. (a) Graph of the size of the inhibition zone (mm) as a function of cement composition. Antimicrobial activity was the greatest in the case of cements that had SrHA/SrCaHA powder on their surface indicating that contact inhibition was the primary mode of bacterial inhibition. Zones of inhibition produced after overnight incubation at 37°C of SrHA and SrCaHA containing cement discs on supplemented LB agar seeded with *E.coli* biofilm, (b) Controls, (c) 10% SrHA, (d) 20% SrHA, (e) 10% SrCaHA, (f) 20% SrCaHA, (g) SrHA powder on 20% SrHA cement surface, and (h) SrCaHA powder on 20% SrCaHA cement surface. .... 83
- Figure 20. SEM micrographs of fractured surfaces of  $\eta$ -TSBCs containing (a) 20% SrCaHA and (c) 20% SrHA microspheres subjected to fracture toughness testing. Backscattered SEM micrographs of the  $\eta$ -TSBCs containing (b) 20% SrCaHA and (d) 20% SrHA

microspheres. The black arrows indicate the crack propagation around the SrHA/SrCaHA microspheres or agglomerates rather than through the microspheres. 91

Figure 21. Fluorescence micrographs of MC3T3 preosteoblast cells cultured on  $\eta$ -TSBCs containing (a) 10% SrHA and (b) 10% SrCaHA microspheres. Red fluorescence = dead cells, green fluorescence = live cells, blue fluorescence = SrHA/SrCaHA microspheres. The white arrows in (a) indicate dead cells on areas devoid of SrHA, while white arrows on (b) indicate live cells on top of the SrCaHA microspheres. 10X magnification..... 93

Figure 22. (a) SrCaHA and (b) SrHA powders compressed into discs for contact angle measurements. As can be seen from the light micrographs, the (c) SrCaHA and (d) SrHA surfaces are very hydrophilic showing contact angles lower than 90°. It was difficult to quantify the contact angle measurements due to absorption of the water droplet by the sample discs. .... 100

**List of Tables**

Table 1. The elemental content analysis results of Ca, Sr, and P from the EDX spectrum of SrHA and SrCaHA samples. Calculated Sr/P, (Ca+Sr)/P, and Sr/(Sr+Ca) ratios of the prepared strontium-substituted hydroxyapatites by EDX (see Figure 2(b) (mean ± SD, n = 3).... 29

Table 2. Nominal ionic concentrations of SBF in comparison to those in human blood plasma (84). ..... 108

Table 3. Order and amount of reagents required for preparing 1000 ml of SBF (84). ..... 109

# Chapter 1

---

## 1 Introduction

Acrylic bone cements have been developed primarily for augmentation and fixation of prostheses and total joint arthroplasties, in order to provide stabilization of the implant and transfer of mechanical loads between the implant and bone. Osteoporosis is well known for deteriorating the structural strength of bone and leading to stresses that exceed the strength of vertebrae, resulting in osteoporosis-induced vertebral compression fractures (5). Lately, bone cements have found applications in spinal applications for treating vertebral compression fractures. Galibert and Deramond (6) first conceived the technique of percutaneous vertebroplasty (VP) with polymethylmethacrylate (PMMA), as a reinforcement procedure for treatment of vertebral compression fractures. The vertebroplasty procedure involves direct injection of PMMA bone cement and a contrast agent, typically barium sulfate, into fractured vertebral bodies using fluoroscopic guidance (7). This procedure was designed to alleviate pain and stabilize fractured vertebral bodies in patients suffering primarily from osteoporotic compression fractures and metastatic bone diseases (8). Kyphoplasty (KP), another procedure to treat vertebral compression fractures, was developed in the 1990's (9)(10). The kyphoplasty procedure involves introduction of an inflatable bone tamp into the compressed vertebral body in order to create a cavity in the centrum of the vertebrae, with the intent to expand and restore the vertebral body to its original height (10). The cavity created by this action is then filled with PMMA bone cement to stabilize the vertebral body and restore the normal load transmission patterns

from vertebrae to vertebrae (10). The desired properties of PMMA bone cement for VP/KP procedures differ in comparison to the properties of PMMA cements used in total joint arthroplasties, and are as follows: easy handling and injectability into the collapsed vertebral body, high radiopacity, lower viscosity (not too low), longer setting times (~ 15 mins), lower curing temperature, requisite mechanical properties (comparable to those of healthy vertebral body), low cost, slower resorption rates, biocompatibility, and excellent bioactivity (5, 7, 8).

Although PMMA is the most commonly used material for vertebral augmentation procedures presently, there are certain concerns associated with its use in VP/KP applications. PMMA exothermic reaction can cause thermal necrosis and burns to the surrounding tissue (11). Suppression of cell growth, DNA synthesis and glucose metabolism resulting in cytotoxicity has also been observed due to release of toxic monomer and PMMA debris (11). PMMA is non-resorbable and has no biologic potential to remodel or integrate with the surrounding bone tissue. The lack of bioactivity and osteoconductivity of PMMA results in the loss of bonding between cement and bone (7). The differences in the mechanical properties of PMMA filled vertebrae and the adjacent vertebral body leads to adjacent vertebral fractures (5). Hence, significant interest by the orthopedic surgeons has been expressed for developing bone cements capable of promoting bone regeneration or integrating into the surrounding bone and having mechanical properties similar to cancellous bone.

Biomaterial-associated infections are also not uncommon in orthopedic surgery. PMMA like any other biomaterial is susceptible to infections caused by bacteria and microorganisms (12). Over the past few decades, antibiotics have been incorporated in

PMMA bone cements in order to prevent and cure orthopedic implant infections (13).

PMMA comes in direct contact with bone, physiological fluids, and blood which results in the formation of a conditioning film by plasma proteins (12). This conditioning film can then allow microorganisms to adhere and form biofilms on the biomaterial surface.

Antibiotic-loaded bone cements essentially consist of PMMA matrix, radiopacifiers, and an antibiotic such as gentamicin (14), tobramycin (15), or erythromycin (16). Ethell et al. (17) incorporated ceftiofur, liquid and powder gentamicin, and amikacin antibiotics into PMMA and hydroxyapatite (HA) cement and studied their elution characteristics. They found that HA cement had greater elution of antibiotics than PMMA and the gentamicin- and amikacin-loaded HA cement released bactericidal concentrations of antibiotic for at least 30 days. It has been believed that the antibiotic release from the bone cements is mainly a surface phenomenon as the bulk of PMMA is essentially impermeable. In vitro studies by Van de Belt et al. (18) also confirm that only a minor portion (5-8 %) of the gentamicin incorporated in bone cements is eluted. However, there have also been theories favoring a bulk diffusion model for antibiotic release rather than an exclusive surface release mechanism. Recently, Van de Belt et al. (19) suggested that the initial release when the antibiotic-loaded cement is exposed to a fluid is mainly a surface phenomenon, whereas sustained release over several days is a bulk diffusion phenomenon. Moreover, antibiotic cements have an optimum surface for bacterial colonization and prolonged exposure to antibiotics can allow for bacterial resistance to be developed (20, 21). Van de Belt et al. (19) reported that *Staphylococcus Aureus* (S. Aureus) biofilm formation was reduced on gentamicin loaded cements as compared to unloaded cements, but only for a short duration during the initial burst release of the antibiotic after which the bacterial strain developed

resistance against gentamicin. Also, when antibiotics are added to PMMA before mixing as a prophylactic measure, they can affect the mechanical properties of the cured PMMA (13). It has been shown in literature that adding different antibiotics to PMMA in quantities less than 2 g per standard polymer packet does not adversely affect the mechanical properties, although concentrations exceeding 2 g does weaken them (22, 23). Therefore there is an urge for developing alternate filler materials that can impart antibacterial properties to bone cements. Preliminary work by Guida et al. (4) has shown that incorporation of strontium and fluoride into glass ionomer cements improved antibacterial properties of the cement, with the bactericidal action of strontium being more significant than fluoride. However, the mechanistic action of  $\text{Sr}^{2+}$  on bacteria is less well understood than that of silver (Ag) (24). Little is currently known with respect to bacterial resistance to strontium, due to limited number of published studies on the *in vitro* or *in vivo* antibacterial applications of the ion. To this effect, the focus of our work was to develop a bioactive and antibacterial two-solution bone cement based on strontium-containing hydroxyapatite (SrHA) that could be used primarily for VP/KP as well as other applications.

Acrylic polymethylmethacrylate (PMMA) bone cement is currently the only material used for augmentation and anchoring of total joint arthroplasties (25, 26). Most commercial bone cements are available in powder-liquid formulations. The powder consists of PMMA polymer, radiopacifier and initiator such as benzoyl peroxide, whereas the liquid component consists of monomer methylmethacrylate (MMA) and an activator (e.g. *N,N*-dimethyl *p*-toluidine (DMPT)) (25). The surgeon mixes the powder and liquid components to initiate the polymerization of the cement and when the powder-liquid mixture reaches a dough-like consistency, the surgeon applies the cement at the surgical site for implant fixation. Even

though the mechanical and physical properties of acrylic cements are widely studied and well understood in literature, there are a number of drawbacks associated with these cements such as high exothermic temperature, chemical necrosis due to residual monomer, stiffness mismatch between cement and bone, aseptic loosening due to lack of integration with surrounding bone, and lack of bioactivity, as discussed previously (25, 27). Therefore, there is a vast interest in the development of new cement formulations to overcome a number of drawbacks associated with the application of this material *in vivo*. The standard two-solution bone cement (STSBC) developed in our laboratory has emerged as an experimental alternative to the commercial powder-liquid formulations (28, 29) where the powder and liquid components are pre-mixed in a two compartment polypropylene cartridge with one side containing the initiator and the other side containing the activator. Thus, when the two sides of the cartridges are mixed using a static mixing nozzle, the cement extruded is already in the dough stage exhibiting a combination of clinical advantages that include ease of mixing and delivery, reduced porosity, and better control of setting characteristics that can be optimized by variations in the initiation chemistry of the cement (28). Nevertheless, a few pitfalls associated with the STSBC, such as high initial viscosity and lower polymer concentration calls for a further investigation of approaches to improve and optimize the material for extended applications such as vertebroplasty (VP) and kyphoplasty (KP).

Therefore, the STSBCs have been modified with cross-linked PMMA nanospheres ( $\eta$ -TSBC) to reduce viscosity, increase polymer concentration and lower the exotherm temperature (30, 31). However, these cements still lack the capacity to integrate with the adjacent bone tissue. To that effect, the first goal of this study was to develop  $\eta$ -TSBCs with improved bioactivity for injection into fractured vertebral bodies. Strontium-substituted

hydroxyapatite (SrHA) microspheres were fabricated and added to the cement mixture in order to achieve a balance between the need of ideal viscosity, adequate mechanical and radiographic properties, while simultaneously increasing bioactivity and antibiotic properties. The second aim of this study was to evaluate the effect of the inclusion of the bioactive filler material on the mechanical properties of the cement. Finally, the third goal was to investigate whether addition of SrHA microspheres allowed for improvement in the antibiotic properties of  $\eta$ -TSBC, since strontium is known to impart antibiotic properties (32). The original idea of this work was conceived as a way of achieving improved bioactivity, radiopacity, and antibiotic properties with addition of only a single filler material with the ultimate goal of optimizing the physical and mechanical properties of this formulation for applications such as cemented arthroplasties as well as VP and KP. The bioactive properties are expected to improve the integration of the cement with the surrounding bone tissue via formation of chemical bonds with the hydroxyapatite (HA) present naturally in the bone.

The dissertation is organized along the following lines. It begins with an overall background of the current technologies in the field of bone cements, followed by goals and hypotheses of the work, then followed by three separate chapters written in manuscript form describing major topics studied. The final sections are devoted to summarize the work and also present a discussion of areas of future research that could be aimed at improving some of the pitfalls of the present study.

## Chapter 2

---

### 2 Background and significance

Compressive vertebral fractures caused by trauma are very common in patients with osteoporosis. Percutaneous VP and KP are new techniques developed to stabilize vertebral bodies post compression fractures caused by osteoporosis and other lesions (33, 34). Because both these procedures involve percutaneous injection of bone cement into the fractured vertebrae under real-time fluoroscopy, the most desirable properties of bone cements for use in VP and KP are very high radiopacity, easy injectibility, low setting temperature, bioactivity to allow for osseointegration thus enhancing bone strength, and mechanical properties resembling those of non-osteoporotic vertebrae (5, 7, 27). Since most commercial formulations of bone cement do not meet the viscosity criteria for use in the spine, surgeons usually alter the polymer-to-monomer ratio recommended by manufacturers by diluting the cement with higher monomer concentrations in order to decrease viscosity and increase the handling and injection times (35). Radiopaque substances like barium sulfate ( $\text{BaSO}_4$ ) and zirconium dioxide ( $\text{ZrO}_2$ ) have been added to bone cements in concentrations ranging from 5 to 30 wt % in order to facilitate visualization under fluoroscopy (36). Some studies have reported deleterious effects of  $\text{BaSO}_4$  in the mechanical performance of the bone cements due to clumping and poor adhesion with the cement matrix (36), as well as an increase in the *in vivo* cytotoxicity caused by  $\text{BaSO}_4$  particles released during wear (35).

Two-solution bone cement is a viable alternative to current powder-liquid formulations, having several advantages in comparison to commercial cements (28, 29, 37). A major limitation to the use of STSBC in applications requiring injection through small needles or cannulas is the higher initial viscosity of the material (28). Since the concentration of monomer is already higher in STSBC (polymer-to-monomer (P:M) ratio 0.9:1) compared to powder-liquid cements, a further reduction in the P:M ratio to make this material more suitable for VP/KP applications could lead to even higher exothermal temperatures and concentrations of residual monomer, which might have a direct impact on the mechanical properties of the material and increase *in vivo* cytotoxicity. Nevertheless, STSBC can find suitable application in VP/KP given its viscosity can be tuned by incorporation of cross-linked PMMA microspheres and nanospheres in the polymer phase (31).

## **2.1 Two-solution bone cements containing PMMA nanospheres ( $\eta$ -TSBC)**

It has been observed that the viscosity of STSBC can be manipulated by subtle changes in the P:M ratio and by addition of cross-linked PMMA microspheres (20 -100  $\mu\text{m}$  in diameter) and nanospheres (300-330 nm in diameter) in the polymer phase (30, 31). The STSBC contains dissolved linear PMMA chains as compared to the modified  $\eta$ -TSBC, in which a cross-linked dispersed particle phase is added to the linear PMMA, and this cross-linked phase does not dissolve but undergoes swelling in the monomer, thereby controlling the cement viscosity (31).  $\eta$ -TSBCs exhibit a high degree of pseudoplasticity, which is expected to facilitate injection of cements in VP/KP applications reducing the risk of cement extravasation by viscosity recovery at the delivery site (31). Additionally, it is observed that inclusion of the PMMA nanospheres in the cement lowers polymerization

temperatures and increases setting times (12-20 mins) in comparison to the STSBC (~ 7 mins) while maintaining the flexural strength (30, 31). With the inclusion of the cross-linked phase a higher P:M ratio is also successfully achieved in comparison to STSBC. Furthermore, the mechanical properties of  $\eta$ -TSBCs are comparable or superior to the properties measured for the STSBC and it is feasible to prepare these cement formulations at higher radiopacifier concentration up to 20% wt/vol of  $ZrO_2$  without affecting the mechanical properties significantly (30).  $\eta$ -TSBCs exhibit several advantages over the STSBC formulation for VP/KP applications, however, it still lacks in its ability to integrate with the adjacent bone tissue to form a stronger bone and cement interface, and also in its bactericidal characteristics. The  $\eta$ -TSBCs lack bioactivity and the ability to form apatite on its surface.

## **2.2 Modification of $\eta$ -TSBC to improve bioactivity**

A solution to the above mentioned problem is to develop bioactive cement particularly designed to produce a better interface between the cement and bone. Also, a bioactive filler that is able to provide adequate radiopacity, bioactivity, and bactericidal properties all at once, should be considered for incorporation into the  $\eta$ -TSBC. According to a review by Harper et al. (38), there are two ways to go about development of bioactive cements; firstly to improve the existing PMMA cement by addition of different bioactive filler particles, e.g. HA added to PMMA cement (39), and secondly, develop an all-bioactive cement, e.g. calcium phosphate cements (CPC). CPC is self-setting, capable of degradation, biocompatible, and has good bone conductivity, all of which are properties that make it advantageous over PMMA (11). Bone Source, an injectable CPC

cement developed by Stryker Orthopedics, was designed primarily to repair cranial defects. Turner et al. (40) tested both PMMA and Bone Source cement in a canine vertebral body defect and observed that both materials were well integrated histologically. They also observed that CPC underwent resorption and remodeling and demonstrated excellent biocompatibility and osteoconductivity in comparison to PMMA cement. However, a major drawback with CPC is its rapid resorption rate which does not provide enough time for the bone tissue to grow into the vertebral body defect (5). While treating an osteoporotic vertebral fracture by cement augmentation, if the cement resorption is faster than the new bone formation then it will have a contrary effect, as the induced resorption will weaken the vertebral body further promoting its collapse (8).

Calcium sulfate cements, mainly known as plaster of Paris, have been used as a bone graft substitute in various sites (7) due to its injectibility and osteoconductivity. Turner et al. (41) have studied calcium sulfate bone graft substitute in a canine medullary defect model and reported progressive resorption of the bolus of calcium sulfate within the defect over a period of 13 weeks. Their histological evaluation at 13 weeks demonstrated prominent osteoblastic rimming of the newly woven bone for all of the medullary defects treated with calcium sulfate. However, these cements also have drawbacks such as rapid resorption rates, low viscosity and difficult handling characteristics (7). Due to its rapid resorption (42, 43), these cements are not expected to support spinal alignment while it is undergoing remodeling, hence they would not be appropriate for use in vertebral augmentation procedures. Another drawback associated with these CPC and calcium sulfate cements is that they exhibit thixotropic properties due to which when pressurized in a confined space such as a delivery tube, they dewater

from the suspension leaving a chalk that cannot advance through the delivery tube or percolate through the bone interstices (8). The all-bioactive cements also are known to have poor mechanical properties due to their faster resorption rates (5).

Since most commercial cements in current use are PMMA based, PMMA has been largely investigated as the matrix material for bioactive cements. A variety of filler particles have been incorporated into PMMA cements to improve bioactivity. Bone particles (44) and growth hormones (45) have been used to impart bioactivity in PMMA, however, glass ceramics (46) and HA (47, 48) are more promising and most studied fillers. Shinzato et al. (49) developed PMMA cements with bioactive glass beads at concentrations varying from 40 to 70 wt % and introduced the cements into the intramedullary canals of rat tibiae to evaluate osteoconductivity over a period of 39 weeks. Their histological analysis revealed new bone formation along the cement surfaces within 4 weeks, even at 40 wt% glass bead concentrations. Furthermore, in another study Shinzato et al. (46) also compared addition of glass beads, apatite and wollastonite containing glass ceramic (AW-GC) powder, and sintered HA powder into PMMA cements at concentrations of each filler amounting to 70 wt%. The cements were applied to the intramedullar canals of rat tibiae and osteoconductivity was determined at 2, 4, and 8 weeks post operation. At each time interval studied, Shinzato et al. (46) reported a higher osteoconductivity for the glass bead cements in comparison to AW-GC and HA cements. PMMA and alpha tricalciumphosphate ( $\alpha$ -TCP) bioactive composite cement was investigated *in vitro* and *in vivo* by Fini et al. (50), using MG-63 human osteoblast cultures and PMMA+ $\alpha$ -TCP implants in rabbit femoral trabecular bone, respectively. They observed new bone formation inside the PMMA+ $\alpha$ -TCP porosity

indicating that the implants osseointegrated successfully in the trabecular tissue *in vivo*, while a positive effect on osteoblast cultures was demonstrated *in vitro* by increased levels of osteocalcin and pro-collagen. However, the differences in the newly formed bone and the pre-existing normal tissue confirmed that the bone mineralization around the bioactive composite material was a slow process.

Kobayashi et al. (51) studied the effect of introduction of three bioactive fillers namely, apatite-wollastonite (AWC), tricalcium phosphate (TCP) and HA, on the cement mechanical and biological properties. They concluded that AWC had superior biological and mechanical properties in comparison to the other two fillers due to early and uniform apatite formation on the cement surface (51). HA has been used widely as a bioactive filler as it is the inorganic component of the bone tissue *in vivo* (39, 52, 53). However, pure HA containing cements have been known to exhibit poor mechanical characteristics (54). Sogal and Hulbert (55) and Dove and Hulbert (56) investigated mechanical properties of HA reinforced PMMA cements. They studied the influence of HA powder with varying particle sizes on the static and dynamic mechanical properties. The static tests revealed that with an average particle size of 96  $\mu\text{m}$  HA particles could only be added up to 10% wt concentration without decreasing the tensile strength. A higher concentration of 20 % wt HA resulted in a decrease in strength with all sizes of HA. Besides imparting bioactivity characteristics to the cements, HA filler has two main drawbacks: i) in most cases, the amount of filler that can be incorporated without deleterious effects on the mechanical or handling properties is so small that the improvement in bioactivity is not likely to be very large; (ii) the glass or ceramic fillers tend to make PMMA even more brittle (38).

Atomic substitutions have also been made in HA structure using magnesium, zinc, strontium, or silver cations in order to improve the biological response of HA (57). However, strontium substitution has been the most effective in promoting osteoblast differentiation along with blocking osteoclastic bone resorption (58). Strontium uptake and retention in the skeleton is also similar to calcium, and it can be cleared by urinary and fecal excretions (58). Strontium ranelate is being developed as an antiresorptive drug for treating osteoporosis since strontium promotes osteoblast differentiation and is easily incorporated into bone via surface exchange or ionic substitution with calcium (59, 60). Li et al. (54) developed bispheno-A-glycidyl methacrylate (Bis-GMA) bioactive cements exploring a different matrix material in comparison to PMMA. They incorporated strontium-substituted hydroxyapatite (SrHA) nano powder into Bis-GMA matrix, and concluded that combination of strontium-HA was more beneficial than pure HA, as it served as a radiopacifier and provided improved mechanical and bioactive properties. However, the Bis-GMA dental resins were reported to have an uncured surface due to inhibition of polymerization reaction by oxygen resulting in the incompletely polymerized oligomers to leach from the cement surface (61, 62). Lin et al. (1) observed an increase in antibacterial properties with increase in strontium substitution in HA nano particles compared to pure HA nano particles. They carried out static (inhibition zone test) and dynamic (shake flask method) antibacterial tests for HA, SrHA (totally substituted) and SrCaHA (partially substituted) nanoparticles against *Escherichia coli*, *Staphylococcus aureus*, and *Lactobacillus* strains. They observed that SrHA particles exhibited antibacterial ability while statically or dynamically contacting the test bacteria, whereas HA and SrCaHA nanoparticles had antibacterial ability only when they

dynamically contacted the test bacteria. However they observed both SrHA and SrCaHA nanoparticles to have higher antibacterial ratio than HA, and amongst them, SrCaHA had the best antibacterial ratio indicating antibacterial properties improved after substitution of calcium ions with strontium in HA nanoparticles.  $\eta$ -TSBCs formulated in our laboratory for VP/KP applications also lack bioactivity and have PMMA as the primary matrix material. Thus, in this study we explored the feasibility of modifying the  $\eta$ -TSBCs by introducing SrHA microspheres to impart bioactivity, radiopacity and antibacterial properties, all at once.

### **2.3 Applications of bioactive $\eta$ -TSBCs**

Compressive vertebral fractures caused by trauma are very common in patients with osteoporosis. Although VP and KP offer potential benefits, the choice of filler material will depend on the eventual development of the cement with good biomechanical and biological properties along with good radiopacity and cost-effectiveness.  $\eta$ -TSBC has been shown to be a suitable alternative for VP/KP applications due to its better injectibility, radiopacity and mechanical properties (30, 31). With the introduction of bioactive filler such as SrHA,  $\eta$ -TSBC is expected to improve in its biological response, which would make it suitable for applications in cemented arthroplasties along with VP and KP. This additional filler will not only impart bioactivity, but also impart radiopacity and antibacterial properties to the PMMA matrix based cement. This would be expected to be cost effective as no other additive or filler would be required in the polymer phase to achieve all of the aforementioned properties. We also envision the use of this injectable, antibiotic, and bioactive cement as an adhesive for acute treatment of fractures and injuries

caused on the battlefields where an immediate stability and relief along with appropriate infection control is required. The bioactive  $\eta$ -TSBC may also find suitable applications as filler or scaffold materials in critical size defects in craniofacial and maxillofacial surgeries (63, 64). Some studies have reported deleterious effects of bioactive fillers in the mechanical performance of bone cements (5, 36, 53). Since it is desired to incorporate the highest amount possible of SrHA microspheres to obtain higher bioactivity and bone growth promotion, it is also important to predict the effect of increasing filler concentration on the various properties of  $\eta$ -TSBCs. The following chapters provide a detailed investigation of the bioactive and antibacterial properties of  $\eta$ -TSBCs containing SrHA microspheres, along with evaluation of the effect of SrHA incorporation on their static mechanical properties.

## Chapter 3

---

### 3 Goals and hypotheses

#### 3.1 First goal: Fabricate two-solution bone cements containing strontium-substituted hydroxyapatite (SrHA) microspheres and characterize their bioactive properties

The first goal of this work focused on synthesis of SrHA microspheres for addition into the  $\eta$ -TSBC formulation. A simple hydrothermal synthetic route was sought for the production of SrCaHA/SrHA (partial and total strontium substitution of calcium) microspheres. The bioactive performance (apatite forming ability) of the SrHA containing cements was evaluated *in vitro* in a simulated body fluid (SBF) over a period of one month. The effect of increasing microsphere concentration and the type of SrHA microspheres (degree of strontium substitution in HA) on bioactivity was investigated and compared to  $\eta$ -TSBC formulation without any filler.

#### *Hypotheses:*

- The addition of SrHA/SrCaHA microspheres in the  $\eta$ -TSBC formulation will allow for preparation of cements with improved bioactivity via increased apatite forming ability on the cement surface when soaked in SBF, in comparison to the control  $\eta$ -TSBCs.
- It is also hypothesized that with higher concentration of SrHA/SrCaHA in the cement and lower percentage of strontium substitution in the microspheres there will be an increase in apatite formation.

- **Expected outcome:** Increased apatite formation due to faster dissolution and release of calcium ions from the SrHA/SrCaHA microspheres exposed at the cement surface that would then help in forming apatite nuclei which can grow spontaneously by consuming calcium and phosphate ions from the surrounding simulated body fluid.

### **3.2 Second goal: Evaluate the effect of composition (degree of strontium substitution) and concentration of SrHA microspheres on the flexural, compressive, and fracture toughness properties of $\eta$ -TSBCs**

The second goal of this work focused on evaluating the effect of addition of SrHA/SrCaHA microspheres on the static mechanical properties of  $\eta$ -TSBCs. The concentration as well as the type of SrHA filler was varied. The compressive, flexural, and fracture toughness properties were evaluated. These cements are expected to exhibit adequate mechanical properties for use in VP/KP applications.

#### ***Hypotheses:***

- The incorporation of SrHA/SrCaHA microspheres at increasing concentration will decrease the flexural and fracture toughness properties of  $\eta$ -TSBC
- **Expected outcome:** An increase in the microsphere concentration may cause non-homogeneous distribution and aggregation of these particles in the cement resulting in poor adhesion to the cement matrix and weakening of the cement. Introduction of

these microspheres is expected to increase brittleness in the  $\eta$ -TSBC formulation due to weaker ductility of the bioactive filler.

- The compressive properties of the SrHA/SrCaHA cements will increase with increasing filler concentration due to increasing ceramic-like properties imparted by SrHA/SrCaHA microspheres.
- **Expected outcome:** Increase in the concentration of microspheres may increase aggregation in the  $\eta$ -TSBC formulation creating internal flaws from which cracks can propagate in tension, but not in compression as these particles can behave as load carriers.
- The type of microspheres, SrHA/SrCaHA, is not expected to have a significant effect on the mechanical properties as they are structurally (morphology and size) similar and differ only in the amount of strontium substitution.

### **3.3 Third goal: Investigate the antibiotic properties of the $\eta$ -TSBC containing bioactive strontium-substituted hydroxyapatite microspheres and determine the mechanism behind bacterial inhibition**

The third goal of this work focused on testing the antibiotic properties of  $\eta$ -TSBC with incorporation of SrHA/SrCaHA microspheres at different concentrations. The short-term and long-term antibiotic properties were evaluated *in vitro* by culturing *E.coli* biofilm on cement surfaces for 24 hours and 14 days, respectively. The two proposed mechanisms for bacterial inhibition were: 1) contact inhibition, direct contact of bacteria with the SrHA/SrCaHA microspheres present on the cement surfaces, or by 2) surface dissolution

of strontium ions from the SrHA/SrCaHA microspheres. In order to determine the mechanism of biofilm growth inhibition, agar gel inhibition zone assays were performed.

***Hypotheses:***

- The capacity to inhibit bacterial growth would increase with increasing concentration and percentage of strontium substitution in SrHA/SrCaHA microspheres added to  $\eta$ -TSBCs, as increase in the amount of strontium which is a natural antibiotic, would result in improved antibiotic properties.
- **Expected outcome:** The primary mechanism for bacterial inhibition is expected to be via contact inhibition, as the SrHA/SrCaHA microspheres are expected to be embedded firmly into the cement matrix not allowing for dissolution of enough strontium ions into the surrounding fluid to cause bacterial inhibition. The cement surface however, could be expected to have some exposed SrHA/SrCaHA particles which could cause biofilm inhibition upon direct contact with bacteria.

## Chapter 4

---

### 4 Injectible, bioactive two-solution bone cements with strontium-substituted hydroxyapatite (SrHA) microspheres

Injectable, radiopaque two-solution bone cements ( $\eta$ -TSBC) have been formulated with improved bioactivity. The bioactive components were partially (50%) and totally (100%) substituted strontium-hydroxyapatite microspheres (SrCaHA and SrHA, respectively), which were introduced in the cements at concentrations of 10%, 20%, and 30% wt/vol. The *in vitro* bioactivity of the cements was tested by introducing cement samples directly in a simulated body fluid (SBF) solution maintained at 37°C (pH of 7.4) for 30 days to mimic *in vivo* conditions. Precipitation of an apatite-like layer was observed for all the cement formulations containing SrHA and SrCaHA microspheres. The deposited apatite layer was characterized for morphology using scanning electron microscopy (SEM), and for composition, using Fourier transform infra-red spectroscopy (FTIR) and energy dispersive x-ray (EDX) analysis. Radiopacity of the cements was observed to increase linearly with increasing SrHA/SrCaHA filler concentration. A significant increase was observed in the atomic percentages of calcium, oxygen, and phosphorus on all of the SrHA/SrCaHA cement surfaces after 30 days in SBF indicating the presence of apatite. However, no significant differences were observed in the bioactivity between all formulations of SrHA and SrCaHA cements. This study showed that the apatite formation ability of SrHA and SrCaHA cements was effective in improving the bioactivity of current polymethylmethacrylate (PMMA) containing  $\eta$ -TSBCs.

## 4.1 Introduction

Polymethylmethacrylate (PMMA) was and still is the gold standard for fixation of total hip prosthesis, percutaneous vertebroplasty (VP), and kyphoplasty (KP) (5, 7, 37, 38, 57). However, PMMA is bioinert, biologically non-degradable, and hydrophobic, which hinders the formation of biological apatite, a major inorganic component of natural bone, on the surface of this polymer (5, 8, 11, 65, 66). Due to this lack in bioactivity of acrylic cements, bioactive bone cements have been developed to overcome the problems of conventional PMMA (38, 39, 51, 52, 67-69). Unlike PMMA cements, the bioactive cements can integrate with the living tissue via the apatite layer formed on the cement surface owing to rapid formation of chemical bonds with the hydroxyl groups of HA in the surrounding bone tissue. In an attempt to balance the mechanical and biological characteristics, since PMMA naturally does not allow formation of apatite on its surface, a variety of bioactive fillers based on calcium phosphates, hydroxyapatite powders or bioactive glass-ceramics have been used in combination with PMMA to form acrylic-ceramic formulations (4, 11, 51, 52, 65, 69-72).

Calcium phosphates are known to have excellent biocompatibility and osteoconductivity; however, they have weaker mechanical strengths compared to PMMA cements, to be considered for the use of load bearing applications (8, 57). Recently, a number of alternatives to the basic MMA/PMMA system have been explored including bioactive filler and bisphenol A diglycidylether dimethacrylate (Bis-GMA) systems that have improved bioactivity (53, 66, 73). Comparing cements based on Bis-GMA and PMMA, it has been reported that for the PMMA cements the bioactive filler remained embedded in the cement matrix leading to failure of formation of apatite layer. However,

Bis-GMA cements tend to have uncured surfaces due to inhibition of polymerization reaction by oxygen resulting in the incompletely polymerized oligomers to leach from the cement surface that has a cytotoxic effect (61, 62). Also, a more recent study by Hernandez et al. (74) has demonstrated *in vitro* and *in vivo* bioactivity of PMMA cements charged with bioactive components such as SrHA nano powder (10% Sr substitution). They explain that when the cement is implanted at the dough stage in the body or directly in simulated body fluid (SBF), the PMMA cement is not completely polymerized and a partial dissolution of the cement surface can leave the bioactive particles exposed to the medium, leading to their bioactive response. It is thus clear that PMMA based cements can offer alternative bioactive solutions to VP and KP techniques.

Lately Li et al. (66) and Ni et al. (75) have reported Bis-GMA cement formulations composed of strontium-containing hydroxyapatite (SrHA) nanopowder that demonstrated good radiopacity and suitable *in vivo* bioactivity. Hydroxyapatite (HA), as a natural component of bone mineral, has been used as a graft material for bone repair, augmentation, and substitution for decades (8, 38). However, its biological performance itself requires improvement as it has limited intrinsic osteoconductive properties (76) and as mentioned earlier they provide weaker mechanical strengths in load bearing applications. Many studies (76-78) however, have looked into ionic-substitutions of HA with strontium (SrHA) which results in the distortion of its structure and a significant increase in the solubility of HA with a constant release of strontium and calcium ions leading to eventual precipitation of apatite in the surrounding fluid, thus improving the biological response of HA. Strontium is also a trace element found in human body having the ability to not only increase osteoblast-related gene expression and alkaline phosphatase

(ALP) activity of mesenchymal stem cells, but also inhibit osteoclast differentiation (2, 58, 59, 79, 80). Strontium has chemical similarity to calcium, thus it allows for radiographic visualization without the need for additional radio contrast material and can be readily substituted for calcium in bone *in vivo* (59). Strontium is also known to impart antibacterial properties (1, 4). SrHA has also been reported to have stronger mechanical properties and better bioactivity than pure HA (66, 76). *In vivo* studies by Ni et al. (73, 75) and Cheung et al. (70) on cements containing SrHA nanopowder (10% Sr) showed that SrHA cement could bond directly to the adjacent bony tissue which facilitated new bone formation along the cement surface indicating good bioactivity and osteoconductivity.

Our group has developed modified two-solution bone cements containing cross-linked PMMA nanospheres ( $\eta$ -TSBC) for applications of VP and KP (81, 82). In this study, we have developed bioactive bone cement by incorporating SrHA with the aim of improving the bioactivity of  $\eta$ -TSBC for VP and KP applications. We have synthesized SrCaHA and SrHA microspheres by hydrothermal synthesis with the Sr substitution degree, respectively, at 50% and 100%. In this chapter, we report the study of the *in vitro* bioactivity of  $\eta$ -TSBCs containing SrHA/SrCaHA microspheres in the presence of simulated body fluid (SBF) and test their ability to form apatite on their surfaces.

## **4.2 Materials and Methods**

### **4.2.1 Preparation and characterization of SrHA/SrCaHA microspheres**

The SrHA and SrCaHA microspheres (2-5  $\mu\text{m}$  in diameter) were synthesized as described by Zhang et al. (2, 83) and the atomic ratios of Sr/P and (Ca+Sr)/P were set as

1.67. To this end, a solution of 3 mmol of strontium nitrate [ $\text{Sr}(\text{NO}_3)_2$ ] and 0.3 g of surfactant hexadecyl-trimethylammonium bromide (CTAB) in 40 ml of deionized water was prepared along with a second solution composed of 6 mmol trisodium citrate ( $\text{Cit}^{3-}$ ) and 2 mmol of ammonium dihydrogen phosphate [ $\text{NH}_4\text{H}_2\text{HPO}_4$ ] in 25 ml of deionized water. After vigorously stirring the individual solutions for 30 minutes the two solutions were mixed and allowed to stir for another 20 minutes. The as-obtained mixing solution was then transferred to a Teflon bottle held in stainless steel pressure vessel (Parr Instruments), sealed and maintained at  $180^\circ\text{C}$  for 24 hours. The SrCaHA microspheres were prepared using the same hydrothermal procedure, however in this case the first solution contained a total of 3 mmol of calcium nitrate [ $\text{Ca}(\text{NO}_3)_2$ ] and [ $\text{Sr}(\text{NO}_3)_2$ ] with a [ $\text{Sr}/(\text{Sr} + \text{Ca})$ ] molar ratio of 0.5 in the reaction mixture. The chemical compositions of the powders were investigated using Fourier transform infrared microscopy (FTIR). The morphology and elemental composition of the samples were inspected using a scanning electron microscopy (SEM) equipped with an energy dispersive X-ray system (EDX, JEOL 5600). The atomic percentages of C, O, P, Sr, and Ca were obtained using the exCalibur software of the EDX set up. The software performs a semi-quantitative analysis by applying a ZAF correction (atomic number, absorptivity and fluorescence correction) after detection and calculation of net intensities of x-rays from the x-ray detector. Net intensities are collected and a Gaussian peak deconvolution is performed to get initial estimates of the concentrations of each element. In order to compute the net intensities, the software calculates the net region of interest (ROI) integrals and then applies the ZAF corrections in order to correct the intensities for overlaps and peaks fractions.

#### 4.2.2 Bone cement preparation

The two-solution bone cements containing cross-linked polymethylmethacrylate nanospheres ( $\eta$ -TSBC), used as controls, were prepared as described by Rodrigues and co-workers (81, 82) at a polymer to monomer ratio of 1:1 and cross-linked PMMA nanospheres to linear PMMA ratio of 1.5:1. For the preparation of  $\eta$ -TSBCs, benzoyl peroxide (BPO) (Aldrich), *N, N*-dimethyl *p*-toluidine (DMPT) (Aldrich) and methylmethacrylate (MMA) (Fluka) were used as received without further purification.  $\eta$ -TSBCs had two polymer phases: 1) dissolved linear PMMA ( $P_1$ ), and 2) dispersed cross-linked PMMA nanospheres ( $P_b$ ). These two components were massed and mixed together forming the powder phase (P). The total volume of MMA was split and added to two graduated cylinders, in which one was mixed with 1.25 g of BPO (1.25 g/100 ml of MMA) and other with 0.7 ml DMPT (0.7 ml/100 ml of MMA). The two mixtures BPO/MMA and DMPT/MMA were transferred to two polypropylene cartridges followed by the addition of the powder phase and remaining MMA. The cartridges were sealed, vigorously agitated by hand, and placed on a rotating drum mixer for 18 h. Following mixing, the cartridges were stored upright at 4°C for 48 hours before use. In order to prepare the  $\eta$ -TSBCs containing strontium substituted microspheres, the SrHA and SrCaHA microspheres were added to the polymer phase at concentrations of 10, 20, and 30% wt/vol of MMA and the mixing procedure remained the same as described above for the  $\eta$ -TSBCs. The cements were then injected into square molds (0.5 inch in length and 1mm in thickness) and allowed to polymerize to create samples for the bioactivity tests.

#### 4.2.3 Optical density measurements

Optical density measurements were obtained from digital X-ray images taken in air at an X-ray tube voltage of 41 kV (82). Three cylindrical (6 mm in diameter and 12 mm height) cement specimens each of the fixed composition of  $\eta$ -TSBC containing 0 (controls), 5, 10, 20, and 30% wt/vol SrHA and SrCaHA microspheres were imaged under the X-ray and their degree of contrast was compared with that of  $\eta$ -TSBC containing 20% wt/vol zirconium dioxide ( $ZrO_2$ ). The radiopacity of SrHA/SrCaHA cements were compared to the 20%  $ZrO_2$  composition, as this cement had contrast value similar to the commercially available Kyphx cement containing 30% wt barium sulphate (82). Radiopacity is determined by looking at the contrast of the X-ray images. Contrast is determined using the following equation defined by Kjellson et al. (84)(83)(83);

$$\text{Contrast} = (I_{\max} - I_{\min}) / I_{\max}$$

where  $I_{\max}$  represents transmittance through the background (brightness) and  $I_{\min}$  the transmittance of the subject. Image J was used to measure the gray scale of the specimens and of the immediate background (82). The average contrast and standard deviations were calculated for each group of samples. The differences in contrast with increasing concentration of SrHA/SrCaHA microspheres were statistically evaluated using two-way ANOVA with a Tukey post-hoc test at a level of significance of 95%.

#### 4.2.4 *In vitro* bioactivity

The *in vitro* test was performed in a simulated body fluid (SBF) medium. From various studies in literature it has been concluded that examination of apatite formation on a material in SBF can be useful for predicting the *in vivo* bone bioactivity of a material

(74, 85, 86). The SBF medium was prepared at pH 7.4 as per Kokubo et al. (85) with ion concentrations nearly equal to human blood plasma (Appendix C). Three square cement samples of 0 (controls), 10, 20, and 30% SrHA and SrCaHA compositions were evaluated for *in vitro* bioactivity by immersion in SBF at 37°C for a period of 30 days. All of the cement surfaces were examined before immersion in SBF by SEM equipped with an EDX system (JEOL 5600). After 30 days of immersion, the samples were extracted from the solution, rinsed with deionized water and allowed to dry in a dessicator. The desiccated cement surfaces were once again examined under SEM and EDX with an accelerating voltage of 15 kV to test whether deposition of apatite had occurred. The study of the composition of the deposited apatite layer on the SrCaHA cement surfaces was carried out by FTIR spectroscopy. A line scan spectra with EDX on the 20% SrHA cement surface was also obtained along the areas devoid in apatite going across areas containing the apatite layer, and the changes in the intensity of 5 elements namely, carbon (C), phosphorus (P), oxygen (O), calcium (Ca), and strontium (Sr), were recorded. The cross-section of 10% SrHA and SrCaHA cement samples after immersion in SBF for 30 days were also evaluated using SEM and EDX to test for the presence of apatite formation in the bulk of the cement. The apatite layer thickness was measured from the SEM micrographs of all cement surfaces using ImageJ software by NIH. The changes in the pH of SBF medium were measured at pre-determined time intervals (0, 1, 2, 3, and 4 weeks) using a pH meter. The differences in the apatite thickness and atomic percentage for C, O, P, Ca, and Sr before and after submersion in SBF with increasing concentration of SrHA/SrCaHA microspheres were statistically evaluated using two-way ANOVA with a Tukey post-hoc test at a level of significance of 95%.

## 4.3 Results

### 4.3.1 Characterization of SrHA/SrCaHA microspheres

The SrHA and SrCaHA microspheres were synthesized directly by hydrothermal treatment at 180 °C for 24 hours. Figure 1 (a, b) shows SEM micrographs of typical SrHA and SrCaHA samples. It can be seen that the microspheres are about 2-5  $\mu\text{m}$  in diameter and are not random aggregates but are ordered self-assembly of nanosheets. Figure 1 indicates that the nanosheets are assembled in a radial form from the center to the surface of the microsphere, as also observed by Zhang and co-workers (77) using transmission electron microscopy. In Figure 1(c), the FTIR result indicates the presence of characteristic peaks representing the phosphate ( $\text{PO}_4^{3-}$ ) and carbonate ( $\text{CO}_3^{2-}$ ) groups. The bands centered at 1080 and 1018  $\text{cm}^{-1}$  wave numbers were ascribed to the asymmetric stretching vibrations of the P-O, and the band at 949  $\text{cm}^{-1}$  was assigned to the symmetric stretching mode of the P-O in  $\text{PO}_4^{3-}$  groups. In addition, two groups of bands observed in the low wave number region from 490 to 630  $\text{cm}^{-1}$  (center: 560, 595  $\text{cm}^{-1}$ ) were due to the bending vibrations of the O-P-O in  $\text{PO}_4^{3-}$  groups. The range of 1300-1600  $\text{cm}^{-1}$  clearly showed the existence of the carbon-related impurities from the organic additives employed during the synthesis.

The EDX spectrum (Figure 1(d)) of the SrHA product shows the presence of strontium (Sr), phosphorus (P), oxygen (O), and carbon (C) peaks, while that of SrCaHA sample shows the presence of the additional calcium (Ca) peaks between binding energies 3-4 keV. Table 1 lists the element content analysis results of Ca, Sr, and P. As compared with the pre-set atomic ratios, the measured atomic % ratios of Sr/P,

(Ca+Sr)/P, and Sr/(Sr+Ca) were maintained roughly as intended values, indicating the reaction was performed according to the predetermined stoichiometric ratios.

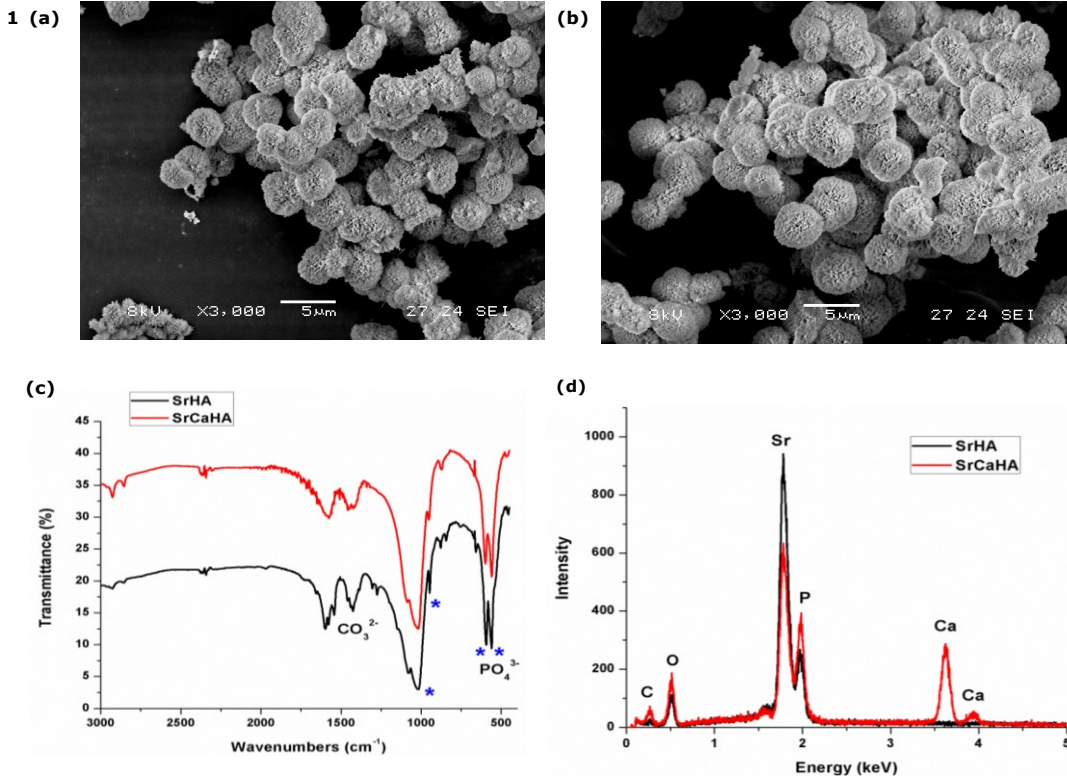


Figure 1. SEM micrographs of as prepared, self-assembled (a) SrHA and (b) SrCaHA microspheres (2-5  $\mu\text{m}$  in diameter). (c) FTIR spectra of SrHA and SrCaHA powders indicating the presence of the phosphate ( $\text{PO}_4^{3-}$ ) peaks. Asterisk represents the significant phosphate peaks. (d) EDX spectra of SrHA and SrCaHA powders. The spectrum for SrCaHA powder shows the additional calcium peaks indicating half-substitution of calcium ions with strontium ions.

Table 1. The elemental content analysis results of Ca, Sr, and P from the EDX spectrum of SrHA and SrCaHA samples. Calculated Sr/P, (Ca+Sr)/P, and Sr/(Sr+Ca) ratios of the prepared strontium-substituted hydroxyapatites by EDX (see Figure 2(b) (mean  $\pm$  SD, n = 3)

Sample	Ca (at %)	Sr (at %)	P (at %)	Measured atomic % ratio	
SrHA	0	40.43 $\pm$ 1.83	24.21 $\pm$ 1.08	Sr/P	1.66 $\pm$ 0.005
SrCaHA	15.76 $\pm$ 0.52	18.35 $\pm$ 3.3	20.45 $\pm$ 1.7	(Ca+Sr)/P	1.67 $\pm$ 0.019
				Sr/(Sr+Ca)	0.51 $\pm$ 0.004

### 4.3.2 Optical Density

Radiographs of the various cement formulations were obtained as illustrated in Figure 2(a-j), and the optical densities of all compositions are compared in Figure 2(k). Specimens containing no filler (0%, Controls) were not completely transparent to X-rays. There was a significant linear increase in the contrast values with increasing concentration of SrHA ( $r^2 = 0.94$ ) and SrCaHA ( $r^2 = 0.98$ ) microspheres ( $p < 0.05$ ). However, no significant differences were observed in the contrast values between the SrHA and SrCaHA cement compositions at each concentration. The 20% and 30% SrHA composition were significantly different than the controls (0%) and 5% SrHA cements ( $p < 0.05$ ), while the 5% and the 10% SrHA compositions were not significantly different. Similar results were observed for the SrCaHA cement compositions. The 30% SrHA and the 30% SrCaHA compositions were observed to have higher contrast values that were comparable to the contrast value observed for 20% ZrO<sub>2</sub> η-TSBC. However, the 20% SrHA and SrCaHA cements also provided radiographic contrast values of  $0.55 \pm 0.05$  and  $0.50 \pm 0.08$ , respectively.

These results fall in between the contrast values reported by Kjellson et al. (84) for acrylic bone cement specimens containing 5% (contrast value 0.339) and 15% (contrast value 0.73) ZrO<sub>2</sub> imaged under similar X-ray tube voltage (40 kV) and conditions applied in this study. Also, cements containing ZrO<sub>2</sub> and strontium were expected to have opacities higher than those cements containing barium sulfate when imaged at an accelerating voltage of 40 kV because this voltage produces its peak intensity at a photon energy of 20kV which is just above the zirconium (~18 kV) and

strontium (~16 kV) k border (84). The cements containing ZrO<sub>2</sub> and strontium filler were expected to have similar opacities.

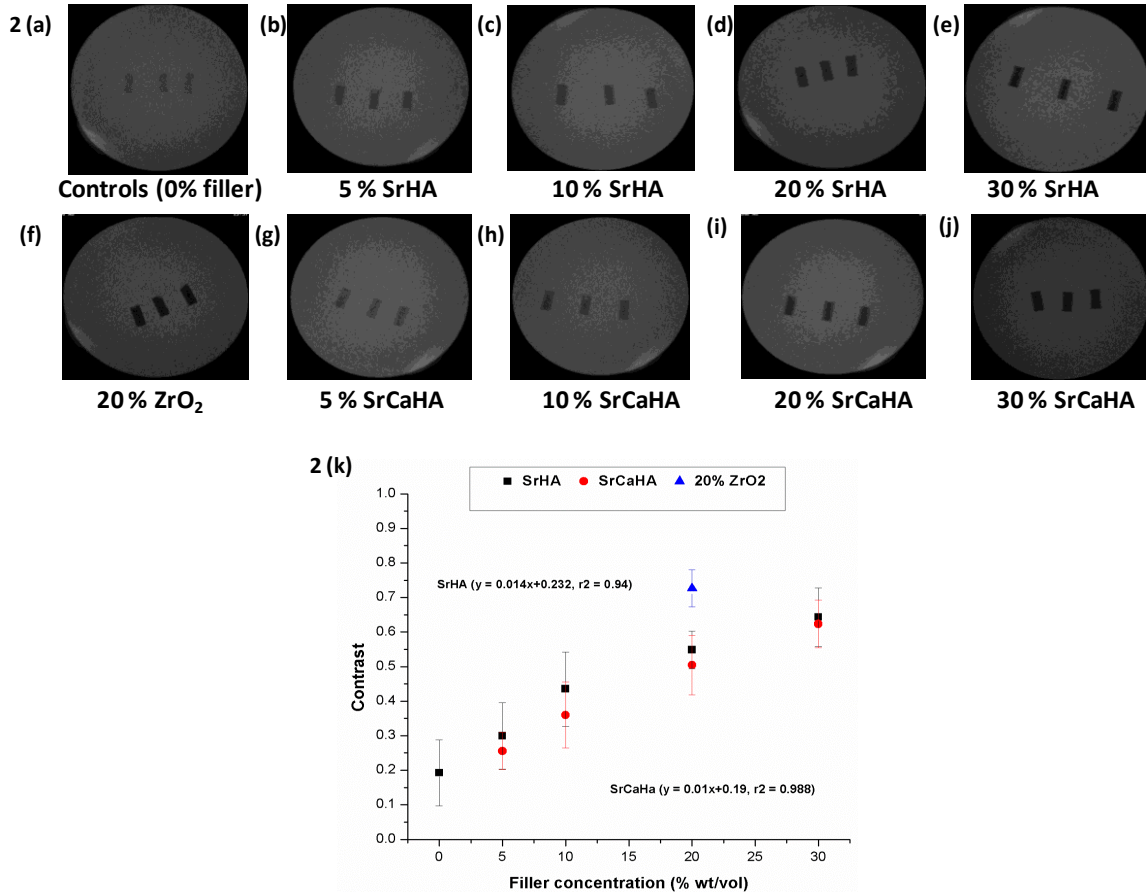


Figure 2. Radiographic images of  $\eta$ -TSBC prepared at (a) 0% (controls), (b) 5% SrHA, (c) 10% SrHA, (d) 20% SrHA, (e) 30% SrHA, (f) 20% ZrO<sub>2</sub>, (g) 5% SrCaHA, (h) 10% SrCaHA, (i) 20% SrCaHA, and (j) 30% SrCaHA. Cements prepared at 0% SrHA/SrCaHA were not completely transparent to X-rays. (k) Comparison of the radiographic contrast values of  $\eta$ -TSBC preparations with increasing concentration of SrHA/SrCaHA microspheres. The data showed a significant linear increase in radiopacity with increasing SrHA/SrCaHA microsphere concentration.

### 4.3.3 Bioactivity

The bioactivity of cements was evaluated *in vitro* after 30 days of immersion in SBF. All of the SrCaHA and SrHA cement surfaces presented deposition of small

particles which were identified as apatite by SEM and EDX analysis. The SEM micrographs and EDX spectra of the resulting SrCaHA and SrHA surfaces are shown in Figure 3(a-d) and 4(a-d), respectively, together with that of their initial surfaces. For the control cements containing no microspheres, no deposition of apatite was found as observed from the SEM micrograph and EDX analysis before and after immersion in SBF (Figure 3(a), 4(a)). The surface composition of the SrCaHA and SrHA cements before and after soaking was analyzed by EDX and the recorded spectra are shown in Figures 3(a-d) and 4(a-d). The intensity of the signals corresponding to calcium, phosphorus, and oxygen atoms increased on the SBF soaked surfaces of the SrHA and SrCaHA samples of all concentrations, and a decrease in the signal assigned to carbon was also observed that could be explained by the deposition of apatite on their surfaces.

The composition of the deposited apatite layer on the SrCaHA cement surfaces was also analyzed by FTIR and the FTIR spectra for 10, 20, and 30% SrCaHA samples are shown in Figure 5. The FTIR spectra of all the SrCaHA samples soaked in SBF showed a band at  $1730\text{ cm}^{-1}$  corresponding to the stretching vibration of the carbonyl groups of PMMA and the band at  $1025\text{ cm}^{-1}$  corresponding to the vibration of the phosphate groups of the hydroxyapatite, indicating that the surface became richer in apatite. Figure 6(a, b) compares the EDX spectra and Figure 6(c, d) quantifies the atomic percentages of C, P, O, Ca and Sr atoms before and after being soaked in SBF, for all concentrations of SrHA and SrCaHA cements. There were significant increases ( $p < 0.05$ ) observed in the atomic percentages of P, O, and Ca and a significant decrease in the atomic percentage of C, on all samples except the controls, after being soaked in SBF for 30 days. However, no significant differences were observed in the atomic percentages of

all the elements between the SrHA and SrCaHA compositions at all concentrations before being soaked in SBF. Also, no significant differences were observed in the atomic percentages of all the elements between the SrHA and SrCaHA compositions at all concentrations after being soaked in SBF.

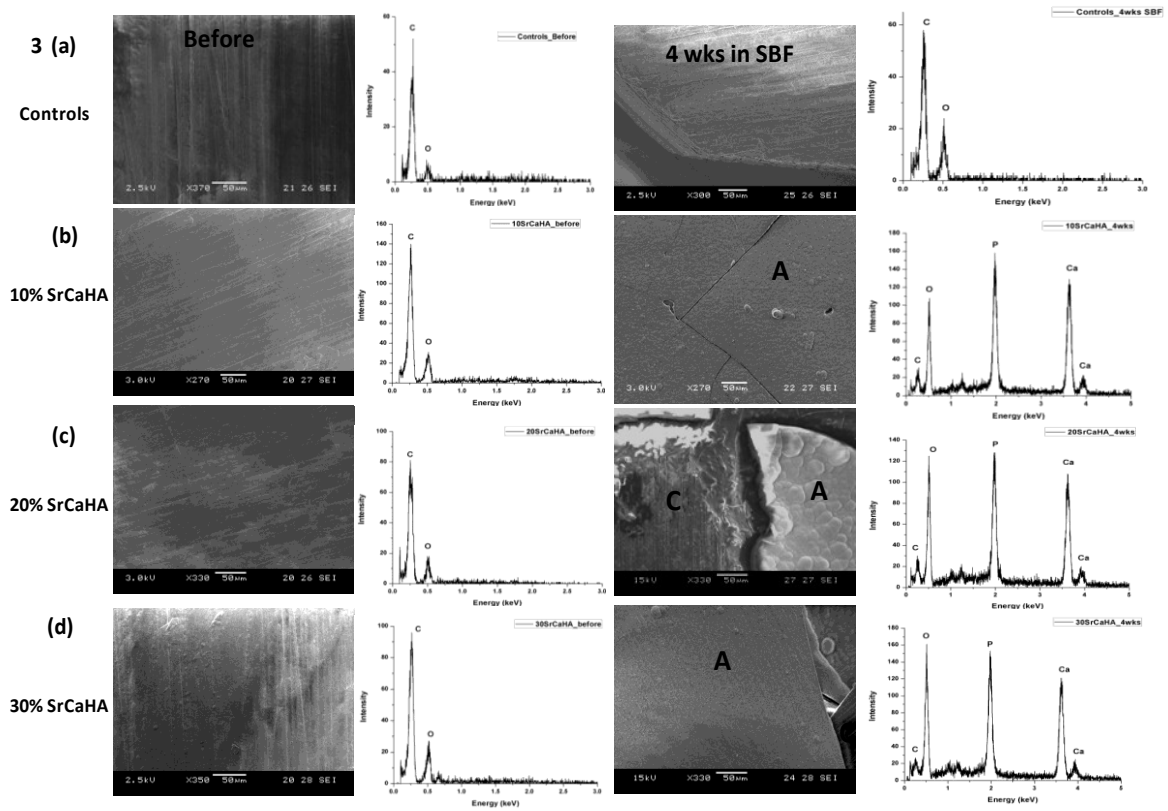


Figure 3. SEM micrographs and EDX spectra of the SrCaHA cement surfaces before (left panel) and after immersion in SBF at 37°C for 30 days (right panel). From top to bottom: (a) Control (0% wt/vol), (b) 10% wt/vol SrCaHA, (c) 20% wt/vol SrCaHA, and (d) 30% wt/vol SrCaHA. Apatite formation was observed on all the SrCaHA containing cement surfaces after 30 days in SBF along with an increase in the atomic percentage of calcium, phosphorus, and oxygen. (A = apatite layer, C = PMMA cement)

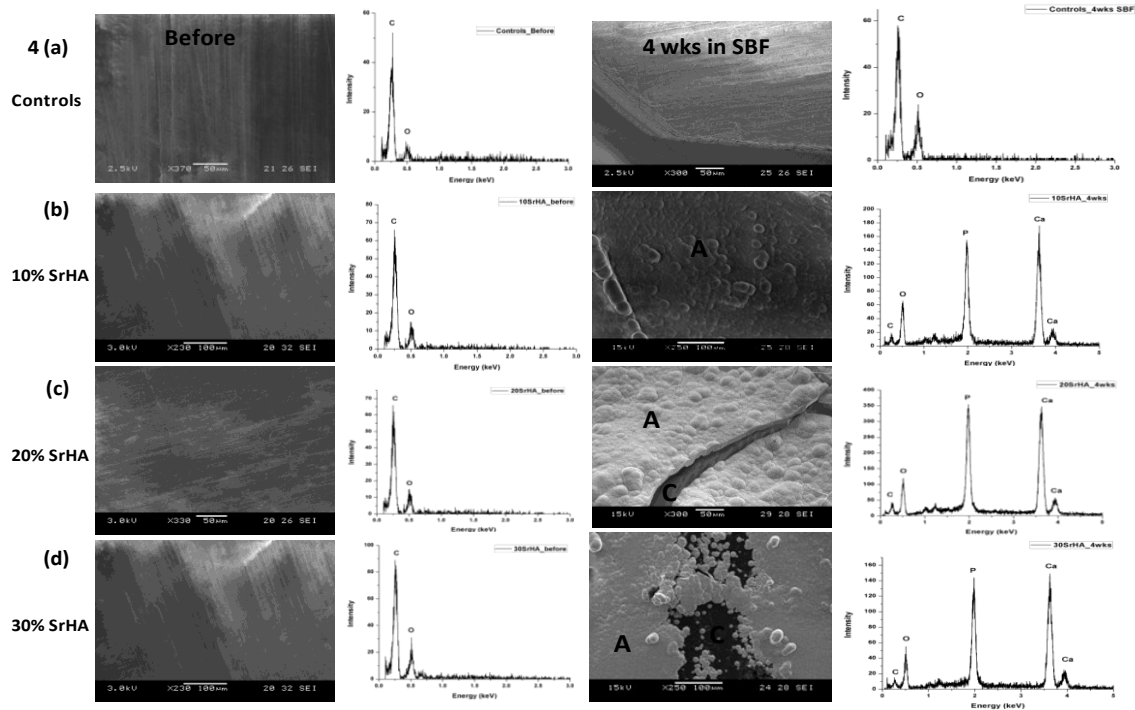


Figure 4. SEM micrographs and EDX spectra of the SrHA cement surfaces before (left panel) and after immersion in SBF at 37°C for 30 days (right panel). From top to bottom: (a) Control (0% wt/vol), (b) 10% wt/vol SrHA, (c) 20% wt/vol SrHA, and (d) 30% wt/vol SrHA. Apatite formation was observed on all the SrHA containing cement surfaces after 30 days in SBF along with an increase in the atomic percentage of calcium, phosphorus, and oxygen. (A = apatite layer, C = PMMA cement)

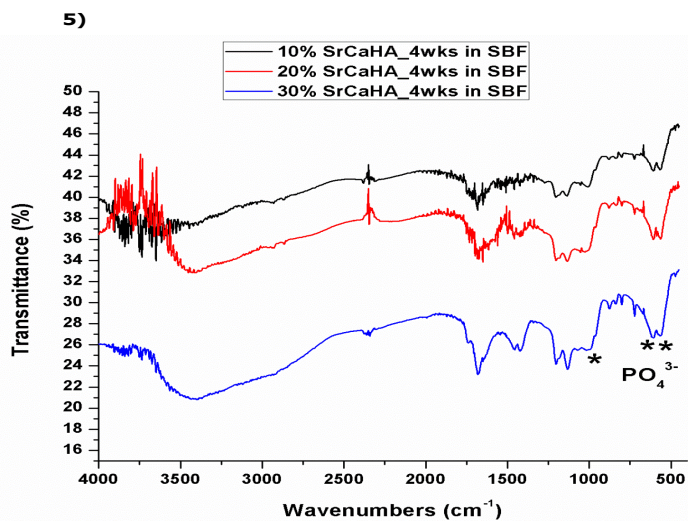


Figure 5. FTIR spectra of apatite layer formed on the surface of 10%, 20%, and 30% wt/vol SrCaHA cements soaked in SBF at 37°C for 30 days. All of the spectra obtained showed the presence of phosphate peaks (Asterisks) confirming the presence of apatite.

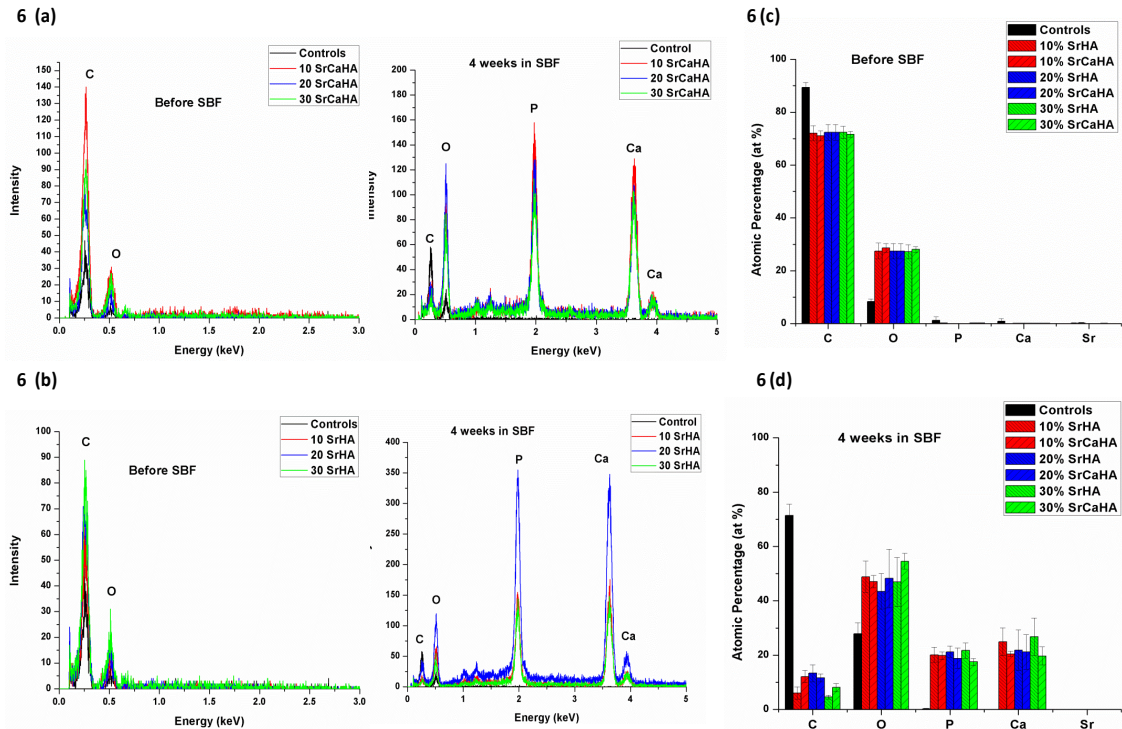


Figure 6. (a) EDX spectra of 0, 10, 20 and 30% SrCaHA samples before and after immersion in SBF for 30 days. (b) EDX spectra of 0, 10, 20 and 30% SrHA samples before and after immersion in SBF for 30 days. Changes in the atomic percentages of C, O, P, Ca, Sr on the 0, 10, 20 and 30% SrCaHA and SrHA sample surfaces (c) before and (d) after immersion in SBF for 30 days. A significant increase in the atomic percentages of O, P, and Ca for all the SrHA and SrCaHA cement compositions was observed after 30 days in SBF. However, no significant changes were observed in the atomic percentages of all the 5 elements for the control samples, before and after immersion in SBF.

The SEM micrograph of a 20% SrHA cement surface, shown in Figure 7(a), revealed a distinct region of apatite layer (A) and a region of the cement without apatite (C). A line-scan EDX (Figure 7(b)) performed along the line plotted (500 points) on the SEM micrograph in Figure 7(a), showed a progressive increase in the intensity of O, P, and Ca levels as one moves from the cement surface onto the apatite layer formed. The increase in the Ca, O, and P intensities at the cement-apatite interface also validates the formation and presence of apatite on the cement surface after being soaked in SBF. The cross-sections of the 10% SrHA and SrCaHA cement samples, soaked in SBF for 30 days, were evaluated for presence of apatite in the bulk of the cement using SEM and

EDX as shown in Figure 8. Figure 8 (a, b) shows the SEM micrograph of the cross-sections of the 10% SrCaHA and 10% SrHA cement surfaces, respectively. The EDX spectra of the cross-sectional areas, shown in Figure 8(c), showed no presence of any calcium or phosphorus peaks corresponding to apatite. Also, the quantification of the atomic percentages (Figure 8(d)) of the elements from the EDX spectra in Figure 8(c) showed that only carbon and oxygen were present in both the cement cross-sections, indicating no formation of apatite in the bulk of the cement.

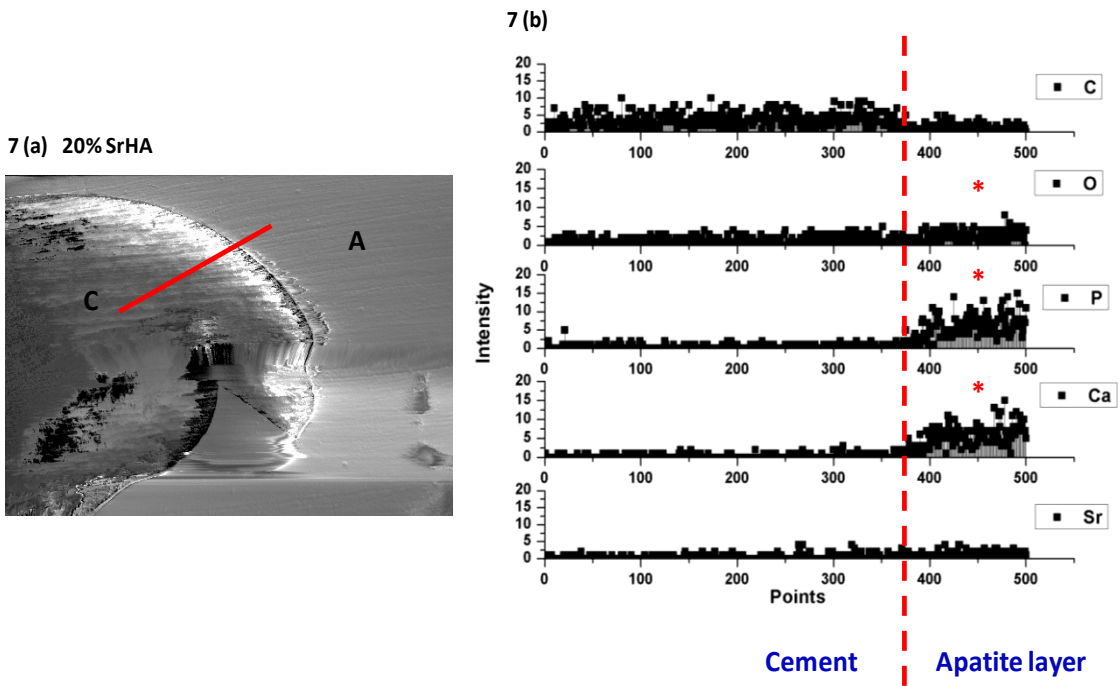


Figure 7. (a) SEM micrograph of a 20% SrHA cement surface after being soaked in SBF at 37°C for 30 days, having regions devoid of apatite (C) and regions having apatite (A) formed on its surface. (b) EDX line scan spectra, performed along the line plotted (500 points) on the SEM micrograph region in Figure 7(a), showing a progressive increase in the intensity of O, P, and Ca levels as one moves from the cement surface onto the apatite layer formed.

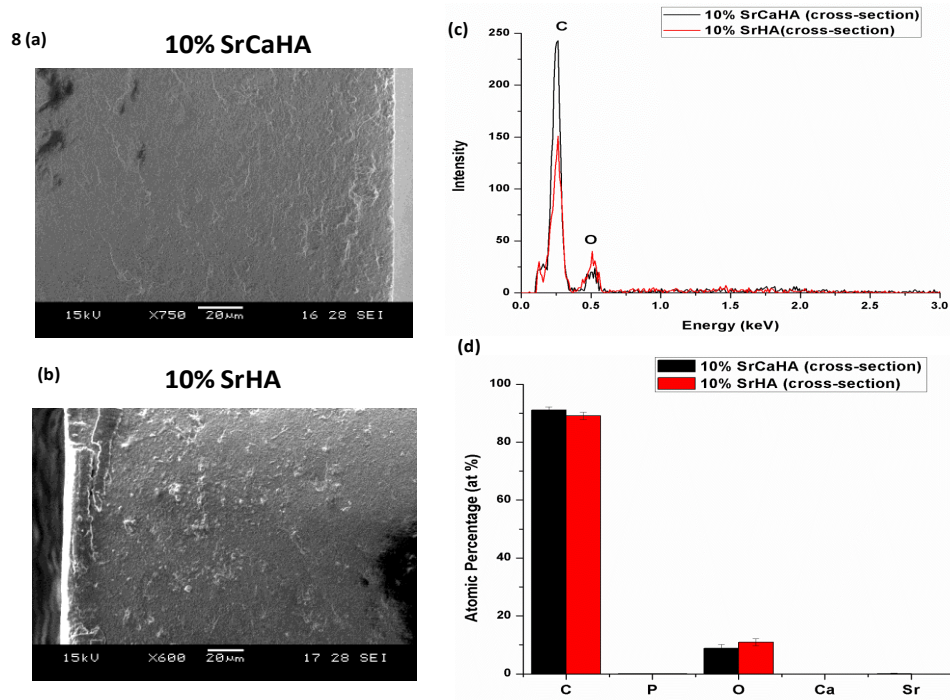


Figure 8. SEM micrographs of cross-section of the (a) 10% SrCaHA and (b) 10% SrHA cement samples soaked in SBF for 30 days. (c) EDX spectra across the cross-section of the 10% SrCaHA and 10% SrHA cement surfaces and the (d) Atomic percentage of the elements analyzed by EDX spectra. The EDX spectra of the cross-section surfaces of both the cement compositions clearly showed no presence of any apatite, indicating that apatite was not formed in the bulk of the cement.

Figure 9(a-d) shows SEM micrographs depicting different thicknesses of the apatite that were observed on various cement surfaces. The thickness of the apatite layer formed on all of the SrHA and SrCaHA cement compositions was measured using ImageJ and was plotted as a function of filler concentration as seen in Figure 9(e). The thickness of apatite layer on SrCaHA cements was observed to decrease significantly with increasing SrCaHA concentration ( $p < 0.05$ ). However, no particular trend was observed in the thickness of the apatite layer with increasing SrHA concentration. The 20% SrHA cement surface had significantly thicker apatite layer in comparison to 10 and 30% SrHA compositions. The changes in the pH of SBF were also measured at timed

intervals over a period of 30 days. Figure 10 shows a graph of pH versus time which illustrates a gradual significant increase ( $p < 0.05$ ) in the pH of SBF containing 10 and 20% SrHA and SrCaHA cement samples, up until 4 weeks. However, no significant changes were observed in the pH of SBF containing the control cement samples, and the pH remained constant at 7.4 over a period of 4 weeks. The increasing alkalinity of SBF containing SrHA and SrCaHA samples could possibly be explained by increase in calcium ion concentration in the solution during apatite formation on the cement surfaces.

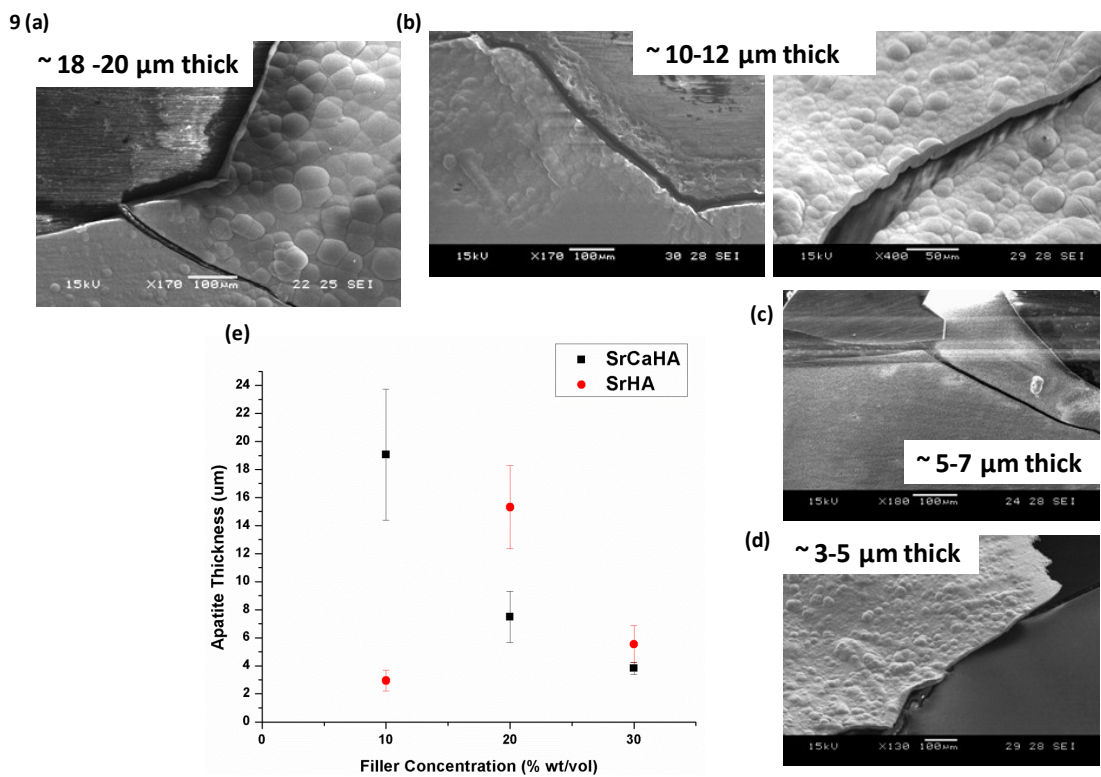


Figure 9. SEM micrographs indicating the different thicknesses of the apatite layer formed on surfaces of various cement compositions (a) 20 μm in thickness, (b) 10 μm in thickness, (c) 5 μm in thickness, (d) 3 μm in thickness. (e) Apatite layer thickness measured as a function of the filler concentration. A decrease in apatite thickness was observed for the SrCaHA cements with increasing filler concentration, whereas no particular trend in the apatite thickness was observed for the SrHA cements with increasing filler concentration.

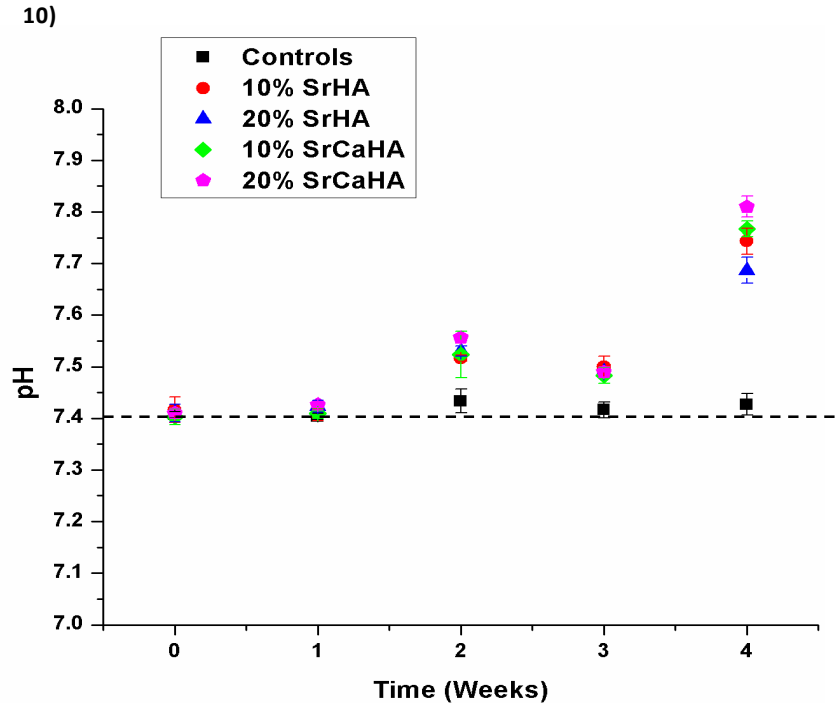


Figure 10. The changes in the pH of SBF medium containing controls (0% filler), 10% SrHA, 20% SrHA, 10% SrCaHA, and 20% SrCaHA cement samples ( $n = 3$ ), over a period of 4 weeks. The pH vs. time graph illustrated that pH of the SBF containing control samples remained constant at 7.4, whereas the pH of SBF containing SrHA and SrCaHA cement samples increased significantly over a period of 4 weeks as compared to the control samples, indicating the relative alkaline effect on the pH of the medium due to addition of apatite.

#### 4.4 Discussion

The FTIR comparison of SrHA and SrCaHA powders is shown in Figure 1(c).

The decrease in the wave numbers of the P-O bonds is attributed to the substitution of strontium ions ( $\text{Sr}^{2+}$ ) for calcium ions ( $\text{Ca}^{2+}$ ) into the lattice of apatite. The radius of  $\text{Sr}^{2+}$  (0.112 nm) is bigger than the radius of  $\text{Ca}^{2+}$  (0.100 nm), which consequently decreases the bonding strength of the P-O bonds (1). These changes further confirm that  $\text{Sr}^{2+}$  can substitute  $\text{Ca}^{2+}$  and enter the lattice of apatite. The detected carbon in the EDX spectra of the microspheres (Figure 1(d)) (as also observed in the FTIR spectra (Figure 1(c))), indicates that some carbon impurities have been induced into the SrHA/SrCaHA host

lattices and/or the surface due to the organic additives employed during their hydrothermal synthesis. Hernandez and co-workers developed PMMA cement containing SrHA nano powder (10% Sr substitution) that had radiopacity similar to that provided by addition of 30% wt/vol barium sulfate radiopacifier which met the requirements of vertebroplasty (68). The radiopacity of cements prepared at higher concentrations (20 and 30% wt/vol) of SrHA/SrCaHA microspheres were observed to have similar contrast values as measured for cements prepared with  $ZrO_2$  (82), suggesting they can provide sufficient radiographic contrast for VP and KP applications. This observation is important considering that SrHA/SrCaHA microspheres were added to two-solution cements instead of  $ZrO_2$  in order to impart radiopacity and bioactive properties, without incorporation of any additional filler material. As expected, the radiopacity increased linearly with increasing concentration of SrHA and SrCaHA microspheres.

Bioactivity of a material *in vivo* is determined through its ability to deposit an apatite layer on its surface, which in the long term facilitates formation of new bone matrix providing direct contact between the implant and bone (87). This phenomenon can be reproduced *in vitro* by immersing the material in SBF, a fluid with ion concentrations similar to human blood plasma but free of proteins and cells. The most employed SBF is that proposed by Kokubo et al. (85) and it has been used in the conditioning of the samples in this work. In this study, all compositions of SrHA and SrCaHA cements exhibited the ability to induce apatite formation on their surfaces after a month in SBF. The presence of apatite layer and the capacity to form apatite on these surfaces was an indication that these cements had improved bioactivity compared to the control  $\eta$ -TSBCs. EDX analysis also revealed decreased levels of C and increased levels of Ca, P, and O on

these cements after 30 days in SBF indicating presence of apatite. A similar increase in Sr, Ca, and P signal and a decrease in signal assigned to C were also observed by Hernandez et al. (74) after soaking PMMA cements containing SrHA nanopowder (10 mol % Sr substitution) in SBF for 28 days. They suggested these elemental changes to be a result of apatite deposition on their cement surfaces. They cured their cements in air as well as directly in SBF and suggest the growth of apatite particles was mainly produced within the superficial pores left by dissolved initial particles. However, Hernandez et al. (74) incorporated SrHA nanopowder at concentrations of only 10 wt % and 20 wt % and observed apatite formation only on cement surfaces containing 20 wt% SrHA nanopowder that was pre-treated with MMA. We observed apatite formation even on our  $\eta$ -TSBC cement surfaces containing lower concentrations (10% wt/vol) of SrHA/SrCaHA microspheres, which is a promising result. The FTIR analysis also confirmed presence of apatite. However, the type or concentration of microspheres did not significantly affect the apatite formation ability of the SrHA/SrCaHA cements. The formation of the apatite layer on a HA surface *in vivo* has already been described by Kokubo et al. (52). The most commonly proposed mechanism for bioactivity involves dissolution of calcium and phosphate ions with subsequent supersaturation of these ions near the implant vicinity leading to their precipitation and formation of biological apatite (80, 88). However, an *in vivo* study by Wong et al. (89) looking at the mineralization of SrHA nano powder/Bis-GMA bioactive cement injected into the cancellous bone of the ilium of rabbits, suggested that dissolution of SrHA (10 mol% Sr substitution) into the debris by the bone remodeling process increased the concentration of calcium and phosphorus at the bone-SrHA cement interface. The crystalline SrHA thus formed an amorphous layer on the cement surface

which then dissolved into the surrounding solution leading to oversaturation and precipitation of apatite crystals. They proposed that the cells resorbed and modified the surface of SrHA cement to promote osseointegration. Also, many studies (69, 76, 90) indicate that introduction of Sr introduces more lattice distortions to the structure of HA increasing its solubility and release of Ca which in turn increases the ionic activity of apatite in the surrounding fluid, inducing apatite formation. In our study, we varied the amount of Sr substitution in HA at 50 mol % and 100 mol % and thus the SrHA/SrCaHA microspheres exposed at the cement surfaces are expected to have higher solubility when subjected to SBF solution. Interestingly, we also observed a gradual increase in the alkalinity of the pH of SrHA/SrCaHA containing  $\eta$ -TSBCs after 4 weeks in SBF indicating an increase in concentration of  $\text{Ca}^{2+}/\text{Sr}^{2+}$  ions. This could be one of the possible mechanisms of formation of apatite on our SrHA/SrCaHA  $\eta$ -TSBCs. The SrHA/SrCaHA microspheres exposed at the cement surfaces could facilitate faster dissolution of  $\text{Ca}^{2+}$  ions into the SBF. The nucleation and formation of apatite on SrHA cements could also be explained due to super saturation of Sr ions in the fluid and interaction with Ca ions in the surrounding SBF medium, since Sr can be easily exchanged by Ca. The SEM micrograph of 30% SrHA sample after 4 weeks in SBF (Figure 4(d)) also showed evidence of individual dome like formations of apatite on some areas of the cement surfaces indicating that the microspheres provided sites of nucleation for apatite formation followed by gradual growth and progression of these dome structures into layers of apatite. Such an increase in pH has also been observed by Boanini et al. (91) who studied the effect of SrHA (10 mol% Sr substitution) and HA nano powder on rat osteoblasts. They measured the calcium and Sr cumulative releases from compacted discs of SrHA and HA powder in

physiological solution over a period of 14 days, and found that the sum of Ca and Sr released from SrHA was always greater than the extent of Ca release from pure HA. Fathi et al. (86) also tested the bioactivity of HA nanopowder versus conventional HA in SBF for a period of 14 days and measured the changes in pH of SBF at timed intervals. They concluded that pH value was dependent on the solubility of HA and drastic changes were seen in the pH of SBF containing HA nanopowder, suggesting it dissolves faster than conventional HA.

The decrease in the apatite layer thickness with increasing concentration of SrCaHA microspheres was not expected. The apatite layer formed on the SrCaHA surfaces was attached loosely to the cement surface and flaked off easily upon drying and preparing the cement for SEM analysis. While performing the SEM analysis it could be possible that some of the apatite layer was detached and thus the thickness measurements from these SEM images were not an accurate representation of the actual apatite thickness. Future work would involve looking at better techniques to measure apatite thickness such as a profilometer. The apatite thickness observed for SrHA samples in our study did not follow a particular trend with increasing SrHA concentration. Also the apatite layer found on SrHA samples seemed better adhered to the cement surface and thinner in comparison to SrCaHA samples. Although, it is important to note that the apatite thickness measurements on the SrHA/SrCaHA samples ranged from 5 – 20  $\mu\text{m}$  in thickness, indicating provision of a thick apatite layer for interaction with the surrounding tissue *in vivo*. In order to determine whether the formation of apatite was present in the bulk of the cements, we also looked at the cross-sections of the 10% SrHA and SrCaHA cement

samples and did not find presence of apatite. This suggested that the apatite formation on our SrHA and SrCaHA samples was limited only to the cement surfaces.

The formation of apatite on the cement surfaces is also known to promote cellular attachment and spreading increasing the bioactivity. Xue et al. (79) investigated the *in vitro* bioactivity of compacted discs of SrHA (10 mol% Sr substitution) powder and its effect on cell attachment, proliferation, and differentiation by culturing osteoprecursor cells. Their results suggested the presence of Sr stimulated cell differentiation and enhanced alkaline phosphatase (ALP) and osteopontin expression indicating mineralization. Ni et al. (76) studied a series of strontium substituted HA powders for their structure, composition, dissolution behavior, and the effect on osteoblastic differentiation, in which 0, 1, 5, and 10% calcium was substituted with strontium. They cultured rat mesenchymal stem cells (MSCs) with the culture media containing Sr ions released from the strontium-substituted HA powders. They suggested that 5-10 mole % Sr substitution in HA enhanced osteogenic differentiation of MSCs. Most of the above mentioned studies from literature have evaluated properties of strontium-substituted HA nano powder with increasing amount of strontium substitution or have only evaluated incorporation of one composition of SrHA nanopowder (10 % Sr substitution) into Bis-GMA resin cements. However, varying the percentage of strontium substitution in HA powders being incorporated into PMMA bone cements have not been evaluated thus far. A further study by Ni et al (92) conducted the MTT test and looked at the ALP activity, mRNA expression and mineralization nodules of MSCs subjected to SrHA conditioned media. They observed no differences in the osteoblast proliferation between groups, but observed an increase in the effect for mRNA expression and mineralization nodules with 5

and 10 wt % Sr substitutions. Recently, Zhang et al. (2) compared the effect of strontium substitution (10, 40, and 100%) of HA on osteoblasts and found 10% SrHA powder group had the best performance. They did not find osteoblasts on the 100% SrHA surface indicating that higher substitutions of strontium may appear to be toxic to the cells. Even though strontium substitution favors osteoblastic cell differentiation, the optimal concentration of strontium remains divisive. In our study the 50 and 100% Sr substituted HA microspheres were incorporated into the  $\eta$ -TSBCs and were not shown to differ in their ability to form apatite on the cement surfaces at each concentration. Although we had higher strontium substitutions in our HA microspheres, most of these particles are expected to be embedded in the PMMA matrix with contact available primarily at the cement surfaces for osteoblast cells. Thus, in such a case the higher substitution of strontium might not essentially be toxic to the osteoblasts and would be an interesting follow up study in order to evaluate the effect of varying strontium-substitution in HA microspheres. The *in vitro* performance of the  $\eta$ -TSBCs containing SrHA and SrCaHA microspheres in SBF is encouraging and future work would look at the *in vivo* bioactivity and biocompatibility. The biomechanical evaluation of these cements is reported in the next chapter.

#### **4.5 Conclusions**

This work demonstrated that addition of SrCaHA or SrHA microspheres to  $\eta$ -TSBCs improved bioactivity in comparison to the control cements. Apatite formation was observed on all of the SrHA/SrCaHA cement compositions irrespective of the amount of strontium substitution in HA and the concentration of SrHA/SrCaHA microspheres.

Addition of SrHA and SrCaHA microspheres provided good radiographic contrast necessary for VP and KP applications, eliminating the need of adding an additional radiopacifier. Apatite formation on cement surfaces was observed even at lower concentrations of the SrHA/SrCaHA bioactive filler. Further investigation using osteoblast cell cultures evaluating the effect of different strontium substituted HA microspheres in  $\eta$ -TSBC needs to be performed. This improvement in bioactivity makes the  $\eta$ -TSBC a good alternative to the powder- liquid cements for VP/KP applications.

## Chapter 5

---

### 5 Biomechanical evaluation of two-solution bone cements with strontium-substituted hydroxyapatite microspheres

This chapter reports the effect of increasing concentration (0, 10, and 20 % wt/vol) and strontium substitution of hydroxyapatite (HA) microspheres on the flexural, compressive, and fracture toughness properties of two-solution bone cement ( $\eta$ -TSBC). The two different types of hydroxyapatite microspheres used were partially (50 %, SrCaHA) and fully (100 %, SrHA) substituted strontium-hydroxyapatite synthesized in our laboratory. Cements prepared with SrHA/SrCaHA microspheres exhibited significantly higher compressive strength than  $\eta$ -TSBC at increasing microsphere concentrations. The flexural properties of the SrHA/SrCaHA cements decreased relative to the control  $\eta$ -TSBCs with increasing filler concentrations, however, they were similar to the 20 % zirconium dioxide ( $ZrO_2$ ) containing  $\eta$ -TSBC. Furthermore, no significant effect of cement composition or SrHA/SrCaHA filler concentration was observed on the fracture toughness properties in comparison to control  $\eta$ -TSBCs. The filler composition (SrHA/SrCaHA) did not significantly affect the static mechanical properties of the modified  $\eta$ -TSBCs at each concentration. The decrease in the mechanical properties may be a consequence of the SrHA/SrCaHA microsphere agglomeration. The fractured surfaces and crack-growth mechanisms were analyzed using scanning electron microscopy (SEM). This study indicates that addition of higher concentrations of SrHA/SrCaHa filler significantly affects the mechanical properties of two-

solution bone cements, while also bringing them closer to the mechanical properties of human cancellous bone that may be advantageous.

## 5.1 Introduction

Acrylic bone cements have been used widely in orthopedic surgery to allow for fast anchorage of the implant and a better distribution of physiological loads between the prosthesis and the bone (25, 27, 37). Kyphoplasty and vertebroplasty procedures involve percutaneous injection of bone cements under real time fluoroscopy image guidance into fractured vertebrae, so the most desirable properties of cements for these applications are high radiopacity, easy injectibility, appropriate mechanical properties resembling those of non-osteoporotic vertebrae, and adequate interdigitation with the cancellous bone (5, 7, 35). Radiopacity is achieved by addition of radio contrast filler, such as barium sulfate ( $\text{BaSO}_4$ ) or zirconium dioxide ( $\text{ZrO}_2$ ), which are known in literature to cause alterations in the biological and mechanical properties of cements (36). The effect of  $\text{BaSO}_4$  on the mechanical properties of bone cements is contradictory, but most studies report deleterious effects of adding  $\text{BaSO}_4$  on the mechanical properties of bone cements (93-98). Ginebra et al. (96) showed that addition of 10 wt %  $\text{BaSO}_4$  to PMMA based cement lowered the tensile strength, fracture toughness, and fatigue crack propagation resistance in comparison to 10 wt%  $\text{ZrO}_2$  filler addition. Wang et al. (95) showed a similar decrease in tensile strength and fracture toughness with addition of 10%  $\text{BaSO}_4$  to Simplex P cement. Vallo et al. (99) reported that presence of  $\text{BaSO}_4$  and  $\text{ZrO}_2$  fillers improved fracture toughness of PMMA cements by promoting interactions between the crack and second phase dispersion. Deb et al. (98) concluded that the presence of the inorganic phase did not affect the tensile

strength of acrylic cements. In comparison to the addition of BaSO<sub>4</sub>, radiopacifiers such as ZrO<sub>2</sub> seemed to have less detrimental effects on mechanical properties of bone cements due to size and morphology of particles that allow for better integration within the PMMA matrix (96). Rodrigues et al. (30) have shown recently that ZrO<sub>2</sub> added to two-solution cements up to concentrations as high as 20 % wt/vol had a less detrimental effect on their static mechanical properties in comparison to BaSO<sub>4</sub>. They also observed that when BaSO<sub>4</sub> was added to η-TSBCs, it affected the viscosity of the cements negatively as mixing BaSO<sub>4</sub> into solutions containing PMMA nanospheres led to the formation of a powdery mixture with difficult handling and injectibility properties.

In view of these studies, alternative fillers and methods have been explored for developing radiopaque as well as bioactive bone cements. Incorporation of bioactive particles such as hydroxyapatite (HA) (53, 100, 101), strontium-substituted hydroxyapatite (SrHA) (66, 70, 73), iodine (36), and glass particles (102), that allow for better integration with the surrounding bone have been studied. Some studies have also concentrated on addition of fibers to reinforce the cement (103, 104). Pourdeyhimi et al. (104) reinforced PMMA cements with short ultra high molecular weight polyethylene fibers and studied their fracture properties. They reported a significant reinforcing effect at a lower concentration of fibers (1 wt %) and observed that beyond this concentration the fracture toughness became insensitive to the increasing fiber content. The fiber reinforced cements possessed increased stiffness but poor intrusion characteristics. Kim et al. (105) added up to 30 wt% of bone mineral particles to Zimmer Regular ® bone cement and observed a linear decrease in the cement tensile strength with increasing amounts of bone particle despite of the decreased percent porosity. Vallo et al. (102) incorporated different weight fractions

(12 -50 wt %) of glass spheres (105 -210  $\mu\text{m}$  in diameter) into a PMMA cement (Subiton, Subiton Laboratories, Buenos Aires, Argentina) and investigated the flexural, compressive and fracture properties. They reported that the glass particles could be added up to 50 wt% with significant increases in the flexural modulus and fracture toughness displaying a reinforcing effect of the filler. However, they also observed through dynamic mechanical analysis an increase in the residual monomer content with increasing glass filler concentration, which could explain the increase in fracture properties and reduction in the compressive strength reported. Incorporation of HA filler has been studied by various groups. Kwon et al. (39, 106) performed *in vivo* studies with HA impregnated PMMA cement with increasing HA concentration up to 30% wt and found that there was new bone formation near the interface between the implant and surrounding bone as the amount of HA filler increased. They also found the interfacial shear strength increased compared with the cement without HA, and was significant when using 30% HA as filler.

The presence of HA not only promotes bone growth, but also modifies the mechanical properties of the cement. However, the effect of HA on the mechanical properties of bone cements is not clear. For example, Vallo et al. (101) tested the flexural, compressive, and fracture toughness properties of PMMA cements with varying amounts of HA nano powder and found an increase in the flexural modulus and fracture toughness when HA was added to radiolucent cements. However, this increase was limited to concentrations up to 15 wt% of HA, due to agglomeration of HA and increase in porosity at higher concentrations. Serbetci et al. (107) reported that presence of HA up to 15 wt% in an acrylic based bone cement increased the compressive strength and provided sufficient compressive fatigue strength, but lowered the tensile properties. Morejon et al. (53) studied the effect of

amount (0, 10, and 30 wt %) and type of HA incorporated into acrylic cement on the compressive, flexural and fracture toughness properties. They observed that inclusion of any type of HA increased the flexural modulus, but decreased the compressive and fracture properties of the cement. However, the mechanical tests carried out by Kwon et al. (39) showed a significant linear decrease in the flexural and diametrical tensile strength with increasing HA concentration up to 30 wt %. Kobayashi et al. (51, 108) studied compressive, bending, tensile strengths, and fracture toughness of three bioactive Bis-GMA based cements containing apatite-wollastonite glass ceramic (AWC), HA, and tricalcium phosphate (TCP), respectively, under wet conditions. They found that the compressive, bending, tensile strengths, and fracture toughness of AWC were significantly higher than those of HA and TCP. Cheung et al. (70) tested the compressive and bending strengths of SrHA cement that they used *in vivo* in vertebroplasty applications, and have reported that these cements had lower compressive and bending properties compared to the AWC cements and current PMMA cements such as Simplex P (Stryker) and Palacos R (Zimmer). These studies indicate that the mechanical properties of the bioactive cements are affected by a number of factors such as matrix chemical composition, filler type, and filler concentration.

In addition to having good bioactive properties, HA or SrHA-filled cements need to have adequate static mechanical properties fulfilling the ASTM standards to be of practical use. This work studies the static mechanical properties, such as compressive and bending strengths, of two-solution bone cements ( $\eta$ -TSBC) filled with SrHA (100 % strontium(Sr)-substituted HA) and SrCaHA (50% Sr-substituted HA) microspheres prepared in the laboratory. The major mechanism for failure in cemented arthroplasties is

gradual loosening of the cement at the bone-cement interface (37). Thus, fracture toughness, which indicates the materials resistance to crack propagation, was also determined. Since it was desired to incorporate the highest amount possible of SrHA/SrCaHA microspheres to obtain higher bioactivity and bone growth promotion, the effect of increasing filler concentration on the mechanical properties of  $\eta$ -TSBCs was also evaluated. Furthermore, the fractured surfaces from the bending and fracture toughness test specimens were studied under scanning electron microscopy (SEM) to determine the fracture mechanisms.

## 5.2 Material and Methods

### 5.2.1 Preparation of SrHA/SrCaHA cements

The SrHA and SrCaHA microspheres (2-5  $\mu\text{m}$  in diameter) were synthesized as described by Zhang et al. (2, 83) and the atomic ratios of Sr/P and (Ca+Sr)/P were set as 1.67. The SrCaHA microspheres were prepared using the same hydrothermal procedure; however in this case the  $[\text{Sr} / (\text{Sr} + \text{Ca})]$  molar ratio was set as 0.5. The two-solution bone cements containing cross-linked polymethylmethacrylate nanospheres ( $\eta$ -TSBC), used as controls, were prepared as described by Rodrigues and co-workers (81, 82) at a polymer to monomer ratio of 1:1 and cross-linked PMMA nanospheres to linear PMMA ratio of 1.5:1. For the preparation of  $\eta$ -TSBCs, benzoyl peroxide (BPO) (Aldrich), *N, N*-dimethyl *p*-toluidine (DMPT) (Aldrich) and methylmethacrylate (MMA) (Fluka) were used as received without further purification. The  $\eta$ -TSBCs were made up of two polymer phases: 1) dissolved linear PMMA ( $P_l$ ), and 2) dispersed cross-linked PMMA nanospheres ( $P_b$ ). These two components were massed and mixed together forming the

powder phase (P). A part of the total volume of MMA was split and added to two graduated cylinders, in which one was mixed with 1.25 g of BPO (1.25 g/100 ml of MMA) and other with 0.7 ml DMPT (0.7 ml/100 ml of MMA). The two mixtures BPO/MMA and DMPT/MMA were transferred to two polypropylene cartridges followed by the addition of the powder phase and remaining MMA. The cartridges were sealed, vigorously agitated by hand, and placed on a rotating drum mixer for 18 h. Following mixing, the cartridges were stored upright at 4°C for 48 hours before use. In order to prepare the  $\eta$ -TSBCs containing strontium substituted microspheres, the SrHA and SrCaHA microspheres were added to the polymer phase at concentrations of 10 and 20% wt/vol of MMA and the mixing procedure remained the same as described above for the  $\eta$ -TSBCs.

### 5.2.2 Compression Testing

Cement cartridges were prepared at 0 (control  $\eta$ -TSBC), 10, and 20 % SrHA and SrCaHA and injected into a Teflon mold consisting of cylindrical holes, each 6 mm in diameter and 12 mm height, to make compression samples as per ASTM standard F451-99a (30, 109). Five cylindrical samples for each composition were allowed to polymerize in the mold for 1 hour followed by 24 hours of curing in air after removal from the mold. All of the specimens were sanded with 600-grit sand paper and were visually inspected for defects. Samples containing external voids or defects greater than 0.5 mm were excluded. The specimens were subjected to compression testing in an MTS system (Sintech 2G) with a 10 kN capacity load cell. The cylindrical samples were tested at room temperature, in air, at a displacement rate of 0.05 mm/s and compressed to 50% strain.

Stress and strain data were obtained by dividing the load and displacement by the cross-sectional area and initial length of the specimens, respectively. Compressive strengths and maximum strain to failure were measured. Compressive modulus was calculated from the slope of the linear region of the stress-strain curve. Two-way ANOVA analysis was applied at a level of significance of 95% to determine the effect of cement composition and SrHA/SrCaHA filler concentration on each variable measured in the compression test (compressive stress, compressive modulus, and strain to failure).

### 5.2.3 Flexural properties

Three point bend flexural tests were performed as per ASTM standard (D790-86 (110)) on five samples of each cement composition. The cement compositions tested were  $\eta$ -TSBC containing 20% zirconium dioxide ( $ZrO_2$ ), and  $\eta$ -TSBC containing SrHA and SrCaHA microspheres at concentrations 0 (control), 10, and 20% wt/vol. The samples were polymerized in a rectangular Teflon mold and polished using sand paper grits 240-600. The samples were on average 11.5 mm wide and 3 mm thick and were tested using an MTS system (Sintech 2G) with a 10 kN capacity load cell. A crosshead speed of 2.54 mm/min and span length of 40 mm were used. The flexural strength ( $\sigma$ ), flexural modulus (E), and maximum strain ( $\epsilon$ ) were calculated according to the following equations (110)

$$\sigma = \frac{3PL}{2bd^2},$$

$$\epsilon = \frac{6Dd}{L^2},$$

$$E = \frac{L^3 M}{4bd^3}$$

where,  $P$  is the maximum load (N),  $L$  is the span length (mm),  $b$  is the sample width (mm),  $d$  is the sample thickness (mm),  $D$  is the maximum deflection at the center of the beam (mm), and  $M$  is the slope of the load/deflection curve (N/mm). The fractured surfaces were studied using SEM to determine fracture mechanisms. Two-way ANOVA statistical analysis was applied at a level of significance of 95% to determine the effect of cement composition and filler concentration on each of the variable measured in the flexural test (flexural strength, flexural modulus, and strain to failure).

#### 5.2.4 Fracture toughness

Fracture toughness tests were performed, as per ASTM standard (E399-83(111)), on five samples of each cement composition. The cement compositions tested were  $\eta$ -TSBC containing 20% zirconium dioxide ( $ZrO_2$ ), and  $\eta$ -TSBC containing SrHA and SrCaHA microspheres at concentrations 0 (control), 10, and 20% wt/vol. Rectangular samples were prepared with average width and thickness of 11.5 mm and 2.5 mm, respectively. A notch was made using a slow speed diamond cut-off wheel and a razor blade was used to impart the final sharp crack tip. The crack length ( $a$ ) used was 45 to 55% of the width of the specimen. The samples were tested at room temperature on a Sintech MTS system (model 2GT) using a crosshead speed of 2.54 mm/min and a span length ( $L$ ) of 40 mm.  $K_{IC}$  (mode I plain strain fracture toughness) was calculated using following equation (111)

$$K_{IC} = \frac{PL}{bW^{3/2}} * \frac{3(\frac{a}{W})^{1/2}[1.99 - (\frac{a}{W})(1 - \frac{a}{W}) * (2.15 - 3.93 \frac{a}{W} + 2.7 \frac{a^2}{W^2})]}{2(1 + 2 \frac{a}{W})(1 - \frac{a}{W})^{3/2}}$$

where,  $P$  is the maximum load (N),  $b$  is the samples thickness (mm),  $W$  is the sample width (mm), and  $a$  is the crack length (mm). The fractured surfaces were studied using SEM to determine fracture mechanisms. Two-way ANOVA analysis was applied at a level of significance of 95% to determine the effect of cement composition and SrHA/SrCaHA filler concentration on the fracture toughness.

## 5.3 Results

### 5.3.1 Compressive properties

Compression tests were performed to investigate the effect of addition of SrHA and SrCaHA microspheres on the mechanical behavior of  $\eta$ -TSBCs as illustrated in Figure 11. The compressive strength of SrHA and SrCaHA cements exceeded minimum specification of 70 MPa (ASTM F451-99a (109)) for all compositions investigated. Figure 11 shows an overall comparison between the compressive properties (compressive strength, compressive modulus, and strain to failure) of the two different cements at increasing concentrations of SrHA and SrCaHA microspheres. The SrHA and SrCaHA cements presented significantly higher compressive strengths in comparison to the plain  $\eta$ -TSBCs, as shown in Figure 11(a). This parameter increased significantly with increasing SrHA/SrCaHA concentration up to 20% ( $p < 0.05$ ). However, mean compressive strengths of SrHA/SrCaHA cements were not significantly different at each

concentration. The behavior of the compressive modulus for the two cement formulations is illustrated in Figure 11(b). Similar to compressive strength, compressive modulus of the SrHA and SrCaHA samples increased significantly ( $p < 0.05$ ) with increasing SrHA/SrCaHA concentration. However, compressive modulus of the 10% SrHA/SrCaHA was not significantly different than the control cements. The type of the microspheres added (SrHA/SrCaHA) in the two-solution cement did not significantly affect the compressive modulus of the material at each concentration. The strain to failure is shown in Figure 11(c) for the two cement formulations and  $\eta$ -TSBC. Strains to failure of the  $\eta$ -TSBC and 10% SrHA/SrCaHA cements were not significantly different. However, there was a significant increase ( $p < 0.05$ ) in strain to failure with increasing microsphere concentration. There was no effect of the type of microsphere on the overall compressive properties of SrHA/SrCaHA cements considering the statistical analysis did not indicate significant differences between SrHA/SrCaHA cements at each concentration in the three parameters evaluated.

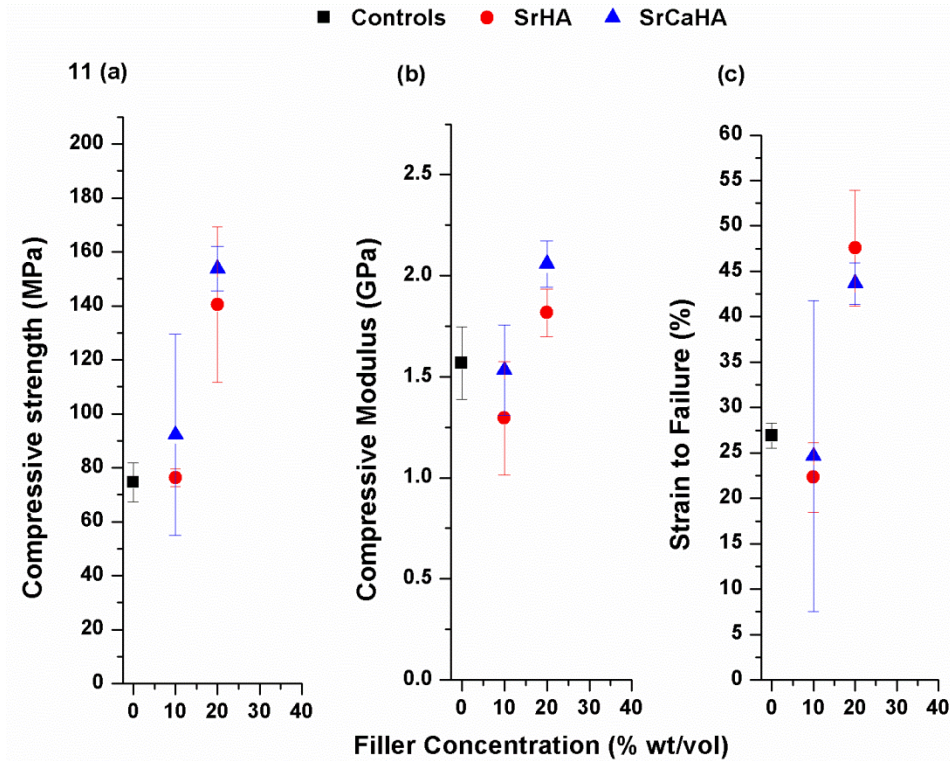


Figure 11. Compressive properties of two-solution bone cements prepared with increasing concentration of SrHA and SrCaHA microspheres. (a) Compressive strength, (b) Compressive modulus, and (c) Strain to failure. Cements prepared with SrHA and SrCaHA microspheres have significantly higher compressive strength than  $\eta$ -TSBCs and the compressive strength increased significantly with increasing SrHA/SrCaHA concentration ( $p < 0.05$ ).

### 5.3.2 Flexural properties

The effect of addition of SrHA/SrCaHA microspheres on the flexural properties of  $\eta$ -TSBCs is illustrated in Figure 12. The flexural properties are compared to the  $\eta$ -TSBC containing 20%  $ZrO_2$  radiopacifier. The flexural strength of  $\eta$ -TSBCs, Figure 12(a), did not change significantly with addition of SrHA/SrCaHA microspheres at 10% wt/vol concentration and were similar to the flexural strength of 20%  $ZrO_2$  composition. The flexural strength of SrHA/SrCaHA cements decreased significantly ( $p < 0.05$ ) at 20% wt/vol composition in comparison to the control samples. However, no significant

differences were observed between the flexural strengths at each concentration of SrHA/SrCaHA. There was no significant effect of SrCaHA concentration on the flexural modulus of the  $\eta$ -TSBC, as shown in Figure 12(b). No significant differences were observed in the flexural modulus between the control, 20% ZrO<sub>2</sub>, and SrCaHA cements. However, a significant decrease in flexural modulus ( $p < 0.05$ ) was observed with increasing SrHA concentration in comparison to control, SrCaHA and 20% ZrO<sub>2</sub> cement samples. Similar results were observed for strain to failure as shown in Figure 12(c). There were no significant differences found in the strains to failure between the control, SrCaHA, and 20% ZrO<sub>2</sub> cement compositions at each concentration. A significant increase ( $p < 0.05$ ) in strain to failure was observed with increasing SrHA concentration.

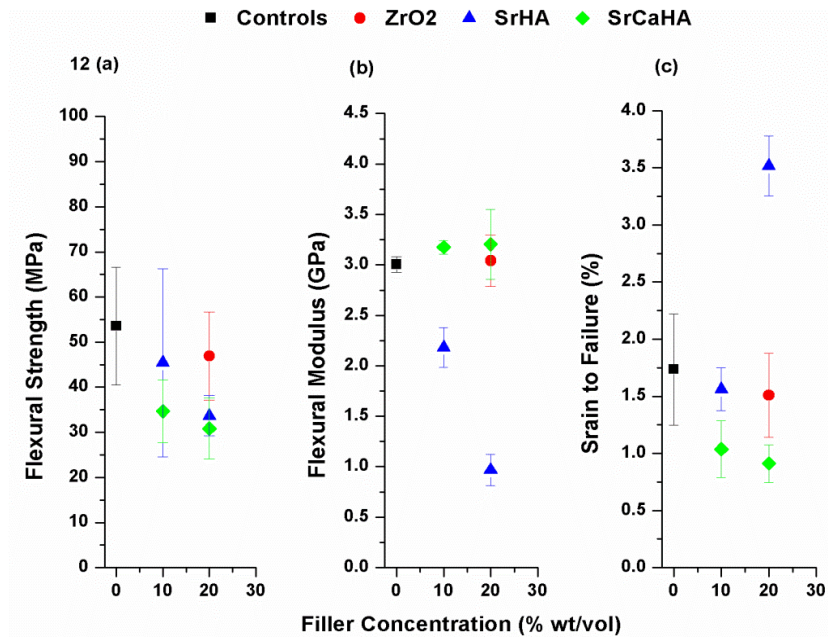


Figure 12. Flexural properties of  $\eta$ -TSBC, and  $\eta$ -TSBC prepared at 10 and 20% SrHA/SrCaHA and 20% ZrO<sub>2</sub>. (a) Flexural strength, (b) Flexural modulus, and (c) Strain to failure. The flexural strength reduced significantly with increasing SrHA/SrCaHA concentration ( $p < 0.05$ ). However, no significant differences were observed between strengths of SrHA and SrCaHA cements and between 20% ZrO<sub>2</sub> and SrHA/SrCaHA containing cement compositions.

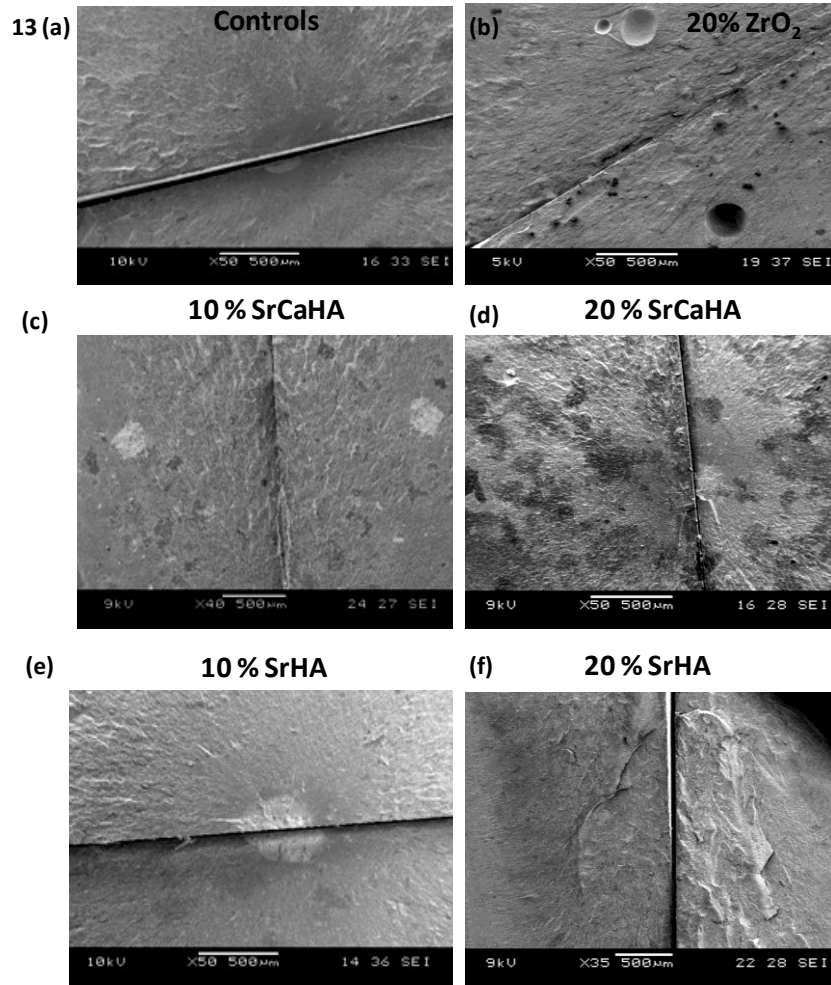


Figure 13. SEM micrographs of the fractured surfaces after flexural testing of the following compositions: (a) Controls (b) 20% ZrO<sub>2</sub> (c) 10% SrCaHA (d) 20% SrCaHA (e) 10% SrHA (f) 20% SrHA.

The 20% SrHA composition had significantly higher strain than all of the compositions. The strain to failure values for SrHA and SrCaHA were significantly different ( $p < 0.05$ ) at each concentration. The SEM micrographs in Figure 13(a-f) show the morphology of the fracture surfaces of flexural samples tested to failure. The fracture surface of  $\eta$ -TSBC, Figure 13(a), showed smooth mirror-like zones with striated areas, which might be an indication of a slow stable crack growth. A homogeneous nano bead-matrix structure can be observed at higher magnifications, in which nanospheres are very

close to each other. The fracture surface of 20% ZrO<sub>2</sub> composition, Figure 13(b), showed poor matrix-bead interface that allowed for crack branching. The ZrO<sub>2</sub> microspheres embedded in the matrix, debonded from the matrix creating pores in the 50-100 μm range. The fracture surfaces of all the SrHA/SrCaHA compositions, Figure 13(c-f), showed a very rough and chalky appearance due to SrHA/SrCaHA agglomerates indicating zones with slow crack propagation and crack arrest. Figure 14 (a,b) shows higher magnification SEM micrographs of fractured surfaces of 20% SrCaHA cements that showed lower strains to failure indicating that this composition is more susceptible to brittle failure. It can be observed that the regions where higher concentrations of nanosphere were present appeared darker in comparison to the region containing SrHA microspheres. These regions that have high concentrations of nanospheres and microspheres are relatively devoid of PMMA matrix. It is hypothesized that these regions of the cement are susceptible to brittle fracture and the inhomogeneous distribution of PMMA nanospheres and SrHA microspheres likely contributes to the lower strains at failure in these cements. In contrast, in regions of the fracture surface where these particles are well dispersed, there is evidence of plastic deformation in the PMMA matrix. The appearance of the fracture surfaces was consistent within each cement type, independent of the SrHA/SrCaHA concentration.

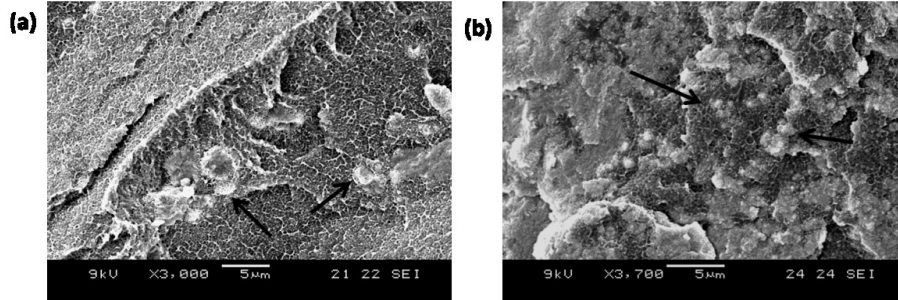


Figure 14. High magnification SEM micrographs of the fractured surfaces of (a) and (b) 20% SrCaHA cements indicating ductile fracture where regions with higher concentration of nanospheres and depleted matrix was observed. Black arrows indicated the regions having SrHA microspheres embedded in the cement matrix (white region).

### 5.3.3 Fracture toughness

The effect of SrHA/SrCaHA microspheres on the fracture toughness of  $\eta$ -TSBC is presented in Figure 15. The results from Figure 15(a) showed that addition of SrHA or SrCaHA microspheres at different concentrations did not significantly affect the fracture toughness of the  $\eta$ -TSBCs. There were no significant changes in the stress intensity factor ( $K_{IC}$ ) between all the compositions and 20%  $ZrO_2$  cements. The SEM micrographs in Figure 15(b-g) show morphology of the fractured surfaces and crack propagation in all of the fracture toughness samples tested to failure. The fractured surfaces for the control samples, Figure 15(b), showed smooth regions at the crack initiation followed by striated areas indicating slow crack growth. The fractured surfaces of 20%  $ZrO_2$  samples, Figure 15(c), showed crack propagation around and not through the  $ZrO_2$  beads/agglomerates, along with debonding of microspheres from the matrix creating pores. All of the fractured surfaces of the SrHA and SrCaHA compositions, Figure 15(c-g) and Figure 16 (a,b), also showed crack propagation around the microspheres and not through the beads, in which the matrix-bead interface allowed for

crack branching. The backscattered SEM micrograph of the 20% SrCaHA fractured surface showed a non homogeneous distribution of SrCaHA particles, with some dispersed particles along with some agglomerates in the matrix. However, cracks were mainly observed to propagate through the nanosphere-PMMA matrix and around the microspheres. Debonding of microspheres from the matrix was not observed, and thus no evidence of porosity was seen with SrHA/SrCaHA compositions.

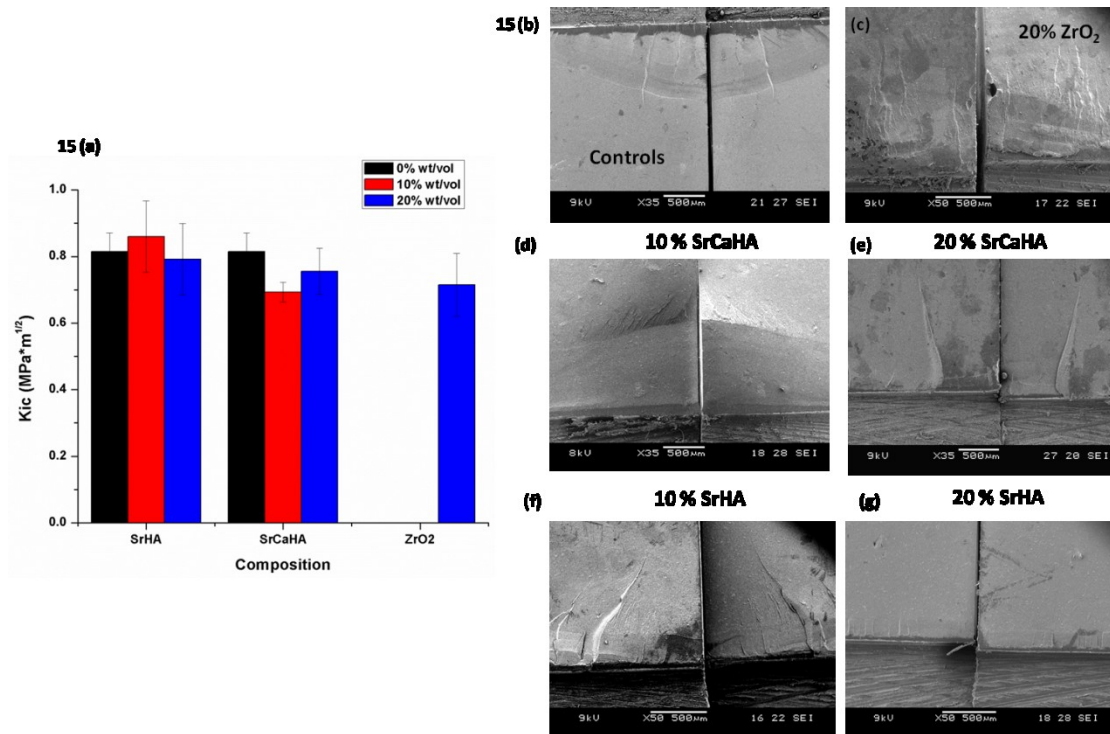


Figure 15. (a) Fracture toughness of  $\eta$ -TSBCs prepared at increasing concentration of SrHA and SrCaHA microspheres. There was no significant effect of addition of SrHA/SrCaHA microspheres on the fracture toughness of  $\eta$ -TSBCs. SEM micrographs of the fractured surfaces depicting the crack propagation in the following cement compositions: (b) Controls (c) 20% ZrO<sub>2</sub> (d) 10% SrCaHA (e) 20% SrCaHA (f) 10% SrHA (g) 20% SrHA.

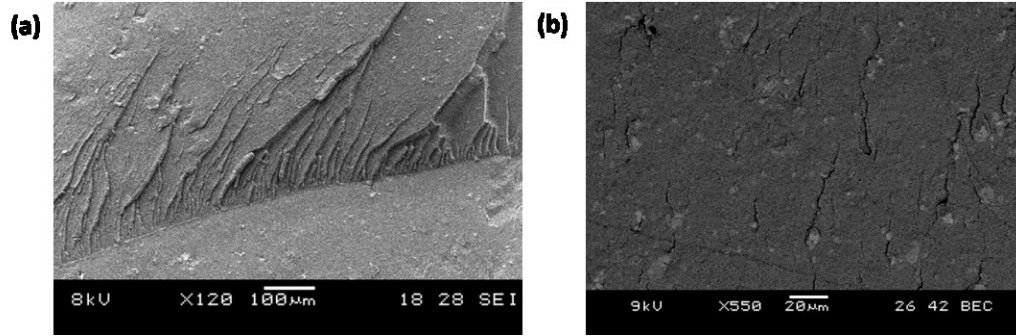


Figure 16. High magnification SEM micrograph of fractured (a) 10% SrCaHA and backscattered SEM micrograph of fractured (b) 20% SrCaHA cement surfaces showing advancement of the main crack via microcracks through the matrix around the SrCaHA beads/agglomerates.

## 5.4 Discussion

The effect of addition of SrHA/SrCaHA microspheres at varying concentrations was evaluated on the mechanical properties of  $\eta$ -TSBC formulation.  $\eta$ -TSBCs containing SrHA/SrCaHA microspheres presented significantly higher compressive strengths in comparison to control  $\eta$ -TSBCs as illustrated in Figure 11. The compressive strength of these two formulations increased significantly with an increase in SrHA/SrCaHA concentration up to 20% wt/vol. The predominant mode of loading in spine *in vivo* is axial compression, hence the measurement of compression strength values of the prepared cements were important. The values of compressive strength reported here for all formulations were higher than the minimum required by the ASTM regulations (70 MPa), and were well within the reported values for commercial cements (77 to 150 MPa) (26). There was no significant effect of the type of microspheres on the compressive strengths at each concentration indicating that both SrHA and SrCaHA microspheres were capable of increasing the compressive strength of the  $\eta$ -TSBC. Kobayashi et al. (108) incorporated 50, 70, and 80 % w/w of HA filler in Bis-GMA cements and investigated the compressive

and bending properties of the cements. They reported compressive strength values as high as  $157 \pm 4$  MPa and  $158 \pm 9$  MPa for their 50 and 70 % HA compositions, respectively. Serbetci et al. (107) also observed an increase in the compressive strength of PMMA bone cement from 96 MPa to 122 MPa with increasing HA concentration up to 14 wt %. They concluded that further increase in filler concentration may lead to decreased compressive properties, as HA particles distributed homogeneously in small quantities can behave as load carriers leading to enhanced mechanical properties; however, an increase in HA concentration may lead to their aggregation and non homogeneous distribution resulting in poor adhesion to the matrix and decreased compressive strength. Furthermore, they explained that the thermal expansion coefficient of HA particles was 10 times less than that of PMMA and hence their volumetric changes post polymerization would not be similar. After polymerization when both the materials shrink, the shrinkage of PMMA matrix would be more than the shrinkage of HA particles, resulting in HA particles that are trapped to be squeezed firmly in the PMMA matrix and causing a hoop stress to be formed adjacent to the HA particles (107). This hoop stress would simulate a weak bonding between HA particles and PMMA matrix and hence, during compressive load application the interface between the two phases would act like a grain boundary resisting propagation of crack. However, when a tensile load would be applied, the direction of the crack propagation would be perpendicular to the direction of the hoop stress and the applied load, wherein the hoop stress would help the crack edges to be separated. They concluded that HA-containing cements were weaker in tension than in compression (107).

Measurements of the flexural properties of SrHA/SrCaHA cements (Figure 12) revealed a decrease in the flexural strength of the  $\eta$ -TSBCs with increasing

SrHA/SrCaHA microsphere concentration. The strain to failure of  $\eta$ -TSBC decreased with addition of SrCaHA microspheres indicating that these compositions were more susceptible to brittle failure. However, the SEM micrographs of the fractured SrHA/SrCaHA surfaces also showed some ductile deformation. The fractured SrHA/SrCaHA surfaces were rougher in comparison to the control cements, and agglomeration of these microspheres was visible at higher concentrations and could be one of the reasons for lower flexural strengths. A decrease in flexural modulus was also observed with increasing SrHA concentration. It can be hypothesized that such a decrease in modulus could be a result of incomplete polymerization, resulting in a lower glass transition temperatures ( $T_g$ ) and changes in the density of the polymerized samples. A further evaluation of the effect of changes in polymerization reaction due to addition of ceramic SrHA filler needs to be performed using differential scanning calorimetry in order to measure the changes in the  $T_g$ . Also, density gradient columns can be used in order to measure the changes in the densities of the cured samples. Furthermore, no porosity was observed on the fractured SrHA/SrCaHA cement surfaces, indicating that the introduction of SrHA/SrCaHA microspheres to the cement mixture did not cause bubbling during polymerization giving rise to porosity. Incomplete polymerization could result in a lower molecular weight for the PMMA matrix, along with an increase in the residual monomer content; both of which could impact the mechanical properties of the polymerized cements. An increase in the concentration of residual monomer in the cement could have a plasticizing effect, thereby increasing the strain to failure of these materials. However, a decrease in the molecular weight of the polymerized matrix will ultimately result in cements with lower flexural strength. Thus these parameters need to

be evaluated in future studies to better understand the mechanical behavior of these cements. Agglomeration of the SrHA/SrCaHA microspheres results in poor integration of these particles with the surrounding PMMA matrix. These regions may be more susceptible to crack initiation, leading to an overall reduction in the mechanical properties of these cements. Future efforts should be focused on obtaining polymerized cements with a homogeneous distribution of both PMMA nanospheres and SrHA microspheres throughout the PMMA matrix. A linear decrease in flexural properties with increasing HA (irregular in shape, sized 420-1000  $\mu\text{m}$ ) concentration up to 30 wt% has been observed by Kwon et al. (39). They incorporated HA powder at concentrations 0, 10, and 30 wt% into commercially available bone cement CMW1<sup>TM</sup> (CMW laboratories, UK). Cheung et al. (70) tested SrHA nano powder (10% Sr substitution) containing Bis-GMA resin cement and observed a similar decrease in the flexural properties as compared to commercially available PMMA cements. They reported a bending strength around 31 MPa, similar to the flexural strengths observed in this study for SrHA/SrCaHA containing  $\eta$ -TSBCs. They conclude that this decrease in bending strength and bending modulus is beneficial as it would bring these values closer to those observed for human cancellous bone and would reduce the fractures caused to the adjacent vertebrae due to the problem of modulus mismatch between the bone-bone cement (70). Leong et al. (112) also incorporated SrHA powder (10% Sr substitution) in a Bis-GMA resin blend at concentration of 40 wt% and tested their compressive and bending properties. They too report a reduced bending strength of  $31.3 \pm 3.2$  MPa for SrHA-Bis-GMA cements in comparison to the Simplex P (80 MPa) and Palacos R (79.6 MPa) commercial PMMA cements tested. However, it is important to note that the flexural strengths of

SrHA/SrCaHA  $\eta$ -TSBCs at each concentration were not significantly different to the 20% ZrO<sub>2</sub>  $\eta$ -TSBC composition, indicating that these microspheres can be incorporated into the  $\eta$ -TSBC to impart radiopacity and bioactivity instead of ZrO<sub>2</sub> without any further detrimental effect to their mechanical properties than has been observed by Rodrigues et al. (30).

The fracture toughness ( $K_{IC}$ ) results are shown in Figure 15. There was no significant effect of the addition of increasing concentration of SrHA/SrCaHA microspheres on the fracture toughness of  $\eta$ -TSBC. Once again, there were no significant differences between all compositions of SrHA/SrCaHA cements and 20% ZrO<sub>2</sub>  $\eta$ -TSBC, indicating that inclusion of these microspheres were not detrimental to the fracture toughness properties of  $\eta$ -TSBC. Vallo et al. (101) studied the fracture toughness properties of PMMA cements (Subiton, Subiton Laboratories) containing increasing concentrations of HA and observed that the  $K_{IC}$  values increased with increasing HA concentration up to only 2.5 wt% HA inclusion ( $K_{IC}$  value 1.62 MPa\*m<sup>1/2</sup>). At higher concentrations of HA, they observed that the fracture toughness ( $K_{IC}$ ) decreased monotonically with filler content. The fractured SrHA/SrCaHA surfaces, examined under SEM in this study, appeared very rough indicating considerable crack branching. At higher magnifications it was observed on SrHA/SrCaHA surfaces that the crack propagation stopped once it found a bead or agglomeration of these microspheres and continued around agglomerates. Despite a reduction in  $K_{IC}$  value in comparison to STSBC (1.73 MPa\*m<sup>1/2</sup>),  $\eta$ -TSBCs containing SrHA/SrCaHA microspheres studied here had  $K_{IC}$  values similar to  $\eta$ -TSBC ( $0.8 \pm 0.05$  73 MPa\*m<sup>1/2</sup>) and  $\eta$ -TSBC with 20% ZrO<sub>2</sub> ( $0.71 \pm 0.09$  73 MPa\*m<sup>1/2</sup>) and were within the reported values for commercial cements (0.88 – 2.2 MPa\*m<sup>1/2</sup>) (113, 114).

However, due to the variation in type and concentration of bioactive fillers, cement matrix composition, and the mechanical properties tested across various studies, it is difficult to make a suitable comparison of our results to the values that have been reported in literature. The SrHA/SrCaHA filled  $\eta$ -TSBCs tested here have adequate mechanical properties to be used for vertebroplasty (VP) / kyphoplasty (KP) applications. The variation in the amount of strontium-substitution in the SrHA microspheres incorporated into  $\eta$ -TSBC did not have a significant effect on any of the static mechanical properties tested. This was expected, as these microspheres had the same morphology, size, and structure and differed only in their chemical composition that would pre-dominantly have an effect on the bioactivity and antibacterial properties. Hernandez et al. (68, 74) investigated compressive properties of PMMA cements containing SrHA nanopowder (10% Sr) at concentrations of 10 and 20 wt% in air at room temperature as well as after storing the specimens in SBF for a month at body temperature. They reported decreased compressive strength and modulus for the SrHA cements stored in SBF for a month, due to the plasticizing effect introduced by absorbed water. These observations necessitate a follow up study that would determine changes in the cement mechanical properties under physiological conditions after formation of apatite on their surfaces (through either being soaked in SBF *in vitro* or after apatite formation *in vivo*).

## 5.5 Conclusions

Overall, this study evaluated the flexural, compressive, and fracture toughness properties of  $\eta$ -TSBCs containing increasing concentrations of SrHA and SrCaHA microspheres. Inclusion of SrHA/SrCaHA microspheres caused an increase in compressive

strength and compressive modulus with increasing SrHA/SrCaHA concentration, which makes them suitable for VP/KP applications. The flexural properties of SrHA/SrCaHA cements at higher concentrations (20% wt/vol) were lower than  $\eta$ -TSBCs; however, the obtained values were still similar to  $\eta$ -TSBC containing 20% ZrO<sub>2</sub>, indicating no further detrimental effect on the  $\eta$ -TSBC properties while replacing ZrO<sub>2</sub> with SrHA/SrCaHA in order to impart radiopacity and improve bioactivity. No significant changes were observed in the fracture toughness properties of  $\eta$ -TSBCs with incorporation of SrHA/SrCaHA microspheres at increasing concentrations. The fractographic analysis revealed the presence of areas of ductile fracture and microsphere agglomeration that could explain the decrease of mechanical properties of SrHA/SrCaHA  $\eta$ -TSBCs. Further studies investigating the effect immersion of SrHA/SrCaHA  $\eta$ -TSBCs in SBF at body temperature on their mechanical properties need to be performed.

## Chapter 6

---

### 6 *In vitro* evaluation of antibacterial properties of two-solution bone cements containing strontium-hydroxyapatite microspheres

In this chapter, the antimicrobial properties of two-solution bone cement ( $\eta$ -TSBC) containing strontium-substituted hydroxyapatite microspheres (Sr HA (100% Sr substitution), SrCaHA (50% Sr substitution)) were investigated *in vitro* by culturing *Escherichia coli* (E. coli) K12/pRSH103 biofilm. It was hypothesized that the capacity to inhibit bacterial growth would increase with increasing concentrations of strontium hydroxyapatite microspheres in  $\eta$ -TSBC and with increasing percentage of strontium substitution in strontium hydroxyapatite microspheres. The concentration of the SrHA/SrCaHA microspheres in the cements was varied at 0 (controls), 5, 10, and 20 % w/vol. The cements containing 20% wt/vol of SrCaHA or SrHA microspheres exhibited the greatest reduction in biofilm formation, 80% and 88% respectively, in comparison to the plain control cements. However, there were no significant differences between cements containing 20% wt/vol of SrCaHA and SrHA microspheres. At lower concentrations (5% and 10% wt/vol), the cements containing SrCaHA microspheres reduced biofilm growth more significantly than the cements containing SrHA microspheres. Additionally, the long-term effects of biofilm inhibition by cements containing 0, 10, and 20% wt/vol SrHA microspheres were studied over a period of 14 days where the 10% and 20% compositions were found to continually inhibit biofilm growth up to day 14.

## 6.1 Introduction

Polymethylmethacrylate (PMMA) was one of the first biomaterials produced by the chemical industry and it is still the most common material used in joint replacements and orthopedic surgeries (12). However, most medical devices as well as biomaterials are associated with 60-70% of all nosocomial infections (115, 116). The use of PMMA, like any other biomaterial, entails a risk of attracting infectious microorganisms. Biomaterial-associated infections pose great surgical problems as infected implants generally require surgical removal and since removal is not always easy, patients suffer severe discomfort (117). These infections are a result of bacterial adhesion and subsequent colonization leading to the inevitable biofilm formation at the implantation site (116). Buchholz (118) first incorporated antibiotics in PMMA bone cements in order to reduce infection and many studies have been performed since then with different materials and antibiotics (13). Apart from gentamicin sulphate, antibiotics such as erythromycin, tobramycin, vancomycin, and clindamycin have also been studied as additives for bone cements (13). Hernandez et al. (119) studied the antibiotic release of ciprofloxacin (CFX) and vancomycin (VM) from PMMA cements immersed in PBS for a period of 1 month. They observed a burst effect for VM release, whereas no burst effect was observed for CFX and after a month in PBS, CFX release was almost finished. Beeching et al. (120) conducted a comparative study about persistence of antibacterial activity around antibiotic loaded PMMA bone cement discs seeded on agar plates. The cement discs containing 2.5 wt% of cephalothin, coumermycin, or fusidic acid antibiotics and inoculated with *Staphylococcus aureus* (S. Aureus) bacteria produced inhibition zones for four to eight weeks. They concluded that many factors such as stability and kinetics of antibiotics loaded, diffusibility of antibiotics

in agar, and the susceptibility of the indicator organism affect the size of the inhibition zones. Several of these studies have however shown that antibiotic loaded PMMA cements have relatively low drug elution property with various antibiotics (13). Furthermore, concerns over the prolonged exposure of microorganisms to antibiotics such as gentamycin, vancomycin, or erythromycin, in PMMA cements were raised, suggesting that bacterial resistance could potentially be developed (14, 20, 21). Inclusion of yet another filler material into the bone cement matrix also affects the cement mechanical properties. Additions of antibiotic fillers to bone cements have been known to impact their mechanical properties (12). Hernandez et al. (119) saw a decrease in flexural properties, but no significant decrease in compressive properties of PMMA cements loaded with CFX and VM. All of the above mentioned concerns raise the need for developing alternative filler materials in place of antibiotics.

Recently, strontium substituted hydroxyapatite nano powder was used to coat implant surfaces (3, 24) as an alternative to antibiotics. Strontium (Sr), a trace element found in human body, is thought to be an antibiotic (4), effective in enhancing the bioactivity (57) of biomaterials, and have potential in the treatment of osteoporosis (2, 60). The addition of Sr as a dopant (1 wt% strontium oxide) to hydroxyapatite coating on titanium implants also showed significant positive enhancement of human fetal osteoblast cell proliferation and differentiation activity (24). PMMA bone cement containing strontium substituted hydroxyapatite nano powder (SrHA, 10% Sr) has been reported to have enhanced bioactivity due to release of strontium ions ( $\text{Sr}^{2+}$ ) which not only promotes osteoblast proliferation, but also facilitates precipitation of apatite, thus increasing the mechanical strength of the bone-implant interface (71, 74). Moreover, the antibacterial

properties of the HA nanoparticles have been observed to improve after calcium is partially or totally substituted by strontium indicating that introduction of strontium is a major contributor in imparting antibiotic properties (1). Preliminary work on glass ionomer dental cements (GICs) containing strontium oxide and fluoride fillers also revealed that greatest antibacterial activity was observed with strontium oxide in comparison to fluoride (4). However, they could not explain the mechanism by which strontium cements had greater bactericidal action than fluoride. Deposition of strontium substituted apatites on metal implant surfaces like titanium showed promising levels of microbial inhibition as well as prolonged ability to reduce bacteria over a 30 day period (3). Gentamicin loaded Bis-GMA cement containing SrHA nano powder (10% Sr) was evaluated as a drug delivery system by Liu et al. (121). They confirmed that SrHA-Bis-GMA cements had significant bactericidal action in comparison to PMMA cements as seen by the inhibition of *S. Aureus* by release of gentamicin after 30 days. However, their study also focused on investigating the mechanism of gentamicin elution from SrHA/Bis-GMA cements in comparison to PMMA cements, and not on the antibacterial properties of strontium. There is enough evidence in literature that strontium substituted HA powder does possess bactericidal characteristics. However, due to limited number of published studies on the *in vitro* antibacterial action of the Sr ion, the possible mechanism behind the bactericidal action has not been understood completely. Also, the ability of SrHA bioactive filler to possibly act as an antibiotic agent when added to acrylic bone cements for improving bioactivity has not been tested or studied so far. In this study the antibacterial properties of two-solution bone cements ( $\eta$ -TSBC) containing strontium-calcium hydroxyapatite (SrCaHA, 50% Sr substitution) and strontium hydroxyapatite (SrHA, 100% Sr substitution)

microspheres were investigated *in vitro* by culturing *Escherichia coli* K12/pRSH103 biofilm. The purpose of this study was to assess the possibility of introducing additional antibiotic properties to two-solution bone cements along with radiopacity and bioactivity by incorporation of SrHA/SrCaHA microspheres as a filler material.

## 6.2 Materials and Methods

### 6.2.1 Bone cement preparation

The SrHA and SrCaHA microspheres (2-5  $\mu\text{m}$  in diameter) were synthesized as described by Zhang et al.(2, 83) and the atomic ratios of Sr/P and (Ca+Sr)/P were set as 1.67. The SrCaHA microspheres were prepared using the same hydrothermal procedure; however in this case the  $[\text{Sr} / (\text{Sr} + \text{Ca})]$  molar ratio was set as 0.5. The two-solution bone cements containing cross-linked polymethylmethacrylate nanospheres ( $\eta$ -TSBC), used as controls, were prepared as described by Rodrigues and co-workers (81, 82) at a polymer to monomer ratio of 1:1 and cross-linked PMMA nanospheres to linear PMMA ratio of 1.5:1. For the preparation of  $\eta$ -TSBCs, benzoyl peroxide (BPO) (Aldrich), *N, N*-dimethyl *p*-toluidine (DMPT) (Aldrich) and methylmethacrylate (MMA) (Fluka) were used as received without further purification. The  $\eta$ -TSBCs were made up of two polymer phases: 1) dissolved linear PMMA ( $P_l$ ), and 2) dispersed cross-linked PMMA nanospheres ( $P_b$ ). These two components were massed and mixed together forming the powder phase (P). A part of the total volume of MMA was split and added to two graduated cylinders, in which one was mixed with 1.25 g of BPO (1.25 g/100 ml of MMA) and other with 0.7 ml DMPT (0.7 ml/100 ml of MMA). The two mixtures

BPO/MMA and DMPT/MMA were transferred to two polypropylene cartridges followed by the addition of the powder phase and remaining MMA. The cartridges were sealed, vigorously agitated by hand, and placed on a rotating drum mixer for 18 h. Following mixing, the cartridges were stored upright at 4°C for 48 hours before use. In order to prepare the  $\eta$ -TSBCs containing strontium substituted microspheres, the SrHA and SrCaHA microspheres were added to the polymer phase at concentrations of 5, 10, and 20% wt/vol of MMA and the mixing procedure remained the same as described above for the  $\eta$ -TSBCs. The cements were then injected into square molds (0.5 inch in length and 1mm in thickness) and circular disk molds (6 mm diameter and 1 mm in thickness), and allowed to polymerize for the casting of samples for the antibacterial tests.

### **6.2.2 Antibacterial tests: 24 hours and long-term**

*E. coli* K12 strain RP437/pRSH103 from the study by Hou et al. (122) was used to study the antimicrobial properties of the bone cements. The strain was labeled with a constitutive Ds-Red Express (BD Franklin Lakes, NJ) fluorescent protein. An overnight culture of *E. coli* RP437/pRSH103 was grown in Luria-Bertani (LB) medium containing 1 g/L bacto-tryptone, 5 g/L yeast extract and 10 g/L sodium chloride in deionized water. Tetracycline (10 $\mu$ g/ml) was added as a supplement to help maintain the plasmid pRSH103. The culture was incubated on an orbital shaker at 200 rpm at 37°C in the dark (Orbit Shaker Model 3520, Lab-line Instruments, Melrose Park, IL). Prior to inoculation, all of the cement samples were sterilized with ethanol, dried with a sterile 0.2  $\mu$ m air filter, and placed in a Biological Safety Cabinet (Purifier Logic 34600 Series, Labconco,

Kansas City, MO) for 20 minutes under a UV light source. Following sterilization, three samples from 0, 5, 10, and 20% SrHA and SrCaHA cement compositions were placed in sterile petri dishes containing 20 ml of sterile LB medium with 10 $\mu$ g/ml tetracycline. The optical density at 600 nm (OD<sub>600</sub>) of the overnight culture was measured with a Genesis 5 spectrophotometer (Spectronic Instruments, Rochester, NY) and the dishes were inoculated with the overnight culture at an OD<sub>600</sub> of 0.05. The petri dishes were then placed in an incubator at 37°C in the dark without shaking for 24 hours.

Following incubation for 24 hours, the cement samples were gently washed three times with 0.85 % sodium chloride buffer to remove planktonic cells. The samples were then analyzed for biofilm surface coverage (%) using an Axio Imager M1 fluorescence microscope (Carl Zeiss MicroImaging GmbH, Göttingen, Germany) with a mercury vapor shot-arc lamp at 558 nm (HBO 103 W/2, OSRAM GmbH, Augsburg, Germany). At least five images were randomly taken of each bone cement sample and control, creating 15 images of each composition. The biofilm surface coverage (%) was calculated from the images using the COMSTAT software written on the MATLAB platform (123). Additionally, the long-term effects of biofilm inhibition by cements containing 0, 10, and 20% wt/vol SrHA microspheres were studied over a period of 14 days. In this study, triplicate samples were analyzed on day 1, 6, 10 and 14. The samples were transferred daily to new petri dishes containing fresh LB media supplemented with 10  $\mu$ g/ml of tetracycline. The culture was inoculated daily with cells from overnight culture in which the cell concentration was adjusted to the OD<sub>600</sub> of 0.05. The samples were analyzed for biofilm surface coverage, at each time point, as described above. The

statistical analysis for percentage of biofilm surface coverage was performed using one-way ANOVA with a Tukey post-hoc test at a level of significance of 95%.

### **6.2.3 Antibacterial inhibition zone test**

Antibacterial activity was also evaluated using the agar gel inhibition zone method, which has been employed previously (1, 4, 120). The test bacteria was *E. coli* K12 strain RP437. Sterile LB Agar medium containing 1 g/L bacto-tryptone, 5 g/L yeast extract, 10 g/L sodium chloride, and 15 g/L agar in deionized water was poured into plates. The agar was allowed to gel overnight and the agar plates were then stored at 4°C before use. The *E. coli* culture was incubated on an orbital shaker at 200 rpm at 37°C in the dark for 16 hours (Orbit Shaker Model 3520, Lab-line Instruments, Melrose Park, IL). The optical density at 600 nm (OD<sub>600</sub>) of the overnight culture was measured with a Genesis 5 spectrophotometer (Spectronic Instruments, Rochester, NY). The inoculum suspension from the overnight culture was distributed evenly over the surface of the LB agar gel plates at an OD<sub>600</sub> of 0.05. All of the cement samples were sterilized with ethanol, dried with a sterile 0.2 µm air filter, and placed in a Biological Safety Cabinet (Purifier Logic 34600 Series, Labconco, Kansas City, MO) for 20 minutes under a UV light source. Following sterilization, three cement disc samples of 0, 10, and 20% SrHA and SrCaHA compositions were placed tightly onto the agar gel plates inoculated with *E. coli* and incubated at 37°C for 24 hours. In addition to this, three 20% SrHA discs having SrHA powder on their surface and three 20% SrCaHA discs having SrCaHA powder on their surfaces were also placed onto the agar gel plates and incubated at 37°C for 24 hours. The SrHA/SrCaHA powders were used on the cement surfaces to determine

whether contact inhibition is the primary mode of bacterial inhibition observed in these cement compositions. Disc diameters were measured and the size of the inhibition zone was calculated as follows:

$$\text{Size of the inhibition zone (mm)} = (\text{diameter of zone of inhibition} - \text{diameter of the disc}) / 2$$

If the inhibition zone was less than 5-7 mm, the test inhibitor could be determined to have the antibacterial property at the condition of static contact with the bacteria. The statistical analysis for size of the inhibition zone was performed using one-way ANOVA with a Tukey post-hoc test at a level of significance of 95%.

## 6.3 Results

### 6.3.1 24 hour antibacterial study

The antibacterial activities of the SrHA and SrCaHA containing cements were evaluated by analyzing *E.coli* biofilm formation on these materials, after 24 hours, using fluorescence microscopy. To provide a quantitative comparison of biofilm growth, the images were analyzed with COMSTAT and the percentage of biofilm coverage was calculated and plotted as shown in Figure 17(a). Antibacterial activity of the SrCaHA and SrHA cement was clearly confirmed by growth inhibition of *E. coli* in Figure 17(b-h). Figure 17(a, e, h) showed that the 20% SrHA and 20% SrCaHA composition exhibited significantly higher ( $p < 0.05$ ) reduction in biofilm formation, 80% and 88% respectively, in comparison to the plain control cements. A linear decrease ( $r^2 = 0.99$ ) in biofilm surface coverage was observed with increasing SrHA microsphere concentration, as expected. However, the biofilm surface coverage for 5% SrHA composition was not significantly

different from the control cements as also observed from Figure 17(a, b-d). The 10% SrHA samples had a  $2.53 \pm 0.56$  % surface coverage, which was a 33% reduction in biofilm growth compared to the control cement. The surface coverage on 5% and 10% SrCaHA composition was not significantly different from each other (Figure 17(f, g)), although it was significantly different from the control and the 20% SrCaHA samples ( $p < 0.05$ ). At lower concentrations (5% and 10% wt/vol), the cements containing SrCaHA microspheres reduced biofilm growth more significantly ( $p < 0.05$ ) than the cements containing SrHA microspheres.

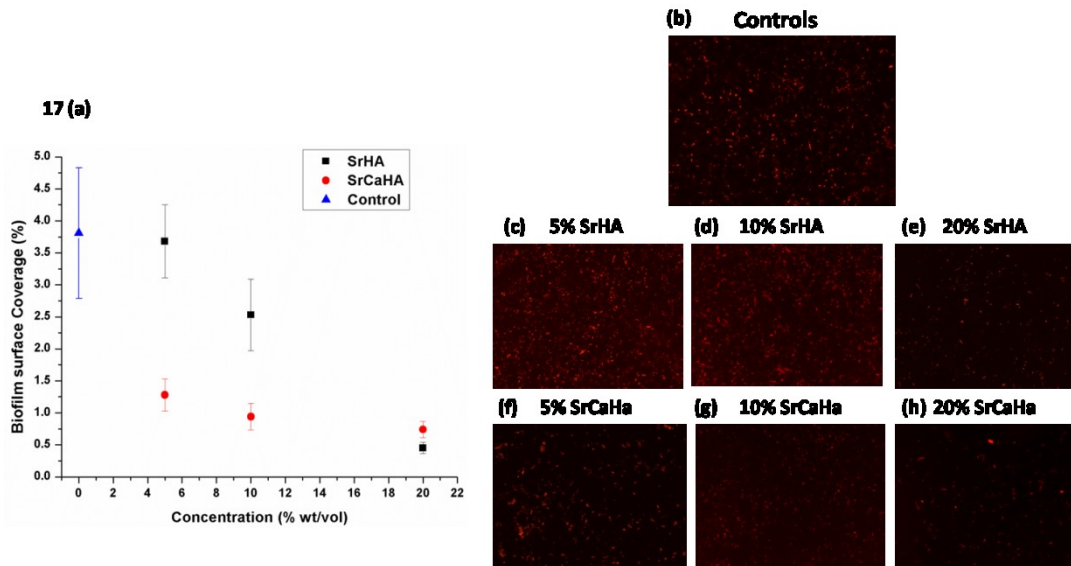


Figure 17. Antibacterial study with *E.coli* for 24 hours. (a) Graphical representation of the biofilm surface coverage (%) as a function of the concentration of SrHA and SrCaHA filler. The 20% SrHA and SrCaHA compositions showed the strongest biofilm inhibition compared to the controls. A significant linear decrease in biofilm coverage was observed with increasing concentration of SrHA filler. Fluorescence micrographs of *E.coli* biofilm formation on (b) Controls, (c) 5% SrHA, (d) 10% SrHA, (e) 20% SrHA, (f) 5% SrCaHA, (g) 10% SrCaHA, (h) 20% SrCaHA samples (all at 20X magnification). Maximum biofilm coverage is observed on control, 5% SrHA, and 5% SrCaHA samples.

### 6.3.2 Long-term antibacterial tests

In order to evaluate the long-term inhibition of biofilm formation, the 10% and 20% SrHA samples were challenged with *E.coli* RP437 pRSH103 in LB medium for varying periods of time (up to 14 days). Figure 18(a) showed that the 20% SrHA composition was successful in continually inhibiting biofilm growth until day 14 in comparison to the control samples. After incubation for 1 day, only several attached cells could be seen on the 20% SrHA samples (Figure 18(b)). In contrast, the control and 10% SrHA samples were extensively covered by *E.coli* biofilm. The 10% SrHA samples significantly ( $p < 0.05$ ) reduced the biofilm coverage up until day 6 (Figure 18(c)), after which there were no significant differences observed in biofilm coverage in comparison to the control cements. When incubated for 14 days, the 20% SrHA surface still had only  $11.99 \pm 1.71\%$  biofilm coverage, while the surface coverage on the control and 10% SrHA was  $21.23 \pm 3.45\%$  and  $16.00 \pm 3.61\%$ , respectively. *E.coli* clusters were apparent on both, control and 10% SrHA samples, at day 14 (Figure 18(e)) covering the entire surface of the cements.

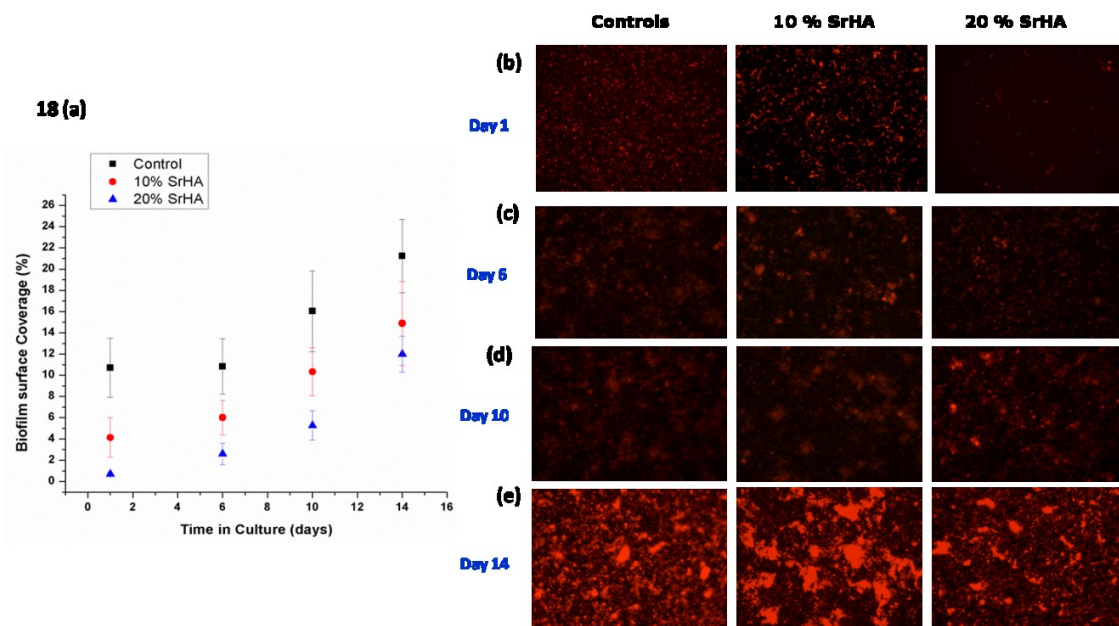


Figure 18. Long-term antibacterial study. (a) Graph of the *E. coli* biofilm surface coverage (%) as a function of time in culture. The 20% SrHA samples showed continued significant biofilm inhibition up till day 14 as compared to controls. The fluorescence micrographs of *E. coli* biofilm formation on controls, 10% SrHA, and 20% SrHA samples on (b) day 1 (c) day 6 (d) day 10 and (e) day 14 (all at 20X magnification). The least amount of biofilm growth was visible on the 20% SrHA samples on day 14.

### 6.3.3 Inhibition zone test

The results from the inhibition zone test are shown in Figure 19(a-h). The results demonstrated that none of the inhibition zones of SrHA/SrCaHA cements to the test bacteria were more than 7 mm. The largest inhibition zones were observed with the cement discs containing SrHA/SrCaHA powder on their surfaces (Figure 19(g,h)). Figure 19(a) indicated that there were no significant differences in the size of the inhibition zones between different SrHA and SrCaHA cement compositions. Each cement composition exhibited some degree of antibacterial activity, although it was observed to be the greatest for 20% SrCaHA cement having SrCaHA powder on its surface ( $p < 0.05$ ).

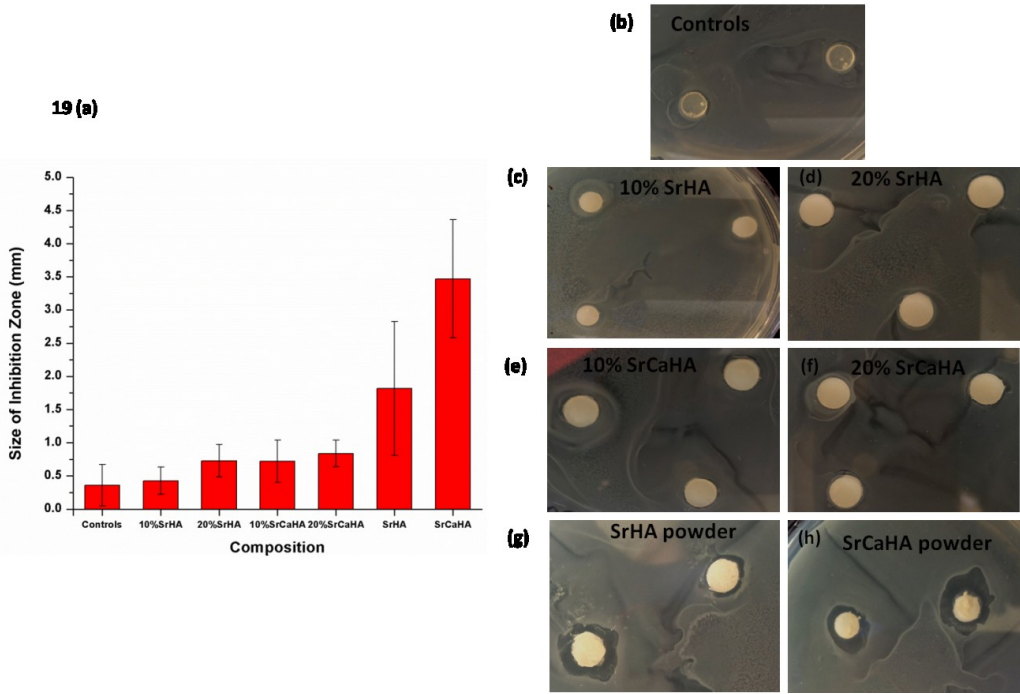


Figure 19. Antibacterial inhibition zone test. (a) Graph of the size of the inhibition zone (mm) as a function of cement composition. Antimicrobial activity was the greatest in the case of cements that had SrHA/SrCaHA powder on their surface indicating that contact inhibition was the primary mode of bacterial inhibition. Zones of inhibition produced after overnight incubation at 37°C of SrHA and SrCaHA containing cement discs on supplemented LB agar seeded with *E.coli* biofilm, (b) Controls, (c) 10% SrHA, (d) 20% SrHA, (e) 10% SrCaHA, (f) 20% SrCaHA, (g) SrHA powder on 20% SrHA cement surface, and (h) SrCaHA powder on 20% SrCaHA cement surface.

## 6.4 Discussion

The SrHA and SrCaHA cements were observed to successfully inhibit biofilm formation. However, as expected, higher concentrations (20% wt/vol) of SrHA and SrCaHA cements were the most effective in reduction of biofilm coverage. A linear decrease in biofilm growth was observed with increasing SrHA concentration indicating that the bactericidal action was dependent on the amount of SrHA microspheres

incorporated. The results of this study agree with previous observations that substitution of strontium in hydroxyapatite used as a coating on implants can improve their antibacterial properties (1, 3, 4, 24, 76, 121). The 5% and 10% SrCaHA samples were found to inhibit biofilm formation more significantly than the 5% and 10% SrHA cements, while the 20% SrCaHA and 20% SrHA samples provided similar levels of biofilm inhibition. This may suggest that the calcium had an additive effect on the antimicrobial properties of strontium. A study by Ni et al. (71, 75) has evaluated the performance of non-acrylic strontium hydroxyapatite bone cement *in vivo*, and observed that the presence of 10% strontium substitution in hydroxyapatite added to the cement increased the amount of calcium in the serum by about 17% compared to plain bone cements. Also, the binding of biofilms to fibrinogen/fibrin has been shown to be inhibited by calcium ions (124) implying calcium could have a synergistic role in inhibiting biofilm formation. The mechanistic action of Sr<sup>2+</sup> on bacteria is less well understood than that of silver (Ag). Little is currently known with respect to bacterial resistance to strontium, due to limited number of published studies on the *in vitro* or *in vivo* antibacterial applications of the ion. Based on the previous studies (1, 3, 24) testing the bactericidal action of SrHA nano powders, we suggest two possible mechanisms by which strontium could inhibit bacterial growth: 1) by contact inhibition, upon static contact with SrHA/SrCaHA microspheres on the cement surface, 2) by elution of Sr<sup>2+</sup> ions into the surrounding physiological media via dissolution of SrHA/SrCaHA microspheres available at the cement surface. Preliminary work by Guida and co-workers (4) on glass ionomer cements that were modified with strontium and fluoride ions, for dental applications, suggested that the antibacterial activity was greatest in the case of cements that contained strontium oxide. This study also indicated that the antibacterial

effect was associated more with the release of strontium ions than fluoride ions. Lin et al. (1) studied the antibacterial properties of hydroxyapatite along with fully and partially substituted strontium hydroxyapatite powders and concluded that SrHA and SrCaHA nanoparticles had higher antibacterial ratio compared to pure HA indicating that antibacterial properties improved after calcium had been partially or totally substituted. This study suggested that the reason behind improved antibacterial properties might be due the increased solubility of SrHA and SrCaHA after strontium substitution resulting in the release of more antibacterial strontium ions to inhibit the test bacteria. In our 24 hour study, results suggested bacterial inhibition primarily due to contact with the SrHA/SrCaHA microspheres exposed at the cement surfaces. However, the long-term evaluation of the 10 and 20% SrHA cement surfaces revealed continued inhibition of *E. coli* bacteria up to 14 days in culture in comparison to control cements, indicating possible elution of Sr ions into the culture media. The least biofilm coverage was observed on the 20% SrHA samples after 14 days in culture. However, the observed OD<sub>600</sub> values ranging from 0.590 to 0.895 indicated that the cells in the petri dishes were continuously growing. This demonstrated that leaching of strontium from SrHA /SrCaHA microspheres into the media was not very significant.

O'Sullivan and co-workers (3) have studied the effect of deposition of strontium and silver doped apatite onto titanium surfaces and observed promising levels of initial bacterial inhibition from both the surfaces, with strontium showing a prolonged ability to reduce bacteria numbers over a 30-day period. Their study was the first to suggest that direct contact with the coated substrate surfaces is the major reason of the antibacterial performance and anticolonizing activity. Moreover, their study also suggested that the

beneficial effect of Sr<sup>2+</sup> ions on osteoblast cells created a possibility to produce a surface which inhibits microbial colonization while simultaneously promoting osseointegration (3). Our antibacterial inhibition zone test results using agar gel plate diffusion assay also showed that the antibacterial activity was more pronounced when cement samples had SrHA/SrCaHA microsphere powders readily accessible at the cement surface. The cement compositions where the SrHA/SrCaHA powders were not added on top of the cement surfaces showed comparatively smaller biofilm inhibition zones. All the inhibition zones observed for different cement compositions in this study were less than 7 mm indicating that the primary mode of bacterial inhibition was static contact with SrHA/SrCaHA microspheres or SrHA/SrCaHA powders available at the cement surface. The inhibition zones were expected to be larger than 7 mm if strontium elution and diffusion through agar gel had occurred. On the basis of comparisons of the antimicrobial activity of strontium substituted apatite powders from literature, the data presented in our study suggests that the direct contact of microbes with the SrHA/SrCaHA microspheres present at the cement surface maybe a significant contributing factor for the antibacterial activity of the cement samples, as dissolution of Sr from these particles in the cement matrix is difficult. Future work would include determining the exact metabolic pathways of bacterial inhibition by strontium substituted hydroxyapatite microspheres. Also, in order to provide a better understanding of how these cements may perform *in vivo*, the performance of these cements need to be evaluated *in vitro* in the presence of serum or other common matrix adhesion proteins that are typically present *in vivo* at the implant site. The ability to test the bone cements with *Staphylococcus aureus* and *Staphylococcus epidermidis*, which are

commonly found bacteria in orthopedic infections, would help in determining whether the antibacterial inhibition can be sustained with more virulent strains.

## 6.5 Conclusions

It can be concluded that the antibacterial properties of  $\eta$ -TSBCs improved significantly upon addition of strontium substituted HA (SrHA/SrCaHA) microspheres. This work also validates the possibility of employing strontium-substituted HA microspheres as alternative antibiotic fillers for acrylic bone cements. The 20% SrHA and SrCaHA composition were observed to be the strongest inhibitors of *E. coli* biofilm formation indicating that the antimicrobial properties were dependent on the concentration of SrHA/SrCaHA microspheres incorporated into the cement. Although it is not possible to fully explain the mechanism by which cements containing SrHA/SrCaHA fillers exhibit antibacterial properties, this work provides evidence that static contact of the test bacteria with SrHA/SrCaHA microspheres is an important contributing factor. Development of  $\eta$ -TSBCs containing strontium substituted microspheres provides a useful material for controlling biofilm infections, with promising applications in joint arthroplasties, vertebroplasty, kyphoplasty, and other orthopedic surgeries.

## Chapter 7

---

### 7 Summary

The overall objectives of this work have been accomplished as discussed in the different sections of this dissertation. Foremost, SrHA/SrCaHA microspheres were successfully fabricated with varying amounts of strontium substitution (50 % and 100 %) in HA. The introduction of SrHA/SrCaHA microspheres in  $\eta$ -TSBCs at varying concentrations allowed for evaluation of their efficacy in improving a combination of cement properties, such as radiopacity, bioactivity, and antibacterial properties. It has been shown previously that SrHA nano powder (10% Sr substitution) provides radiopacity (66, 68, 75, 87) when included in bone cements, as Sr falls under the same group of elements such as barium and calcium used in commercially available radiopacifiers. Our work also reports a linear increase in the contrast of  $\eta$ -TSBC with increasing concentrations of SrHA/SrCaHA microspheres. Thus, the goal of introducing SrHA/SrCaHA microspheres in  $\eta$ -TSBCs for improving bioactivity additionally allowed for complete removal of ZrO<sub>2</sub> radiopacifier used previously by Rodrigues et al. (82) to impart radiopacity in  $\eta$ -TSBCs. This was thought to be advantageous as many studies have reported deleterious effects of radiopacifiers, such as BaSO<sub>4</sub> and ZrO<sub>2</sub>, on the mechanical properties of acrylic cements (94-97). Secondly, all of the compositions of SrHA/SrCaHA containing  $\eta$ -TSBCs evaluated for bioactivity using SBF have been shown to have the capacity to form apatite on their cement surfaces. Therefore, both the partially and totally substituted SrHA microspheres proved successful in improving the bioactive properties of acrylic  $\eta$ -TSBCs. Thirdly, introduction of SrHA/SrCaHA microspheres in  $\eta$ -TSBC at higher concentrations was shown to reduce

biofilm formation through bactericidal action of Sr in comparison to control cements. Most commercial cement formulations used currently would require addition of an antibiotic, such as gentamicin sulfate, in order to prevent bacterial infections prevalent during orthopedic surgeries (13, 19, 120). Addition of antibiotics to acrylic bone cement has been studied extensively and is reported to further reduce the mechanical properties of PMMA cement (12, 119). Therefore, the feasibility of completely substituting the ZrO<sub>2</sub> radiopacifier in  $\eta$ -TSBCs with a single bioactive filler that could provide good radio contrast, bioactivity, and antibacterial properties all at the same time provides a cost-effective and superior cement formulation in comparison to the current commercial cement formulations that require addition of different fillers to achieve each of these individual properties.

SrHA nanopowder with 10 mol% strontium substitution in HA was fabricated by Li et al. (66) and was introduced by their group into Bis-GMA resin cements as a bioactive filler. They reported improved *in vitro* as well as *in vivo* bioactivity of Bis-GMA cements. The bioactive properties of Bis-GMA cement consisting of this SrHA nanopowder has been studied extensively thereafter by Ni et al. (73, 75, 76, 88, 92) using *in vitro* and *in vivo* models. Incorporation of HA powder as bioactive filler material has been investigated largely in PMMA based bone cement formulations (38, 39, 47, 52, 125, 126). However, only Hernandez et al. (68, 74) thus far has investigated the incorporation of strontium substituted hydroxyapatite (10% Sr substitution) as a potential bioactive filler material in acrylic based (PMMA) bone cement. Hernandez et. al (74) observed improved ability of apatite formation only on surfaces containing 20 wt% SrHA nanopowder that had been treated with MMA solution. However, we observed apatite formation on our  $\eta$ -TSBC compositions containing SrHA/SrCaHA microspheres even at lower concentrations (10%

wt/vol), which was promising. Most of the above mentioned studies employing SrHA nanopowder in bone cements for imparting bioactivity evaluated only 10 mol% strontium substitution in HA. SrHA nanoparticles with 50 and 100% Sr substitution have been evaluated for their antibiotic properties *in vitro* by Lin et al. (1). However, only Liu et al. (121) incorporated SrHA nanopowder (10% Sr) into a bone cement (Bis-GMA resin) along with gentamicin to investigate SrHA-Bis-GMA as a drug delivery system. They did not however investigate the potential of SrHA to act as an antibiotic filler. In our work, not only did we introduce SrHA microspheres (2-5  $\mu\text{m}$  in diameter) into PMMA cement matrices for improving bioactivity, but we also varied the amount of strontium substitution (50% and 100% Sr) in order to evaluate the effect of higher substitution on bioactivity and antibiotic properties of  $\eta$ -TSBCs. Our study reports no significant effect of strontium substitution or SrHA/SrCaHA concentration on the ability of SrHA- $\eta$ -TSBCs to form apatite on their surfaces. However, the increase in strontium substitution did have a significant effect on the antibiotic properties of SrHA- $\eta$ -TSBCs. SrCaHA- $\eta$ -TSBCs were observed to have greater biofilm inhibition in comparison to SrHA- $\eta$ -TSBCs at lower concentrations. At higher SrHA/SrCaHA concentration both the cement compositions provided similar bioactivity and antibiotic properties. Thus,  $\eta$ -TSBC composition containing 20% SrHA/SrCaHA was believed to have optimal antibiotic and bioactive properties. We also concluded that the primary mechanism of bacterial inhibition observed on SrHA/SrCaHA  $\eta$ -TSBCs was via contact inhibition, upon direct contact of bacteria with SrHA/SrCaHA microspheres available at the cement surfaces.

The 20% SrHA/SrCaHA composition was also shown to have adequate compressive, flexural and fracture toughness properties required for VP/KP applications. It was observed

that inclusion of SrHA/SrCaHA up till 20% wt/vol did not have any further detrimental effect on the static mechanical properties of  $\eta$ -TSBC in comparison to  $\eta$ -TSBCs containing 20% wt/vol ZrO<sub>2</sub> filler. Serbetci et al. (107) has shown reduction in mechanical properties due to increased porosity and agglomeration of HA nanopowder at higher concentrations. The SEM micrographs of the fractured surfaces of 20 % SrCaHA and SrHA cements after a fracture toughness test, are shown in Figure 20 (a,b) and 20 (c,d), respectively. The backscattered SEM micrographs of 20 % SrHA/SrCaHA cements (Figure 20 (b) and (d)) showed that the microspheres were not dislodged from the cement matrix indicating no porosities were caused. The crack was observed to propagate around the SrHA/SrCaHA microspheres or agglomerates rather than through the microspheres. This result was promising, as SrHA/SrCaHA microspheres can be subjected to surface treatments in the future studies to improve interaction with the PMMA nanospheres resulting in improved adhesion and integration with the PMMA matrix and their fracture toughness properties.

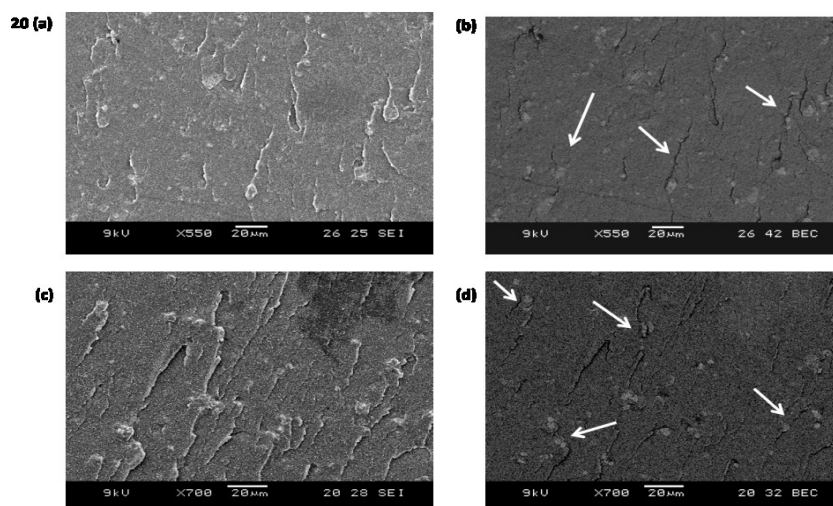


Figure 20. SEM micrographs of fractured surfaces of  $\eta$ -TSBCs containing (a) 20% SrCaHA and (c) 20% SrHA microspheres subjected to fracture toughness testing. Backscattered SEM micrographs of the  $\eta$ -TSBCs containing (b) 20% SrCaHA and (d) 20% SrHA microspheres. The black arrows indicate the crack propagation around the SrHA/SrCaHA microspheres or agglomerates rather than through the microspheres.

Most of the studies evaluating SrHA filler use SrHA nanopowder for incorporation into cements. In this study, we fabricated SrHA/SrCaHA microspheres using the hydrothermal synthetic route suggested by Zhang et al. (127). Zhanglei et al. (83) and Zhang et al. (127) developed Sr-doped HA microspheres that have excellent photoluminescent properties without using expensive rare earth ions, in order to use them as a new, efficient, and low-cost blue luminescent material. Their as-obtained 20% SrHA microspheres were shown to have the highest photoluminescence by a bright blue emission from 350 to 570 nm centered at 424 nm wavelength under UV light excitation. The SrHA/SrCaHA microspheres that were synthesized in this study via the same synthetic route thus also possess the added ability to emit a blue emission peak when exposed to a UV light or under a DAPI filter on the fluorescence microscope (having an excitation in the same range as UV light). Therefore, when we looked at the cement surfaces containing SrHA/SrCaHA microspheres under a fluorescence microscope using a DAPI filter, we could see the SrHA/SrCaHA particles as blue spheres or agglomerates. This property of SrHA/SrCaHA microspheres was utilized to look at the distribution of these particles on the cement surface, which was observed to be heterogeneous throughout the cement surface. This property of the SrHA/SrCaHA microspheres can be beneficial to our future work. Our preliminary cell cytotoxicity studies on 10% SrHA/SrCaHA  $\eta$ -TSBC (not reported here) using MC3T3-E1 pre-osteoblast cells revealed that we could not only use the green (calcein AM dye) and red (ethidium homodimer 1 dye) fluorescence from the live-dead kit to observe the live-dead cells, but also use blue (DAPI) fluorescence to simultaneously observe the location of the SrHA/SrCaHA microspheres with respect to the attached cells. Thus, it was possible to acquire a composite image with the green (live cells), red (dead cells), and

blue (SrHA/SrCaHA microspheres) fluorescence as shown in Figure 21 (a,b). It can be observed from Figure 21(a) that most of the dead cells (red) were found to be present in the areas devoid of the SrHA/SrCaHA microspheres (white arrows), whereas most of the live cells (green) were present on top of the SrHA/SrCaHA microspheres as indicated by white arrows in Figure 21 (b). This preliminary result also confirmed that SrHA/SrCaHA particles are biocompatible and would promote osteoblast cell attachment. This property of SrHA/SrCaHA microspheres can prove beneficial in the future studies as a tool to look at the interaction of osteoblasts with  $\eta$ -TSBC surfaces containing SrHA/SrCaHA microspheres.

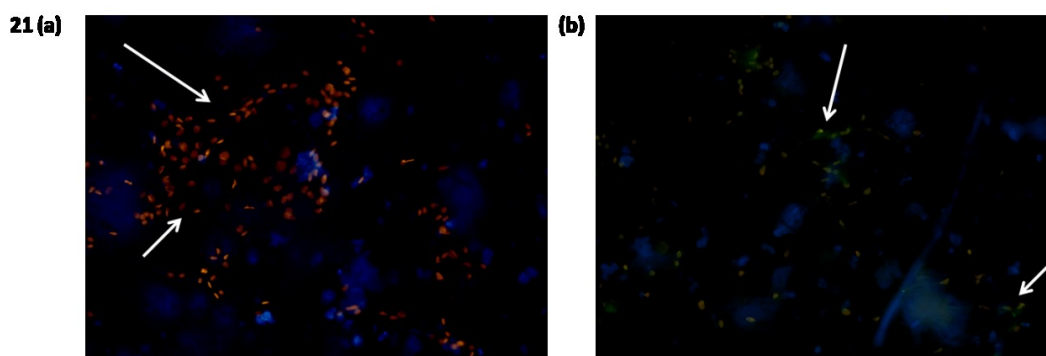


Figure 21. Fluorescence micrographs of MC3T3 preosteoblast cells cultured on  $\eta$ -TSBCs containing (a) 10% SrHA and (b) 10% SrCaHA microspheres. Red fluorescence = dead cells, green fluorescence = live cells, blue fluorescence = SrHA/SrCaHA microspheres. The white arrows in (a) indicate dead cells on areas devoid of SrHA, while white arrows on (b) indicate live cells on top of the SrCaHA microspheres. 10X magnification.

In this work, the variation in strontium substitution did not significantly affect the mechanical or bioactive properties, but significantly affected the antibiotic properties of  $\eta$ -TSBC containing SrHA/SrCaHA microspheres. This indicates that the cement formulations can be modified or altered depending on the requirements of the applications. For example, in the case of cemented arthroplasties where better interfacial strength between bone and

implant is required for long-term stability of prosthesis, both 20% SrHA and SrCaHA formulations could find applications. Whereas, for the case of treating battlefield wounds where preventing infections is a priority along with fracture stabilization, 20% SrCaHA formulation exhibiting superior bioactive as well as antibiotic properties could find applications.

## Chapter 8

---

### 8 Future Work

The results presented in this work consisted of several advantages involving the  $\eta$ -TSBC formulation, right from the synthesis of SrHA/SrCaHA microspheres to the development of  $\eta$ -TSBCs containing these microspheres. The findings of this study will not only serve as a platform for continued improvements in order to better understand properties of these cements, but also provide a basis for solutions to the current drawbacks introduced with these innovations.

Some of the areas that need more in depth study in follow up projects are:

1. Study of initial *in vitro* interaction of osteoblasts with cement surfaces containing SrHA/SrCaHA microspheres:

The material surface and topography influences cell reaction through changes in cell cytoskeleton and also dictates the cell attachment, morphology, and viability. It has been reported that bone formation is dependent on the number of cells and the cell number is largely dependent on cell adherence and proliferation (48). Thus, initial recruitment of cells on a material surface is of great importance to terminal differentiation of cells in contact with a material. An *in vitro* tissue culture model needs to be developed to evaluate the biological response on  $\eta$ -TSBC versus  $\eta$ -TSBC containing SrHA/SrCaHA microspheres. Also, there is a need for evaluation of cell behavior on cement surfaces with an apatite layer formed previously on their surfaces versus cement surfaces without any apatite layer. The changes in cell morphology with different surfaces can be investigated using SEM analysis or time-lapse microscopy. The

capacity for osteoblast differentiation and mineralization can be investigated by monitoring alkaline phosphatase (ALP) and osteopontin activity using fluorescent markers. Dalby et al. (48) investigated the initial response of primary human osteoblast-like cells (HOB) on PMMA cements containing 17.5% wt HA. They reported significantly higher cell proliferation on HA containing cements in comparison to PMMA cements with cell phenotype retention up to 21 days. They observed flattened cells with small processes on PMMA samples whereas, HA surfaces showed cell processes attaching preferentially to HA particles exposed at the cement surface rather than the polymer matrix indicating physiological compatibility to HA. Another study by this group investigated the effect of increasing HA incorporation into PMMA on osteoblast adhesion and response (47) and found that focal contact formation, cytoskeletal organization, cell proliferation and expression of phenotype increased with increasing HA volume. Jager et al. (128) also observed similar results of increased osteogenic potential of PMMA cement with introduction of HA particles in terms of collagen production and ALP activity. Activity of bone mineralization markers such as ALP and osteopontin have been seen to increase in cells cultured on compacted discs of HA and SrHA powder (79). Hao et al. (129) evaluated osteoconduction and proliferation of mesenchymal (MSC) and osteoblast cells (OB) on SrHA nanoparticles and observed increased OB cell adhesion and proliferation upto 4 days in culture and higher ALP activity with MSC cells. Thus, investigating the interaction between SrHA/SrCaHA microspheres and osteoblasts would be worthwhile to pursue. Also, cells react differently to rough and smooth surfaces, thus it would be worthwhile to investigate how osteoblasts react to a cement surface that already has an apatite layer present on its

surface which would be rougher in comparison to the cement surface without an apatite layer.

2. Investigate the mechanical properties of SrHA/SrCaHA cements after formation of apatite layer in SBF to replicate *in vivo* conditions:

Hernandez et al. (68) have characterized the compressive properties of PMMA cements containing SrHA nanoparticles. They performed compression tests on cement specimens stored in air at room temperature versus specimens stored in SBF for 1 month at body temperature. They reported a decrease in mechanical properties after storage in SBF for a month due to the plasticizing effect introduced by the absorbed water (68). A further decrease in mechanical properties after being stored in SBF would be detrimental for our cement formulations. Thus, measuring the mechanical properties of SrHA/SrCaHA cements after immersion in SBF would be a meaningful investigation. Also, measuring the residual monomer content and relating it with the mechanical properties would provide some insight into the decrease or increase observed in the static mechanical properties on addition of bioactive fillers.

3. Surface modification of SrHA/SrCaHA particles for better integration with PMMA matrix:

Addition of inorganic fillers makes the bone cement brittle because of low ductility of the fillers and the weak interface between the fillers and the cement matrix. We have also observed this phenomenon in our study with lower flexural and fracture

toughness properties of SrHA/SrCaHA cements resulting from agglomeration of SrHA/SrCaHA microspheres. Thus a surface treatment of these particles could provide improved distribution and integration with the cement matrix. HA has a significant fraction of reactive hydroxyl groups that can be made available for grafting of organic molecules onto the surfaces of HA particles. Hernandez et al. (74) treated SrHA nanoparticles with MMA solution for 24 hours before introducing it into their cements and observed immediate improvement in the mixing and injectibility of their cements as the MMA treatment hydrophobises the surface of SrHA particles to some extent. Leong et al. (112) also postulated that surface modification of SrHA filler with MMA will induce matrix/filler interface integration and consequently improve mechanical properties of bioactive cement. Dalby et al. (48) suggests grafting of HA to PMMA using isocyanate groups that may help in maintaining mechanical properties and incorporation of HA particles. Another possibility could be silanization of SrHA/SrCaHA microspheres. Surface treatment by bisphosphonates is also an emerging alternative as they are used widely as drugs for osteoporosis (112). Surface treatment of the SrHA/SrCaHA microspheres will help prevent agglomeration as well as provide their homogeneous dispersion in the cement.

4. Develop techniques in order to have higher concentration of SrHA/SrCaHA microspheres available at the surface of the cements for increasing bioactive and antibacterial response:

It has been observed that most of the bioactive filler material when added to PMMA cements gets embedded into the matrix of the cement and is not available at the

surface of the cement in the concentration needed for inducing bioactivity. Hernandez et al. (74) observed better bioactivity when they polymerized their bioactive cement by directly extruding their cement into the SBF solution at body temperature, replicating *in vivo* conditions. According to them, this method leaves the bioactive particles exposed to the medium which leads to a better bioactive response in comparison to cements cured in air at room temperature. However, they did not discuss the mechanism that drives these bioactive particles to the cement surface. As a preliminary study, we wanted to investigate what would drive these particles to the surface when the cement paste is extruded directly into a solution. We hypothesized that for the SrHA/SrCaHA particles to be driven to the surface when the cement is injected in SBF or deionized water, they would have to be inherently extremely hydrophilic. Thus, SrHA and SrCaHA microsphere powder was compacted into discs (n=3) using the FTIR press as shown in Figure 22 (a, b). The contact angles of SrHA/SrCaHA discs were measured using DROP Image software and sessile drop technique. It was observed that both these powders were intrinsically extremely hydrophilic and absorbed water before we could perform any contact angle measurements. Although, initial pictures of the drop touching the SrHA/SrCaHA discs were captured successfully as shown in Figure 22, indicating their hydrophilicity. These preliminary observations are in line with our hypothesis. Therefore, it would be interesting to explore this technique of extruding and polymerizing the cement directly into SBF at body temperature and then study its bioactive and mechanical properties in comparison to cements cured in air at room temperature. However, one drawback that might need to be addressed with this method would be release of monomer MMA into the SBF solution during cement

polymerization and its sustained release in SBF with continued storage over longer time periods. If a high concentration of monomer is present in the SBF solution, it might affect its ability to form apatite on its surface, and the SBF solution might need to be replaced daily.

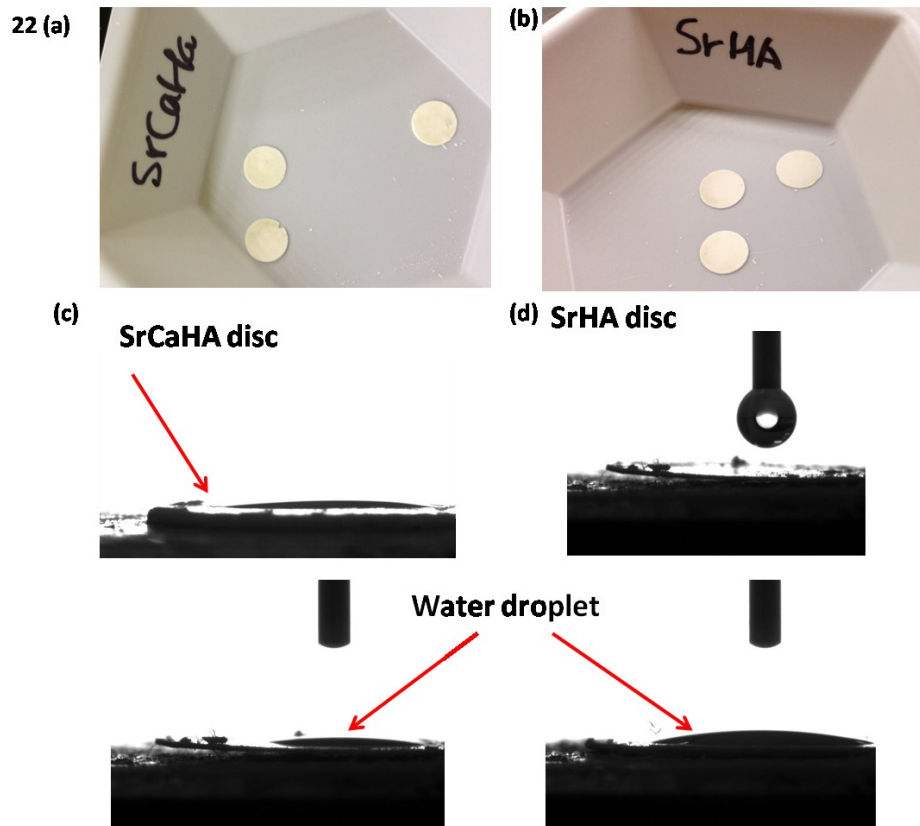


Figure 22. (a) SrCaHA and (b) SrHA powders compressed into discs for contact angle measurements. As can be seen from the light micrographs, the (c) SrCaHA and (d) SrHA surfaces are very hydrophilic showing contact angles lower than  $90^\circ$ . It was difficult to quantify the contact angle measurements due to absorption of the water droplet by the sample discs.

5. Study of the kinetics of polymerization of the  $\eta$ -TSBC containing SrHA/SrCaHA by performing experiments at several curing temperatures. Understand the role of these bioactive fillers on the kinetic parameters, setting times and polymerization exotherms using differential scanning calorimetry (DSC) techniques.
6. Study of the shelf-life of the SrHA/SrCaHA microspheres containing  $\eta$ -TSBCs using DSC techniques. Preliminary experiments, using DSC techniques previously employed for the study of shelf-life of the STSBC formulation (130), indicated shorter shelf-life of  $\eta$ -TSBC in comparison to linear STSBC. However, the large variability obtained between the upper and lower prediction limits using this DSC technique pointed to the need of development of a more efficient method for data acquisition and analysis of DSC profiles.
7. Study the viability of preparation of SrHA-brush-TSBC:

Rather than using linear PMMA for the formation of composite bioactive cement, it would be ideal to graft PMMA brushes on the surface of SrHA/SrCaHA microspheres, thereby eliminating the use of linear PMMA, which could further improve the viscosity of cement mixtures at higher polymer concentrations. This would also improve adhesion between SrHA/SrCaHA microspheres and the polymer matrix. Rodrigues et al. (131) have been successful in grafting PMMA nanospherical brushes on PMMA nanospheres incorporated into STSBCs, through the addition of carbon-carbon double bonds on the surface of the nanoparticles that allowed for grafting of PMMA brushes via radical polymerization. Liu et al. (132) have also studied feasibility of grafting PMMA by using

the reaction of isocyanate groups with the hydroxyl (OH) groups present on the surface of HA particles. They introduced double bonds to the surface of HA via coupling reaction of isocyanate ethyl methacrylate (ICEM) with HA followed by radical polymerization in MMA. The same procedure could be attempted with SrHA/SrCaHA microspheres synthesized in our study, for grafting of MMA via radical polymerization. Details of the procedure are described in the paper by Liu and co-workers (132).

8. Study ex-vivo exothermal and mechanical properties of  $\eta$ -TSBC containing of SrHA/SrCaHA microspheres:

The experimental  $\eta$ -TSBC performed as well as or better than the commercial KyphX cements with respect to exothermic characteristics and mechanical properties in an *ex-vivo* human cadaver study (133). Hence, investigation of polymerization temperatures and level of mechanical augmentation of these novel bioactive  $\eta$ -TSBCs in a vertebroplasty cadaver model in comparison to the performance of a commercial cement used in the treatment of vertebral compression fractures is necessary.

9. Investigate the possibility of using  $\eta$ -TSBCs containing SrHA/SrCaHA microspheres as a treatment for critical size defects in craniofacial and maxillofacial surgeries. Evaluate the feasibility of sintering SrHA/SrCaHA microspheres to develop bioactive resorbable scaffolds for providing bone regeneration while treating critical size defects.

## **Chapter 9**

---

### **9 Appendices**

#### **9.1 Appendix A: Synthesis of cross-linked PMMA nanospheres**

##### **1. Materials**

- Methyl methacrylate (MMA) 99% Fluka – stored in the flammable cabinet
- Ethylene glycol dimetacrylate (EGDMA) 98% Sigma – stored in the refrigerator
- Potassium Persulfate (KPS) – 99% Sigma – stored in the refrigerator
- Deionized (DI) water
- Condenser
- 1000 mL three neck flask
- 2” stir bar
- Thermometer
- Centrifuge tubes (50 mL) - Corning® 50mL centrifuge tubes
- Centrifuge bottles (250 mL Nalgene)

##### **2. Procedure (Boiling-temperature soap-free emulsion polymerization)**

- Fill a three neck flask with 400 mL DI
- Equip the three-necked flask with a condenser keeping cold water running during the entire time of polymerization
- Add a 2” stir bar to the flask

- Stir the solution at low speed (mark 4 in the stir plate) and turn the temperature controller on
- Mix 25 mL MMA and 6.25 mL EGDMA in a beaker. For 25% crosslinking add 8.34 mL EGDMA instead
- Add the mixture to the water and seal the flask
- Raise the mixture to reflux and monitor the temperature (100°C). It takes about one hour and a half for to reach the boiling point
- After the medium had boiled for 5 minutes add 0.4 g of potassium persulfate
- Let the solution mixing at low speed (mark 4) for a couple of minutes for dissolution of the initiator.
- Monitor temperature after addition of the initiator, since the temperature tends to increase after the mixture gets homogeneous. Keep the medium boiling during the entire period of polymerization ( $100 \pm 2^\circ\text{C}$ )
- Increase the stir speed (mark 7.5 on the stir plate) after a milky solution has formed
- Stop the reaction after 2 hours – turn the temperature controller off
- Let the mixture stirring with the condenser assembled for another hour for cooling down

### **3. Drying**

#### **3.1. Centrifugation**

- Add the mixture to 250 mL centrifuge bottles
- Set the centrifuge to 4500 rpm (maximum speed) and 60 minutes
- After 60 minutes of centrifugation collect the supernatant and add distilled water to the bottles for washing of the product. Shake the bottles for mixing of the particles with water. A stick and

white mass deposits at the bottom of the bottles after centrifugation, therefore abrupt shaking is required to loosen the mass from the bottom

- Set the centrifuge to 4500 rpm and 60 minutes
- Collect the remaining water
- Add just a little more water and shake the bottles to loosen the mass of particles from the bottom
- Transfer the solution to 50 mL Corning centrifuge tubes

### **3.2. Freeze-drying**

- Place the 50 mL tubes during 24 hours in a -20°C freezer
- Transfer the tubes from the -20°C freezer to a -80°C freezer
- Keep the tubes under -80°C for at least 12 hours
- Remove the tubes from the freezer and transfer them to freeze-dryer bottles
- Remove the centrifuge tubes caps and cover them with Kim wipes
- Seal the tubes (covered with Kim wipes) with rubber bands
- Keep the particles in the freeze-dryer for at least 48 hours for complete removal of ice crystals.

If crystals are still present, let the particles drying for another couple of hours

- Subject the particles to heat treatment at 90°C for 24 hours for removal of residual initiator
- Keep the particles in a sealed flask 25 mL monomer yields about 17-18 g of crosslinked nanospheres. The procedure can be also done with double the amount of reagents. In this case the stir speed has to be decreased to mark 1 or 2 for the addition of the initiator to avoid spilling of the boiling medium.

## 9.2 Appendix B: Synthesis of SrHA/SrCaHA microspheres

### 1. Materials

- Hexadecyl-trimethylammonium bromide (CTAB)
- Ammonium phosphate ( $\text{NH}_4\text{H}_2\text{PO}_4$ )
- Strontium Nitrate ( $\text{Sr}(\text{NO}_3)_2$ )
- Trisodium citrate ( $\text{Cit}^{3-}$ )
- Calcium nitrate ( $\text{Ca}(\text{NO}_3)_2$ )
- Deionized (DI) water
- 2" stir bar
- Centrifuge tubes (50 ml) - Corning® 15 ml centrifuge tubes
- Parr steel pressure vessel with 125 ml teflon bottle
- Two 100 ml beakers

### 2. Procedure for synthesis of SrHA/SrCaHA microspheres

- Fill one 100 ml with 40 ml DI water, and add a 2" stir bar to the beaker. Label it as solution 1.
- Fill the other 100 ml with 25 ml DI water, and add a 2" stir bar to the beaker. Label it as solution 2.
- For SrHA microspheres, add 0.3 g CTAB and 0.635 g strontium nitrate to solution 1 and allow it to stir for 30 minutes
- For SrCaHA microspheres, add 0.3 g CTAB, 0.32 g strontium nitrate, and 0.35 g calcium nitrate to solution 1 and allow it to stir for 30 minutes.

- For both SrHA/SrCaHA microspheres, add 1.54 g trisodium citrate and 0.26 g ammonium phosphate to solution 2 and allow it to stir for 30 minutes.
- After 30 mins of stirring both the solutions, add solution 2 to the beaker of solution 1 and let it stir for another 20-25 minutes.
- Transfer the mixed solution into 125 ml Teflon bottle from Parr Instruments that can be held in a stainless steel pressure vessel, seal the Teflon cup and the stainless steel pressure vessel and keep it in the vacuum oven at 180°C for 24 hours.
- After 24 hours, take the stainless steel vessel out of the oven, and let it cool down to room temperature naturally.

### **3. Centrifugation and drying**

- Once the steel vessel has cooled down, unscrew the top and remove the Teflon cup.
- You will see white particles settled to the bottom of the cup and a clear solution on the top. In order to get all particles out, mix the solution and try to remove all particles stuck at the bottom of the cup. You will get a milky solution.
- Transfer this solution into 15 ml conical centrifuge tubes and centrifuge for 5 mins at 1000 rpm (centrifuge is placed in the tissue culture lab, next to our lab safety hood)
- After centrifuging, remove the supernatant and add DI water to the test tubes and shake them so the particles settled at the bottom would be resuspended in water.
- Centrifuge the tubes again for 5 mins at 1000 rpm, remove the supernatant, add DI water and resuspend the particles in DI.
- Filter the resuspended particles using a vacuum filter and filter paper. Once all particles are filtered, add ethanol to the funnel containing filtered particles, to clean any excess

organic solvents. Once ethanol is filtered, remove the filter paper and leave it for drying in the oven at 80 degrees for 24 hours.

### 9.3 Appendix C: Protocol by Kokubo et al. (84) for preparation of Simulated Body Fluid (SBF)

Following tables from the Kokubo protocol shows the comparison between the composition of human blood plasma and the as prepared SBF solution and the materials required for the preparation of SBF solution.

Table 2. Nominal ionic concentrations of SBF in comparison to those in human blood plasma (84).

Ion	Ion concentrations (mM)	
	Blood plasma	SBF
Na <sup>+</sup>	142.0	142.0
K <sup>+</sup>	5.0	5.0
Mg <sup>2+</sup>	1.5	1.5
Ca <sup>2+</sup>	2.5	2.5
Cl <sup>-</sup>	103.0	147.8
HCO <sub>3</sub> <sup>-</sup>	27.0	4.2
HPO <sub>4</sub> <sup>2-</sup>	1.0	1.0
SO <sub>4</sub> <sup>2-</sup>	0.5	0.5
pH	7.2–7.4	7.40

Table 3. Order and amount of reagents required for preparing 1000 ml of SBF (84).

Order	Reagent	Amount
1	NaCl	8.035 g
2	NaHCO <sub>3</sub>	0.355 g
3	KCl	0.225 g
4	K <sub>2</sub> HPO <sub>4</sub> · 3H <sub>2</sub> O	0.231 g
5	MgCl <sub>2</sub> · 6H <sub>2</sub> O	0.311 g
6	1.0M-HCl	39 ml
7	CaCl <sub>2</sub>	0.292 g
8	Na <sub>2</sub> SO <sub>4</sub>	0.072 g
9	Tris	6.118 g
10	1.0M-HCl	0–5 ml

**Procedure:**

In order to prepare 1000 ml of SBF, put 700 ml of deionized water with a magnetic stirring bar into 1000 ml plastic beaker. Set it on a heating stir plate and cover it with a parafilm. Heat the water in the beaker to  $36.5 \pm 1.5$  °C under stirring. Dissolve only the reagents of 1<sup>st</sup> to 8<sup>th</sup> order into the solution at  $36.5 \pm 1.5$  °C one by one in the order given in Table 3, taking care of the indications in the following list. The reagents 9<sup>th</sup> (Tris) and 10<sup>th</sup> order (HCl) are dissolved in the following process:

- Never dissolve several reagents simultaneously. Dissolve a reagent only after the preceding one is dissolved completely.
- Since reagent CaCl<sub>2</sub> has a great effect on precipitation of apatite and takes usually granular form and much longer to dissolve, dissolve one granule at a time. Completely dissolve one granule before initiation of dissolution of the next.

- Set the temperature of the solution at  $36.5 \pm 1.5$  °C. If the amount of solution is smaller than 900 ml, add deionized water up to 900 ml in total.
- Insert the electrode of the pH meter into the solution. Just before dissolving Tris, the pH of the solution should be  $2.0 \pm 1.0$ .
- With the solution temperature between 35 and 38°C, preferable to  $36.5 \pm 1.5$  °C, dissolve reagent Tris into the solution little by little taking careful note of the pH change. After adding a small amount of Tris, stop adding it and wait until reagent already introduced is dissolved completely and the pH has become constant.
- Then add more Tris to raise the pH gradually, until pH becomes 7.45 making sure that the temperature is maintained at  $36.5 \pm 1.5$  °C.
- When pH has risen to  $7.45 \pm 0.01$ , stop dissolving Tris, then drop 1 ml – HCl by syringe to lower the pH to  $7.42 \pm 0.01$ , making sure that pH does not decrease below 7.40. After the pH has fallen to  $7.42 \pm 0.01$ , dissolve the remaining Tris little by little until the pH has risen to  $\leq 7.45$ . Repeat this process until the whole amount of Tris is dissolved keeping the pH within 7.42 - 7.45.
- After dissolving the whole amount of Tris, adjust the temperature of the solution to  $36.5 \pm 1.5$  °C and pH to 7.42.
- Pour the pH adjusted solution from the beaker into a 1000 ml volumetric flask. Add deionized water up to the marked line, put a lid on the flask and close it with the plastic film.
- After mixing the solution in the flask, keep it in water to cool it down to 20°C. After the temperature has fallen to 20°C, add the distilled water up to the marked line.

- Prepared SBF should be preserved in plastic bottle with a lid put on tightly and kept at 4-10°C in a refrigerator until used. The SBF should be used within 30 days after preparation.

## 10 References

1. Lin Y, Yang Z, Cheng J, Wang L. Synthesis, characterization and antibacterial property of strontium half and totally substituted hydroxyapatite nanoparticles. *Journal of Wuhan University of Technology--Materials Science Edition*. 2008;23(4):475-9.
2. Zhang W, Shen Y, Pan H, Lin K, Liu X, Darvell BW, et al. Effects of strontium in modified biomaterials. *Acta Biomaterialia*. 2011;7(2):800-8.
3. O'Sullivan C, O'Hare P, O'Leary N, Crean A, Ryan K, Dobson A, et al. Deposition of substituted apatites with anticolonizing properties onto titanium surfaces using a novel blasting process. *Journal of Biomedical Materials Research Part B: Applied Biomaterials*. 2010;95(1):141-9.
4. Guida A, Towler M, Wall J, Hill R, Eramo S. Preliminary work on the antibacterial effect of strontium in glass ionomer cements. *J Mater Sci Lett*. 2003;22(20):1401-3.
5. Lewis G. Injectable bone cements for use in vertebroplasty and kyphoplasty: State-of-the-art review. *J Biomed Mater Res B Appl Biomater*. 2006 Feb;76(2):456-68.
6. Galibert P, Deramond H, Rosat P, Le Gars D. Notre préliminaire sur le traitement des angiomes vertébraux par vertébroplastie acrylique percutanée. *Neurochirurgie*. 1987;33(2):166-8.
7. Lieberman IH, Togawa D, Kayanja MM. Vertebroplasty and kyphoplasty: Filler materials. *Spine J*. 2005 Nov-Dec;5(6 Suppl):305S-16S.

8. Heini PF, Berlemann U. Bone substitutes in vertebroplasty. *Eur Spine J.* 2001 Oct;10 Suppl 2:S205-13.
9. Ledlie JT, Renfro M. Balloon kyphoplasty: One-year outcomes in vertebral body height restoration, chronic pain, and activity levels. *Journal of Neurosurgery: Spine.* 2003;98(1):36-42.
10. Lieberman I, Dudeney S, Reinhardt M, Bell G. Initial outcome and efficacy of “kyphoplasty” in the treatment of painful osteoporotic vertebral compression fractures. *Spine.* 2001;26(14):1631-7.
11. Yang H, Zou J. Filling materials used in kyphoplasty and vertebroplasty for vertebral compression fracture: A literature review. *Artif Cells Blood Substit Immobil Biotechnol.* 2011 Apr;39(2):87-91.
12. Belt H, Neut D, Schenk W, Horn JR, Mei HC, Busscher HJ. Infection of orthopedic implants and the use of antibiotic-loaded bone cements: A review. *Acta Orthopaedica.* 2001;72(6):557-71.
13. Jiranek WA, Hanssen AD, Greenwald AS. Antibiotic-loaded bone cement in aseptic total joint replacement: Whys, wherefores and caveats. Conference summary for 70th annual meeting of the american academy of orthopedic surgeons; ; 2003.
14. van de Belt H, Neut D, Schenk W, van Horn JR, van der Mei HC, Busscher HJ. Staphylococcus aureus biofilm formation on different gentamicin-loaded polymethylmethacrylate bone cements. *Biomaterials.* 2001;22(12):1607-11.

15. Fish DN, Hoffman HM, Danziger LH. Antibiotic-impregnated cement use in US hospitals. *American Journal of Health-System Pharmacy*. 1992;49(10):2469-74.
16. Murray WR. Use of antibiotic-containing bone cement. *Clin Orthop*. 1984(190):89.
17. Ethell MT, Bennett RA, Brown MP, Merritt K, Davidson JS, Tran T. In vitro elution of gentamicin, amikacin, and ceftiofur from polymethylmethacrylate and hydroxyapatite cement. *Veterinary Surgery*. 2004;29(5):375-82.
18. Belt HvD, Neut D, Schenk W, Horn JRv, Mei, Henny C van Der, Busscher HJ. Gentamicin release from polymethylmethacrylate bone cements and staphylococcus aureus biofilm formation. *Acta Orthopaedica*. 2000;71(6):625-9.
19. Van de Belt H, Neut D, Uges D, Schenk W, Van Horn J, Van der Mei H, et al. Surface roughness, porosity and wettability of gentamicin-loaded bone cements and their antibiotic release. *Biomaterials*. 2000;21(19):1981-7.
20. Thornes B, Murray P, Bouchier-Hayes D. Development of resistant strains of staphylococcus epidermidis on gentamicin-loaded bone cement in vivo. *Journal of Bone and Joint Surgery-British Volume*. 2002;84(5):758.
21. Arizono T, Oga M, Sugioka Y. Increased resistance of bacteria after adherence to polymethyl methacrylate. *Acta Orthopaedica*. 1992;63(6):661-4.
22. Lautenschlager E, Jacobs J, Marshall G, Meyer P. Mechanical properties of bone cements containing large doses of antibiotic powders. *J Biomed Mater Res*. 2004;10(6):929-38.

23. Lautenschlager E, Marshall G, Marks K, Schwartz J, Nelson C. Mechanical strength of acrylic bone cements impregnated with antibiotics. *J Biomed Mater Res.* 2004;10(6):837-45.
24. Fielding GA, Roy M, Bandyopadhyay A, Bose S. Antibacterial and biological characteristics of plasma sprayed silver and strontium doped hydroxyapatite coatings. *Acta Biomaterialia.* 2012.
25. Kuehn K, Ege W, Gopp U. Acrylic bone cements: Composition and properties. *Orthop Clin North Am.* 2005;36(1):17.
26. Kühn K. Bone cements: Up-to-date comparison of physical and chemical properties of commercial materials. Springer Verlag; 2000.
27. Lewis G. Properties of acrylic bone cement: State of the art review. *Journal of Biomedical Materials Research Part B: Applied Biomaterials.* 1997;38(2):155-82.
28. Hasenwinkel JM, Lautenschlager EP, Wixson RL, Gilbert JL. A novel high-viscosity, two-solution acrylic bone cement: Effect of chemical composition on properties. *Journal of Biomedical Materials Research Part A.* 1999;47(1):36-45.
29. Hasenwinkel JM, Lautenschlager EP, Wixson RL, Gilbert JL. Effect of initiation chemistry on the fracture toughness, fatigue strength, and residual monomer content of a novel high-viscosity, two-solution acrylic bone cement. *J Biomed Mater Res.* 2002 Mar 5;59(3):411-21.

30. Rodrigues DC, Gilbert JL, Hasenwinkel JM. Two-solution bone cements with cross-linked micro and nano-particles for vertebral fracture applications: Effects of zirconium dioxide content on the material and setting properties. *J Biomed Mater Res B Appl Biomater*. 2010 Jan;92(1):13-23.
31. Rodrigues DC, Gilbert JL, Hasenwinkel JM. Pseudoplasticity and setting properties of two-solution bone cement containing poly(methyl methacrylate) microspheres and nanospheres for kyphoplasty and vertebroplasty. *J Biomed Mater Res B Appl Biomater*. 2009 Oct;91(1):248-56.
32. Lin Y, Yang Z, Cheng J, Wang L. Synthesis, characterization and antibacterial property of strontium half and totally substituted hydroxyapatite nanoparticles. *Journal of Wuhan University of Technology--Materials Science Edition*. 2008;23(4):475-9.
33. Phillips F, Pfeifer B, Lieberman I, Kerr E, Choi I, Pazianos A. Minimally invasive treatments of osteoporotic vertebral compression fractures: Vertebroplasty and kyphoplasty. *INSTRUCTIONAL COURSE LECTURES-AMERICAN ACADEMY OF ORTHOPAEDIC SURGEONS*. 2003;52:559-68.
34. Bono C, Garfin S. Kyphoplasty and vertebroplasty for the treatment of painful osteoporotic vertebral compression fractures. *Advances in spinal fusion*. 2003:33-49.
35. Provenzano MJ, Murphy KPJ, Riley III LH. Bone cements: Review of their physiochemical and biochemical properties in percutaneous vertebroplasty. *Am J Neuroradiol*. 2004;25(7):1286.

36. Lewis G, van Hooy-Corstjens CS, Bhattaram A, Koole LH. Influence of the radiopacifier in an acrylic bone cement on its mechanical, thermal, and physical properties: Barium sulfate-containing cement versus iodine-containing cement. *J Biomed Mater Res B Appl Biomater*. 2005 Apr;73(1):77-87.
37. Lewis G. Alternative acrylic bone cement formulations for cemented arthroplasties: Present status, key issues, and future prospects. *Journal of Biomedical Materials Research Part B: Applied Biomaterials*. 2008;84(2):301-19.
38. Harper E. Bioactive bone cements. *Proc Inst Mech Eng Part H J Eng Med*. 1998;212(2):113-20.
39. Kwon SY, Kim YS, Woo YK, Kim SS, Park JB. Hydroxyapatite impregnated bone cement: In vitro and in vivo studies. *Biomed Mater Eng*. 1997;7(2):129-40.
40. Turner TM, Urban RM, Singh K, Hall DJ, Renner SM, Lim T, et al. Vertebroplasty comparing injectable calcium phosphate cement compared with polymethylmethacrylate in a unique canine vertebral body large defect model. *The Spine Journal*. 2008;8(3):482-7.
41. Turner TM, Urban RM, Gitelis S, Haggard WO, Richelsoph K. Resorption evaluation of a large bolus of calcium sulfate in a canine medullary defect. *Orthopedics*. 2003;26(5):577.

42. Stubbs D, Deakin M, Chapman-Sheath P, Bruce W, Debes J, Gillies R, et al. In vivo evaluation of resorbable bone graft substitutes in a rabbit tibial defect model. *Biomaterials*. 2004;25(20):5037.
43. Glazer PA, Spencer UM, Alkalay RN, Schwardt J. In vivo evaluation of calcium sulfate as a bone graft substitute for lumbar spinal fusion. *Spine J*. 2001 Nov-Dec;1(6):395-401.
44. Liu Y, Park J, Njus G, Stienstra D. Bone-particle-impregnated bone cement: An in vitro study. *J Biomed Mater Res*. 2004;21(2):247-61.
45. Downes S, Wood D, Malcolm A, Ali S. Growth hormone in polymethylmethacrylate cement. *Clin Orthop*. 1990;252:294.
46. Shinzato S, Kobayashi M, Mousa WF, Kamimura M, Neo M, Kitamura Y, et al. Bioactive polymethyl methacrylate-based bone cement: Comparison of glass beads, apatite-and wollastonite-containing glass-ceramic, and hydroxyapatite fillers on mechanical and biological properties. *J Biomed Mater Res*. 2000;51(2):258-72.
47. Dalby M, Di Silvio L, Harper E, Bonfield W. Increasing hydroxyapatite incorporation into poly (methylmethacrylate) cement increases osteoblast adhesion and response. *Biomaterials*. 2002;23(2):569-76.
48. Dalby M, Di Silvio L, Harper E, Bonfield W. Initial interaction of osteoblasts with the surface of a hydroxyapatite-poly (methylmethacrylate) cement. *Biomaterials*. 2001;22(13):1739-47.

49. Shinzato S, Nakamura T, Kokubo T, Kitamura Y. PMMA-based bioactive cement: Effect of glass bead filler content and histological change with time. *J Biomed Mater Res.* 2001;59(2):225-32.
50. Fini M, Giavaresi G, Aldini NN, Torricelli P, Botter R, Beruto D, et al. A bone substitute composed of polymethylmethacrylate and  $\alpha$ -tricalcium phosphate: Results in terms of osteoblast function and bone tissue formation. *Biomaterials.* 2002;23(23):4523-31.
51. Kobayashi M, Nakamura T, Tamura J, Kokubo T, Kikutani T. Bioactive bone cement: Comparison of AW-GC filler with hydroxyapatite and  $\beta$ -TCP fillers on mechanical and biological properties. *J Biomed Mater Res.* 1998;37(3):301-13.
52. Kokubo T. Bioactive glass ceramics: Properties and applications. *Biomaterials.* 1991;12(2):155-63.
53. Morejon L, Mendizabal AE, Garcia-Menocal JA, Ginebra MP, Aparicio C, Mur FJ, et al. Static mechanical properties of hydroxyapatite (HA) powder-filled acrylic bone cements: Effect of type of HA powder. *J Biomed Mater Res B Appl Biomater.* 2005 Feb 15;72(2):345-52.
54. Li YW, Leong JCY, Lu WW, Luk KDK, Cheung KMC, Chiu KY, et al. A novel injectable bioactive bone cement for spinal surgery: A developmental and preclinical study. *Journal of Biomedical Materials Research Part A.* 2000;52(1):164-70.

55. Sogal A, Hulbert S. Mechanical properties of a composite bone cement: Polymethylmethacrylate and hydroxyapatite. *Bioceramics*. 1992;5:213-24.
56. Dove J, Hulbert S. Fatigue properties of a polymethylmethacrylate-hydroxyapatite composite bone cement. Tokyo: Proc 2nd int symp apatite; ; 1995.
57. Shepherd JH, Shepherd DV, Best SM. Substituted hydroxyapatites for bone repair. *J Mater Sci Mater Med*. 2012:1-13.
58. Marie PJ, Ammann P, Boivin G, Rey C. Mechanisms of action and therapeutic potential of strontium in bone. *Calcif Tissue Int*. 2001 Sep;69(3):121-9.
59. Dahl SG, Allain P, Marie PJ, Mauras Y, Boivin G, Ammann P, et al. Incorporation and distribution of strontium in bone. *Bone*. 2001 Apr;28(4):446-53.
60. Meunier PJ, Roux C, Seeman E, Ortolani S, Badurski JE, Spector TD, et al. The effects of strontium ranelate on the risk of vertebral fracture in women with postmenopausal osteoporosis. *N Engl J Med*. 2004;350(5):459-68.
61. Eliades T, Eliades G, Brantley WA, Johnston WM. Residual monomer leaching from chemically cured and visible light-cured orthodontic adhesives. *American Journal of Orthodontics and Dentofacial Orthopedics*. 1995;108(3):316-21.
62. Tanaka K, Taira M, Shintani H, Wakasa K, Yamaki M. Residual monomers (TEGDMA and Bis-GMA) of a set visible-light-cured dental composite resin when immersed in water. *J Oral Rehabil*. 1991;18(4):353-62.

63. Yaszemski MJ, Payne RG, Hayes WC, Langer R, Mikos AG. Evolution of bone transplantation: Molecular, cellular and tissue strategies to engineer human bone. *Biomaterials*. 1996 Jan;17(2):175-85.
64. Mistry AS, Mikos AG. Tissue engineering strategies for bone regeneration. *Adv Biochem Eng Biotechnol*. 2005;94:1-22.
65. Choi SM, Yang WK, Yoo YW, Lee WK. Effect of surface modification on the in vitro calcium phosphate growth on the surface of poly(methyl methacrylate) and bioactivity. *Colloids Surf B Biointerfaces*. 2010 Mar 1;76(1):326-33.
66. Li YW, Leong JCY, Lu WW, Luk KDK, Cheung KMC, Chiu KY, et al. A novel injectable bioactive bone cement for spinal surgery: A developmental and preclinical study. *Journal of Biomedical Materials Research Part A*. 2000;52(1):164-70.
67. Guo D, Xu K, Zhao X, Han Y. Development of a strontium-containing hydroxyapatite bone cement. *Biomaterials*. 2005 Jul;26(19):4073-83.
68. Hernández L, Gurruchaga M, Goñi I. Injectable acrylic bone cements for vertebroplasty based on a radiopaque hydroxyapatite. formulation and rheological behaviour. *J Mater Sci Mater Med*. 2009;20(1):89-97.
69. Landi E, Tampieri A, Celotti G, Sprio S, Sandri M, Logroscino G. Sr-substituted hydroxyapatites for osteoporotic bone replacement. *Acta Biomaterialia*. 2007;3(6):961-9.

70. Cheung KM, Lu WW, Luk KD, Wong CT, Chan D, Shen JX, et al. Vertebroplasty by use of a strontium-containing bioactive bone cement. *Spine (Phila Pa 1976)*. 2005 Sep 1;30(17 Suppl):S84-91.
71. Ni G, Lu W, Chiu K, Li Z, Fong D, Luk K. Strontium-containing hydroxyapatite (Sr-HA) bioactive cement for primary hip replacement: An in vivo study. *Journal of Biomedical Materials Research Part B: Applied Biomaterials*. 2006;77(2):409-15.
72. Silver IA, Deas J, Erecińska M. Interactions of bioactive glasses with osteoblasts in vitro: Effects of 45S5 bioglass<sup>®</sup>, and 58S and 77S bioactive glasses on metabolism, intracellular ion concentrations and cell viability. *Biomaterials*. 2001;22(2):175-85.
73. Ni GX, Lu WW, Chiu KY, Li ZY, Fong DYT, Luk KDK. Strontium-containing hydroxyapatite (Sr-HA) bioactive cement for primary hip replacement: An in vivo study. *Journal of Biomedical Materials Research Part B: Applied Biomaterials*. 2006;77(2):409-15.
74. Hernández L, Parra J, Vázquez B, Bravo AL, Collía F, Goñi I, et al. Injectable acrylic bone cements for vertebroplasty based on a radiopaque hydroxyapatite. bioactivity and biocompatibility. *Journal of Biomedical Materials Research Part B: Applied Biomaterials*. 2009;88(1):103-14.
75. Ni G, Chiu K, Lu W, Wang Y, Zhang Y, Hao L, et al. Strontium-containing hydroxyapatite bioactive bone cement in revision hip arthroplasty. *Biomaterials*. 2006;27(24):4348-55.

76. Ni GX, Shu B, Huang G, Lu WW, Pan HB. The effect of strontium incorporation into hydroxyapatites on their physical and biological properties. *Journal of Biomedical Materials Research Part B: Applied Biomaterials*. 2012.
77. Zhang C, Cheng Z, Yang P, Xu Z, Peng C, Li G, et al. Architectures of strontium hydroxyapatite microspheres: Solvothermal synthesis and luminescence properties. *Langmuir*. 2009;25(23):13591-8.
78. Zhang W, Shen Y, Pan H, Lin K, Liu X, Darvell BW, et al. Effects of strontium in modified biomaterials. *Acta biomaterialia*. 2011;7(2):800-8.
79. Xue W, Moore JL, Hosick HL, Bose S, Bandyopadhyay A, Lu WW, et al. Osteoprecursor cell response to strontium-containing hydroxyapatite ceramics. *J Biomed Mater Res A*. 2006 Dec 15;79(4):804-14.
80. Wong CT, Lu WW, Chan WK, Cheung KM, Luk KD, Lu DS, et al. In vivo cancellous bone remodeling on a strontium-containing hydroxyapatite (sr-HA) bioactive cement. *J Biomed Mater Res A*. 2004 Mar 1;68(3):513-21.
81. Rodrigues DC, Gilbert JL, Hasenwinkel JM. Pseudoplasticity and setting properties of two-solution bone cement containing poly(methyl methacrylate) microspheres and nanospheres for kyphoplasty and vertebroplasty. *J Biomed Mater Res B Appl Biomater*. 2009 Oct;91(1):248-56.
82. Rodrigues DC, Gilbert JL, Hasenwinkel JM. Two-solution bone cements with cross-linked micro and nano-particles for vertebral fracture applications: Effects of zirconium

- dioxide content on the material and setting properties. *J Biomed Mater Res B Appl Biomater*. 2010 Jan;92(1):13-23.
83. Zhanglei N, Zhidong C, Wenjun L, Jinghua Z, Yang L. Synthesis and photoluminescence performance of sr-doped hydroxyapatite. Proceedings of the international conference on circuits, systems, signals; .
84. Kjellson F, Almen T, Tanner KE, McCarthy ID, Lidgren L. Bone cement X-ray contrast media: A clinically relevant method of measuring their efficacy. *J Biomed Mater Res B Appl Biomater*. 2004 Aug 15;70(2):354-61.
85. Kokubo T, Takadama H. How useful is SBF in predicting in vivo bone bioactivity? *Biomaterials*. 2006 May;27(15):2907-15.
86. Fathi M, Hanifi A, Mortazavi V. Preparation and bioactivity evaluation of bone-like hydroxyapatite nanopowder. *J Mater Process Technol*. 2008;202(1):536-42.
87. Ni G, Lu W, Chiu K, Li Z, Fong D, Luk K. Strontium-containing hydroxyapatite (Sr-HA) bioactive cement for primary hip replacement: An in vivo study. *Journal of Biomedical Materials Research Part B: Applied Biomaterials*. 2006;77(2):409-15.
88. Ni GX, Lu WW, Xu B, Chiu KY, Yang C, Li ZY, et al. Interfacial behaviour of strontium-containing hydroxyapatite cement with cancellous and cortical bone. *Biomaterials*. 2006 Oct;27(29):5127-33.

89. Wong C, Chen Q, Lu W, Leong J, Chan W, Cheung K, et al. Ultrastructural study of mineralization of a strontium-containing hydroxyapatite (Sr-HA) cement in vivo. *Journal of Biomedical Materials Research Part A*. 2004;70(3):428-35.
90. Pan H, Li Z, Lam W, Wong J, Darvell B, Luk K, et al. Solubility of strontium-substituted apatite by solid titration. *Acta Biomaterialia*. 2009;5(5):1678-85.
91. Boanini E, Torricelli P, Fini M, Bigi A. Osteopenic bone cell response to strontium-substituted hydroxyapatite. *J Mater Sci Mater Med*. 2011:1-10.
92. Ni G, Yao Z, Huang G, Liu W, Lu WW. The effect of strontium incorporation in hydroxyapatite on osteoblasts in vitro. *J Mater Sci Mater Med*. 2011;22(4):961-7.
93. van Hooy-Corstjens CS, Bulstra SK, Knetsch ML, Geusens P, Kuijer R, Koole LH. Biocompatibility of a new radiopaque iodine-containing acrylic bone cement. *Journal of Biomedical Materials Research Part B: Applied Biomaterials*. 2007;80(2):339-44.
94. van Hooy-Corstjens CS, Govaert LE, Spoelstra AB, Bulstra SK, Wetzels GM, Koole LH. Mechanical behaviour of a new acrylic radiopaque iodine-containing bone cement. *Biomaterials*. 2004;25(13):2657-67.
95. Wang C, Pilliar R. Fracture toughness of acrylic bone cements. *J Mater Sci*. 1989;24(10):3725-38.
96. Ginebra M, Albuixech L, Fernandez-Barragan E, Aparicio C, Gil F, San Roman J, et al. Mechanical performance of acrylic bone cements containing different radiopacifying agents. *Biomaterials*. 2002;23(8):1873-82.

97. Kurtz S, Villarraga M, Zhao K, Edidin A. Static and fatigue mechanical behavior of bone cement with elevated barium sulfate content for treatment of vertebral compression fractures. *Biomaterials*. 2005;26(17):3699-712.
98. Deb S, Vazquez B. The effect of cross-linking agents on acrylic bone cements containing radiopacifiers. *Biomaterials*. 2001;22(15):2177-81.
99. Vallo CI, Cuadrado TR, Frontini PM. Mechanical and fracture behaviour evaluation of commercial acrylic bone cements. *Polym Int*. 1999;43(3):260-8.
100. Chen Q, Wong C, Lu W, Cheung K, Leong J, Luk K. Strengthening mechanisms of bone bonding to crystalline hydroxyapatite in vivo. *Biomaterials*. 2004;25(18):4243-54.
101. Vallo CI, Montemartini PE, Fanovich MA, Porto Lopez JM, Cuadrado TR. Polymethylmethacrylate-based bone cement modified with hydroxyapatite. *J Biomed Mater Res*. 1999;48(2):150-8.
102. Vallo CI. Influence of filler content on static properties of glass-reinforced bone cement. *J Biomed Mater Res*. 2000;53(6):717-27.
103. Saha S, Pal S. Improvement of mechanical properties of acrylic bone cement by fiber reinforcement. *J Biomech*. 1984;17(7):467-78.
104. Pourdeyhimi B, Wagner H. Elastic and ultimate properties of acrylic bone cement reinforced with ultra-high-molecular-weight polyethylene fibers. *J Biomed Mater Res*. 1989;23(1):63-80.

105. Kim YS, Kang YH, Kim JK, Park JB. Effect of bone mineral particles on the porosity of bone cement. *Biomed Mater Eng.* 1994;4(1):37-46.
106. Kwok JC, Afshari F, Garcia-Alias G, Fawcett JW. Proteoglycans in the central nervous system: Plasticity, regeneration and their stimulation with chondroitinase ABC. *Restor Neurol Neurosci.* 2008;26(2-3):131-45.
107. Serbetci K, Korkusuz F, Hasirci N. Thermal and mechanical properties of hydroxyapatite impregnated acrylic bone cements. *Polym Test.* 2004;23(2):145-55.
108. Kobayashi M, Nakamura T, Shinzato S, Mousa WF, Nishio K, Ohsawa K, et al. Effect of bioactive filler content on mechanical properties and osteoconductivity of bioactive bone cement. *J Biomed Mater Res.* 1999 Sep 15;46(4):447-57.
109. ASTM F451-99a. In: *Standard Specification for Acrylic Bone Cement.* ASTM International, West Conshohocken, PA. ; 2007e1.
110. Standard test method for flexural properties of unreinforced and reinforced plastics and electrical insulating materials. ASTM specification D 790-86. *ASTM Standards Philadelphia: American Society for Testing and Materials.* 1990:274-83.
111. Designation A. E399-90. standard test method for plane-strain fracture toughness of metallic materials. *American Society for Testing Materials, Philadelphia, Pennsylvania,* 1990. 1997.
112. Leong JC, Li Z, Lu WW. Development and clinical trial of a novel bioactive bone cement. *Frontiers of Medicine in China.* 2008;2(2):117-26.

113. Nguyen N, Maloney W, Dauskardt R. Reliability of PMMA bone cement fixation: Fracture and fatigue crack-growth behaviour. *J Mater Sci Mater Med*. 1997;8(8):473-83.
114. Topoleski L, Ducheyne P, Cuckler J. Microstructural pathway of fracture in poly (methyl methacrylate) bone cement. *Biomaterials*. 1993;14(15):1165-72.
115. Bryers JD. Medical biofilms. *Biotechnol Bioeng*. 2008;100(1):1-18.
116. Costerton JW, Stewart PS, Greenberg EP. Bacterial biofilms: A common cause of persistent infections. *Science*. 1999;284(5418):1318-22.
117. Gristina AG. Biomaterial-centered infection: Microbial adhesion versus tissue integration. *Science*. 1987;237(4822):1588-95.
118. Buchholz H, Engelbrecht H. [Depot effects of various antibiotics mixed with palacos resins]. *Chirurg*. 1970;41(11):511.
119. Hernandez L, Muñoz ME, Goñi I, Gurruchaga M. New injectable and radiopaque antibiotic loaded acrylic bone cements. *Journal of Biomedical Materials Research Part B: Applied Biomaterials*. 2008;87(2):312-20.
120. Beeching NJ, Thomas MG, Roberts S, Lang SD. Comparative in-vitro activity of antibiotics incorporated in acrylic bone cement. *J Antimicrob Chemother*. 1986 Feb;17(2):173-84.
121. Liu W, Wong C, Fong M, Cheung W, Kao R, Luk K, et al. Gentamicin-loaded strontium-containing hydroxyapatite bioactive bone cement—An efficient bioactive

- antibiotic drug delivery system. *Journal of Biomedical Materials Research Part B: Applied Biomaterials*. 2010;95(2):397-406.
122. Wu J, Hou S, Ren D, Mather PT. Antimicrobial properties of nanostructured hydrogel webs containing silver. *Biomacromolecules*. 2009;10(9):2686-93.
123. Heydorn A, Nielsen AT, Hentzer M, Sternberg C, Givskov M, Ersbøll BK, et al. Quantification of biofilm structures by the novel computer program COMSTAT. *Microbiology*. 2000;146(10):2395.
124. O'Connell DP, Nanavaty T, McDevitt D, Gurusiddappa S, Höök M, Foster TJ. The fibrinogen-binding MSCRAMM (clumping factor) of *Staphylococcus aureus* has a Ca<sup>2+</sup>-dependent inhibitory site. *J Biol Chem*. 1998;273(12):6821-9.
125. Kokubo T, Matsushita T, Takadama H, Kizuki T. Development of bioactive materials based on surface chemistry. *Journal of the European ceramic society*. 2009;29(7):1267-74.
126. Chu K, Oshida Y, Hancock E, Kowolik M, Barco T, Zunt S. Hydroxyapatite/PMMA composites as bone cements. *Biomedical Materials and Engineering*. 2004;14(1):87-106.
127. Zhang C, Cheng Z, Yang P, Xu Z, Peng C, Li G, et al. Architectures of strontium hydroxyapatite microspheres: Solvothermal synthesis and luminescence properties. *Langmuir*. 2009 Dec 1;25(23):13591-8.

128. Jäger M, Wilke A. Comprehensive biocompatibility testing of a new PMMA-HA bone cement versus conventional PMMA cement in vitro. *Journal of Biomaterials Science, Polymer Edition*. 2003;14(11):1283-98.
129. Hao Y, Yan H, Wang X, Zhu B, Ning C, Ge S. Evaluation of osteoinduction and proliferation on nano-sr-HAP: A novel orthopedic biomaterial for bone tissue regeneration. *J Nanosci Nanotechnol*. 2012 Jan;12(1):207-12.
130. Shim JB, Warner SJ, Hasenwinkel JM, Gilbert JL. Analysis of the shelf life of a two-solution bone cement. *Biomaterials*. 2005 Jul;26(19):4181-7.
131. Rodrigues DC, Bader RA, Hasenwinkel JM. Grafting of nanospherical PMMA brushes on cross-linked PMMA nanospheres for addition in two-solution bone cements. *Polymer*. 2011;52(12):2505-13.
132. Liu Q, De Wijn J, Van Blitterswijk C. Covalent bonding of PMMA, PBMA, and poly (HEMA) to hydroxyapatite particles. *Hydroxyapatite/polymer composites for bone replacement*. 1998:113.
133. Rodrigues DC, Ordway NR, Ru-Jyu Ma C, Fayyazi AH, Hasenwinkel JM. An ex vivo exothermal and mechanical evaluation of two-solution bone cements in vertebroplasty. *The Spine Journal*. 2011;11(5):432-9.

## 11 Vita

### SHAILLY H. JARIWALA

Syracuse Biomaterials Institute  
413 Bowne Hall  
Syracuse, NY 13244

Office Phone: 315 443 9209  
Home Phone: 315 439 2806  
E-mail: [shjariwa@syr.edu](mailto:shjariwa@syr.edu)

#### EDUCATION

SYRACUSE UNIVERSITY, Syracuse, New York - Ph.D Bioengineering	May 2013
SYRACUSE UNIVERSITY, Syracuse, New York - M.S. Bioengineering	June 2009
MUMBAI UNIVERSITY, Mumbai, India - B.E. Biomedical Engineering	May 2006

#### RESEARCH EXPERIENCE

Syracuse University, Syracuse New York GRADUATE STUDENT Advisor: Julie M. Hasenwinkel PhD.	September 2007- present
Tata Memorial Hospital and Cancer Research Center Speech Therapy Unit, Mumbai, India UNDERGRADUATE INTERN Advisor: Dr. Mrs. G. K. Bachher	February 2006 - March 2006
Mumbai University, Mumbai, India UNDERGRADUATE RESEARCH ASSISTANT Advisor: Dhananjay Theckedath	January 2005 - January 2006
Jaslok Hospital and Research Center, Mumbai, India UNDERGRADUATE INTERN Advisor: Dr. I.P.Gandhi	July 2005 - November 2005

#### PROFESSIONAL EXPERIENCE

Teaching Assistant, Syracuse University Department of Bioengineering	August 2008 - May 2009
---	------------------------

#### PROFESSIONAL AFFILIATIONS

- Society for Biomaterials (SFB)
- Orthopedic Research Society (ORS)

- Biomedical Engineering Society (BMES)
- Golden Key International Honor Society
- The American Association for the Advancement of Science (AAAS)
- Women in Science and Engineering Future Professoriate Program (WISE-FPP), Student Associate (2008-2009)

## SELECTED CONFERENCE ABSTRACTS

1. Jariwala SH, Hasenwinkel JM. *Injectable, bioactive two-solution bone cements ( $\eta$ -TSBC) with strontium substituted hydroxyapatite microspheres*. Poster presentation at the Annual Meeting and Exposition of Society for Biomaterials, Boston, Massachusetts, April 2013.
2. Jariwala SH, Smith SF, Ren D, Hasenwinkel JM. *In-vitro evaluation of the antibacterial properties of two-solution bone cement ( $\eta$ -TSBC) containing strontium substituted hydroxyapatite microspheres*. Poster presentation at the Biomedical Engineering Society, Atlanta, Georgia, October 2012.
3. Jariwala SH, Hasenwinkel JM. *Injectable, nanospheres containing, two-solution bone cements ( $\eta$ -TSBC) with bioactive strontium-hydroxyapatite (SrHA) microspheres*. Poster presentation at the Biomedical Engineering Society, Hartford, Connecticut, October 2011.
4. Jariwala SH, Hasenwinkel JM, Gilbert JL. *Analysis of the Shelf Life of Nano-Two Solution Bone Cement ( $\eta$ -TSBC)*. Poster presentation at the Orthopedic Research Society, Long Beach, California, January 2011.
5. Jariwala SH, Hasenwinkel JM. *Effect of Microtopography and Surface Modulus on PC12 Cell Neurite Outgrowth*. Poster presentation at the Society for Biomaterials, Washington, Seattle, April 2010.
6. Jariwala SH, Bevilacqua E, Hasenwinkel JM. *Effect of Surface Modulus and Extracellular Matrix (ECM) Adhesion Proteins on PC12 Cell Proliferation and Neurite Outgrowth*. Poster presentation at the Society for Biomaterials, San Antonio, Texas, March 2009.
7. Jariwala SH, D'Souza O, Dave J, Theckedath D, Bachher GK. *Assessment of Changes in Speech due to Pathological Conditions caused by Laryngeal Cancer using Digital Signal Processing Techniques*. D.J.Sanghvi College of Engineering. 2006.